Adsorption and Microwave Regeneration for Controlling Volatile Organic Compounds Emissions from Automotive Paint Booths

by

Mohammadreza Fayaz

A thesis submitted in partial fulfillment of the requirements for the degree of

Doctor of Philosophy

in

Environmental Engineering

Department of Civil and Environmental Engineering

University of Alberta

ABSTRACT

Adsorption is a widely used method for control of organic compounds produced during painting operations. After adsorption, the loaded adsorbent should be regenerated to recover the adsorbates and reuse the adsorbent for subsequent adsorption/regeneration cycles. Accumulation of non-desorbed adsorbates in adsorbent pores (aka heel buildup) is a common challenge associated with adsorbent use, which results in reducing the working capacity and life-time of the adsorbent. The goal of this study is to understand the factors affecting heel buildup and possible ways to mitigate it. In this study, heel buildup associated with volatile organic compounds (VOCs) from painting operations was quantified and analyzed. Then, the performance of microwave heating method during regeneration of adsorbents loaded with high molecular weight VOCs was investigated, in terms of regeneration efficiency and energy consumption, to find proper conditions for preventing or minimizing heel. The effect of regeneration temperature, heating rate, adsorbent porosity, and the dielectric properties of adsorbents and adsorbates on regeneration performance and heel buildup were also investigated. Finally, a non-contact microwave sensor was used to monitor the adsorption progress and the level of heel buildup on beaded activated carbon (BAC) samples.

At the early stage of this study, VOCs commonly present in paint solvents were screened for potential heel buildup on BAC. It was observed that compounds with high molecular weight, high boiling point and low vapor pressure tend to provide high heel.

Comparing the performance of conductive and microwave heating for regeneration of a heavy VOC (n-dodecane), it was observed that the minimum energy needed to completely regenerate the adsorbent (100% desorption efficiency) using microwave heating was 6% of that needed with conductive heating. Moreover, it was confirmed that neither regeneration method

altered the adsorbate composition and adsorbent physical and chemical properties during desorption.

Further investigations were completed to study the effect of regeneration temperature, heating rate and adsorbent porosity on heel formation during microwave regeneration of two BACs (88% and 46% microporous) loaded with 1,2,4-trimethylbenzene (TMB). The results showed that for the higher regeneration temperature (400 °C versus 288 °C), increasing heating rate increased heel buildup by as much as 92% and 169% for the mainly microporous and partially microporous BACs, respectively. The elevated heel formation at higher heating rates could be due to adsorbate coking as a result of exposure to high temperature. Conversely, for the lower regeneration temperature (288 °C), increasing the heating rate did not significantly affect the amount of heel buildup; however, it increased the contribution of coke formation in heel. The results from this study indicate that the heating rate, regeneration temperature and adsorbent porosity could be optimized to allow fast desorption with minimal adsorbate decomposition during microwave regeneration.

To study the effect of dielectric properties of adsorbent and adsorbate on microwave heating performance, BAC (microwave absorbing) and a polymeric adsorbent (microwave transparent) were partially loaded with TMB or 2-butoxyethanol (BE) and then regenerated with microwave heating. Results indicate that for the polymeric adsorbent, required energy for regeneration was primarily provided by microwave dissipation within the adsorbate. Conversely, for BAC, required energy for regeneration was primarily provided by microwave dissipation within the adsorbent.

In the next phase of this study, it was found that during adsorption, the dielectric properties of the adsorbent changed with increased adsorbate loading. Those changes could be

measured by a non-contact high resolution microwave sensor in terms of shift in the quality factor and resonant frequency. It was observed that the difference between the 5% breakthrough time and the time that the quality factor was 0.95 of its final value, was less than 5%. Moreover, for all tests, a proportional relationship between adsorption capacity and the final value of the resonant frequency shift was found.

Further investigation focused on studying the ability of the non-contact high resolution microwave sensor to determine the degree of exhaustion of BAC spent through many adsorption/regeneration cycles. The resonant frequency shift was linearly correlated ($R^2 = 0.81 - 0.93$) with the adsorbent apparent density, Brunauer Emmett Teller (BET) surface area and pore volume. Moreover, the effect of adsorbent porosity on dielectric property variation appeared to be more important than the heel composition. Finally, the ability of the sensor for fast, non-contact measurement, and without sample pretreatment, potentially allows for in-situ measurement and real-time monitoring of continuously operating systems.

I dedicate this dissertation to my beloved family.

My sincere gratitude to my caring and loving parents, Mohammad Hassan and Farideh, whose continuous support, affection, and prays made me overcome difficulties during my education.

This dissertation is also dedicated to my lovely sister, Sara, for her sincere support, consideration, and encouragement.

ACKNOWLEDGEMENTS

TABLE OF CONTENTS

LIST OF TABLES

LIST OF FIGURES

LIST OF ACRONYMS

ACC	Activated Carbon Cloth
ACF	Activated Carbon Fiber
ACFC	Activated Carbon Fiber Cloth
AD	Apparent Density
BAC	Beaded Activated Carbon
BE	2-butoxyethanol
BET	Brunauer-Emmett-Teller
BTR	Breakthrough Time Reduction (over 5 adsorption/regeneration cycles)
COP	Critical Oxidation Potential
DAC	Data Acquisition and Control
DDR	Derivative of Desorption Rate
NLDFT	Nonlocal Density Functional Theory
QSDFT	Quench Solid Density Functional Theory
DTG	Derivative Thermo-Gravimetric
GAC	Granular Activated Carbon
GC-FID	Gas Chromatography–Flame Ionization
MEK	Methyl Ethyl Ketone
PID	Photoionization Detector
PSD	Pore Size Distribution
QSDFT	Quenched Solid Density Functional Theory
SLPM	Standard Liter per Minute
THF	Tetrahydrofuran
TGA	Thermo-Gravimetric Analysis
TMB	1,2,4-trimethylbenzene
VOC	Volatile Organic Compound
VNA	Vector Network Analyzer
XPS	X-Ray Photoelectron Spectroscopy

CHAPTER 1. INTRODUCTION AND RESEARCH OBJECTIVES

1.1 Background and Motivation

1.1.1 Irreversible adsorption

Vehicle painting booths are the primary source of emissions of volatile organic compounds (VOCs) from the automobile manufacturing sector (Kim et al., 2000). The main purpose of a spray booth is to provide operational controls to prevent hazardous volatile solvents from escaping to the atmosphere. The overspray stream from a painting booth contains VOCs and paint particles that should be captured and controlled. The paint particles and a portion of the VOCs can be captured using a water curtain; however, a control technique is still required to capture the VOCs present in the air stream (Chiang et al., 2006).

VOCs emissions can be controlled through several techniques such as adsorption, absorption, oxidation, incineration, biofiltration, condensation, and membrane separation (Chiang et al., 2012, Detchanamurthy and Gostomski, 2012, Dunn and El-Halwagi, 1994, Hashisho et al., 2008, Schnabel et al., 1998, Stehlik et al., Tang and Yang, 2012). Compared to other control techniques, adsorption is more cost-effective and efficient. Activated carbon is widely used in VOCs' adsorption processes because it is inexpensive and has a high internal surface area (Lashaki et al., 2012).

When adsorption is used as a pollution control process, it is usually followed by desorption to recover the adsorbate and recover the adsorbent. In some cases, some of the adsorbate remains on the adsorbent after desorption, which means that the adsorption capacity of the adsorbent decreases after each adsorption/ regeneration cycle. Accumulation of non-desorbed molecules in adsorbent pores is known as heel buildup, resulting in reduced adsorbent life-time

and therefore increased operational cost of the process (Lashaki et al., 2012). Heel buildup could be due to physical adsorption (physisorption), oligomerization, chemical adsorption, and/or adsorbate decomposition (Ania et al., 2004, Ania et al., 2005, Çalişkan et al., 2012, Ha and Vinitnantharat, 2000, Thakkar and Manes, 1987, Vidic et al., 1993, Yonge et al., 1985).

In physisorption, the main driving forces are physical forces such as the Van der Waals forces between the adsorbate molecules and the adsorbent. Sometimes adsorbates which physically adsorb on the surface of activated carbon cannot completely be desorbed due to a low regeneration temperature. Those adsorbates are non-desorbed physisorbed species that usually have high boiling points and molecular weights (Fayaz et al., 2011). By increasing the regeneration temperature (i.e., providing a sufficient driving force for desorption), those compounds can be desorbed (Lashaki et al., 2012). In chemical adsorption or chemisorption, the adsorbate reacts with the available functional groups on the surface of the adsorbent through chemical bonds. Hence, in chemisorption, the heat of adsorption is high and approaches the heat of chemical bonds (Lowell and Shields, 1991). The irreversible adsorption of phenolic compounds onto activated carbon is due to the oxidative polymerization of those compounds on the surface of activated carbon (Lu and Sorial, 2007, Osei-Twum et al., 1996).This is because phenolic compounds lose a hydrogen atom and become phenoxy radicals, and by reacting with each other, those radicals form a polymerized molecule. Previous studies showed that during microwave regeneration, some adsorbate molecules could be decomposed and remain in the pores as coke deposits (Ania et al., 2004, Çalişkan et al., 2012).

Most of previous studies on irreversible adsorption were completed for phenolic compounds in liquid phase (Chatzopoulos et al., 1993, De Jonge et al., 1996, Schnelle and Brown, 2002, Álvarez et al., 2004). There are two studies, completed on heel formation from

VOCs in gas phase. The authors of these studies investigated the effect of regeneration temperature on heel buildup, using conductive heating (Lashaki et al., 2012) and resistive heating (Niknaddaf et al., 2016) techniques and found contradictory result, where for conductive heating increasing regeneration temperature from 288 to 400 °C, reduced heel formation by 61%, however, for resistive heating the same increase in temperature increased heel buildup by up to 19%. While the studies used different adsorbents (beaded activated carbon (BAC) versus activated carbon fibre cloth (ACFC)) and different adsorbates (1,2,4-trimethylbenzene (TMB) versus a mixture of VOCs), it is expected that the difference in the heating mechanism in each study had also contribution to the counter-intuitive results.

1.1.2 Determining adsorption breakthrough time and capacity using a non-contact microwave sensor

Breakthrough time has been recognized as a criterion for switching the loaded adsorbent with a virgin one (Lashaki et al., 2012). Direct measurement of the effluent concentration during adsorption is typically used to determine breakthrough time (Lashaki et al., 2012, Wang et al., 2012). To measure the breakthrough-time, however, the monitoring instruments should be directly in contact with the effluent stream, which might be hazardous for the user or might contaminate and damage the instruments in presence of high boiling point and toxic or corrosive compounds. Therefore introducing an alternative cost-effective technique for non-contact determination of breakthrough time could be industrially relevant.

Adsorption capacity for different concentrations of a VOC stream is typically expressed as adsorption isotherms (Pei and Zhang, 2012). Adsorption isotherms for some VOCs on different adsorbents have been obtained using several techniques such as dynamic column method, static volumetric method and gravimetric method (Cal et al., 1997, Seo et al., 2009, Yun

et al., 1998). Due to limitation of the instruments used in most of these studies, the adsorption isotherm measurements could be completed mainly for low to moderate boiling point VOCs such as acetaldehyde, methyl ethyl ketone, benzene, toluene, xylene and cumene (Benkhedda et al., 2000a, Benkhedda et al., 2000b, Cal et al., 1997, Kim et al., 2007, Lashaki et al., 2012, Ryu et al., 2002, Seo et al., 2009, Yun et al., 1999). Consequently, determination of adsorption isotherm for high boiling point compounds could be industrially relevant.

On the other hand, to evaluate the performance of adsorbents in cyclic adsorption/regeneration, monitoring the progression of heel buildup on adsorbents (degree of exhaustion) could be relevant. A typical method for determining the degree of exhaustion of adsorbents in industry is measuring the apparent density (AD) of the sample. Micropore surface analysis is another characterization techniques used for determining the performance of the spent adsorbent; however it is time-consuming and costly. Also neither of the aforementioned techniques is suitable for real-time monitoring of adsorbent performance. Therefore there is need for developing an in-situ technique for reliable real-time monitoring of the adsorbent degree of exhaustion.

1.2 Objectives

The main goal of this study is to understand factors affecting heel buildup and possible ways to mitigate it. The specific objectives are detailed as follows:

The main objective of Chapter 3 was to identify the VOCs which irreversibly adsorb onto the activated carbon and reduce the adsorption capacity; hence, several adsorption/conductive regeneration tests were completed on BAC loaded with different VOCs.

The principal objective of Chapter 4 was to compare the conductive heating and microwave heating regeneration and assess their performance based on the regeneration

efficiency and energy consumption; therefore, BAC was loaded with a high boiling point VOC (n-dodecane) and regenerated using conductive or microwave heating.

The main objective of Chapter 5 was to investigate the effect of adsorbent porosity, regeneration temperature and heating rate on heel buildup during microwave heating; hence, two BACs with different porosities were loaded with TMB and regenerated at two regeneration temperatures (288 and 400 °C) using several heating rates.

The objective of Chapter 6 was to investigate the effect of dielectric properties of adsorbent and adsorbate on microwave heating regeneration. In this study, two adsorbents with contrasted dielectric properties were loaded with two VOCs with the same boiling point but contrasted dielectric properties. Then the samples were regenerated using microwave heating at constant temperature.

The main objective of Chapter 7 was to introduce microwave resonator sensor as a fast and cost effective technique for monitoring adsorption progression and determining adsorption breakthrough time and capacity of adsorbents. In this study, two adsorbents with contrasted dielectric properties were loaded with two VOCs with the same boiling point but contrasted dielectric properties. During adsorption, the variations in dielectric properties of the adsorbents were monitored using a microwave resonator sensor.

The main objective of Chapter 8 was showing the effectiveness of microwave resonator sensor in estimating performance of spent BACs; hence, several characterization tests were conducted on BACs, previously spent during cyclic adsorption/regeneration to evaluate their adsorption performance. Then the results were compared with those obtained from a microwave sensor.

1.3 Thesis Organization

This thesis has been written in paper-based format. Chapter 1 provides a brief background and motivations for completing this research. Chapter 2 provides a review of the literature and theories related to heel formation, microwave heating and microwave sensing. The above-mentioned objectives are met in chapter 3 to 8, individually. Chapter 9 summarizes the main conclusions and contributions from this study and provides recommendations for future studies.

1.4   References

ÁLVAREZ, P. M., BELTRÁN, F. J., GÓMEZ-SERRANO, V., JARAMILLO, J. & RODRIGUEZ, E. M. 2004. Comparison between thermal and ozone regenerations of spent activated carbon exhausted with phenol. *Water Research,* 38**,** 2155-2165.

ANIA, C. O., MENÉNDEZ, J. A., PARRA, J. B. & PIS, J. J. 2004. Microwave-induced regeneration of activated carbons polluted with phenol. A comparison with conventional thermal regeneration. *Carbon,* 42**,** 1377-1381.

ANIA, C. O., PARRA, J. B., MENÉNDEZ, J. A. & PIS, J. J. 2005. Effect of microwave and conventional regeneration on the microporous and mesoporous network and on the adsorptive capacity of activated carbons. *Microporous and Mesoporous Materials,* 85**,** 7-15.

BENKHEDDA, J., JAUBERT, J. N., BARTH, D. & PERRIN, L. 2000a. Experimental and modeled results describing the adsorption of toluene onto activated carbon. *Journal of Chemical and Engineering Data,* 45**,** 650-653.

BENKHEDDA, J., JAUBERT, J. N., BARTH, D., PERRIN, L. & BAILLY, M. 2000b. Adsorption isotherms of m-xylene on activated carbon: Measurements and correlation with different models. *Journal of Chemical Thermodynamics,* 32**,** 401-411.

CAL, M. P., ROOD, M. J. & LARSON, S. M. 1997. Gas phase adsorption of volatile organic compounds and water vapor on activated carbon cloth. *Energy and Fuels,* 11**,** 311-315.

ÇALIŞKAN, E., BERMÚDEZ, J. M., PARRA, J. B., MENÉNDEZ, J. A., MAHRAMANLIOĜLU, M. & ANIA, C. O. 2012. Low temperature regeneration of activated carbons using microwaves: Revising conventional wisdom. *Journal of Environmental Management,* 102**,** 134-140.

CHATZOPOULOS, D., VARMA, A. & IRVINE, R. L. 1993. Activated carbon adsorption and desorption of toluene in the aqueous phase. *AIChE Journal,* 39**,** 2027-2041.

CHIANG, C. Y., LIU, Y. Y., CHEN, Y. S. & LIU, H. S. 2012. Absorption of hydrophobic volatile organic compounds by a rotating packed bed. *Industrial and Engineering Chemistry Research,* 51**,** 9441-9445.

CHIANG, Y. C., LEE, C. C. & SU, W. P. 2006. Adsorption behaviors of activated carbons for the exhaust from spray painting booths in vehicle surface coating. *Toxicological and Environmental Chemistry,* 88**,** 453-467.

DE JONGE, R. J., BREURE, A. M. & VAN ANDEL, J. G. 1996. Reversibility of adsorption of aromatic compounds onto powdered activated carbon (PAC). *Water Research,* 30**,** 883-892.

DETCHANAMURTHY, S. & GOSTOMSKI, P. A. 2012. Biofiltration for treating VOCs: an overview. *Reviews in Environmental Science and Biotechnology***,** 1-11.

DUNN, R. F. & EL-HALWAGI, M. M. 1994. Selection of optimal VOC-condensation systems. *Waste Management,* 14**,** 103-113.

FAYAZ, M., WANG, H., JAHANDAR LASHAKI, M., HASHISHO, Z., PHILIPS, J. H. & ANDERSON, J. E. 2011. Accumulation of adsorbed of organic vapors from automobile painting operations on bead activated carbon. *Proceedings of the Air and Waste Management Association's Annual Conference and Exhibition, Orlando, FL.*

HA, S. R. & VINITNANTHARAT, S. 2000. Competitive removal of phenol and 2,4-dichlorophenol in biological activated carbon system. *Environmental Technology,* 21**,** 387-396.

HASHISHO, Z., EMAMIPOUR, H., ROOD, M. J., HAY, K. J., KIM, B. J. & THURSTON, D. 2008. Concomitant adsorption and desorption of organic vapor in dry and humid air streams using microwave and direct electrothermal swing adsorption. *Environmental Science and Technology,* 42**,** 9317-9322.

KIM, B. R., ADAMS, J. A., KLAVER, P. R., KALIS, E. M., CONTRERA, M., GRIFFIN, M., DAVIDSON, J. & PASTICK, T. 2000. Biological removal of gaseous VOCs from automotive painting operations. *Journal of Environmental Engineering,* 126**,** 745-753.

KIM, J. H., LEE, S. J., KIM, M. B., LEE, J. J. & LEE, C. H. 2007. Sorption equilibrium and thermal regeneration of acetone and toluene vapors on an activated carbon. *Industrial and Engineering Chemistry Research,* 46**,** 4584-4594.

LASHAKI, M. J., FAYAZ, M., WANG, H., HASHISHO, Z., PHILIPS, J. H., ANDERSON, J. E. & NICHOLS, M. 2012. Effect of adsorption and regeneration temperature on irreversible adsorption of organic vapors on beaded activated carbon. *Environmental Science and Technology,* 46**,** 4083-4090.

LOWELL, S. & SHIELDS, J. E. 1991. *Powder surface area and porosity,* London; New York, Chapman & Hall.

LU, Q. & SORIAL, G. A. 2007. The effect of functional groups on oligomerization of phenolics on activated carbon. *Journal of Hazardous Materials,* 148**,** 436-445.

NIKNADDAF, S., ATKINSON, J. D., SHARIATY, P., JAHANDAR LASHAKI, M., HASHISHO, Z., PHILLIPS, J. H., ANDERSON, J. E. & NICHOLS, M. 2016. Heel formation during volatile organic compound desorption from activated carbon fibre cloth. *Carbon,* 96**,** 131-138.

OSEI-TWUM, E. Y., ABUZAID, N. S. & NAHKLA, G. 1996. Carbon-catalyzed oxidative coupling of phenolic compounds. *Bulletin of Environmental Contamination and Toxicology,* 56**,** 513-519.

PEI, J. & ZHANG, J. S. 2012. Determination of adsorption isotherm and diffusion coefficient of toluene on activated carbon at low concentrations. *Building and Environment,* 48**,** 66-76.

RYU, Y. K., LEE, H. J., YOO, H. K. & LEE, C. H. 2002. Adsorption equilibria of toluene and gasoline vapors on activated carbon. *Journal of Chemical and Engineering Data,* 47**,** 1222-1225.

SCHNABEL, S., MOULIN, P., NGUYEN, Q. T., ROIZARD, D. & APTEL, P. 1998. Removal of volatile organic components (VOCs) from water by pervaporation: separation improvement by Dean vortices. *Journal of Membrane Science,* 142**,** 129-141.

SCHNELLE, K. B. J. & BROWN, C. A. 2002. Air pollution control technology handbook.

SEO, J., KATO, S., ATAKA, Y. & CHINO, S. 2009. Performance test for evaluating the reduction of VOCs in rooms and evaluating the lifetime of sorptive building materials. *Building and Environment,* 44**,** 207-215.

STEHLIK, P., DVORAK, R., BEBAR, L. & PARIZEK, T. Up to date technologies for off-gas cleaning. Proceedings of the 2008 Global Symposium on Recycling, Waste Treatment and Clean Technology, REWAS 2008. 1367-1372.

TANG, F. & YANG, X. 2012. A "deactivation" kinetic model for predicting the performance of photocatalytic degradation of indoor toluene, o-xylene, and benzene. *Building and Environment,* 56**,** 329-334.

THAKKAR, S. & MANES, M. 1987. Adsorptive displacement analysis of many-component priority pollutants on activated carbon. *Environmental science and technology,* 21**,** 546-549.

VIDIC, R. D., SUIDAN, M. T. & BRENNER, R. C. 1993. Oxidative coupling of phenols on activated carbon: impact on adsorption equilibrium. *Environmental Science & Technology,* 27**,** 2079-2085.

WANG, H., JAHANDAR LASHAKI, M., FAYAZ, M., HASHISHO, Z., PHILLIPS, J. H., ANDERSON, J. E. & NICHOLS, M. 2012. Adsorption and Desorption of Mixtures of Organic Vapors on Beaded Activated Carbon. *Environmental Science & Technology,* 46**,** 8341-8350.

YONGE, D. R., KEINATH, T. M., POZNANSKA, K. & JIANG, Z. P. 1985. Single-solute irreversible adsorption on granular activated carbon. *Environmental Science and Technology,* 19**,** 690-694.

YUN, J. H., CHOI, D. K. & KIM, S. H. 1999. Equilibria and dynamics for mixed vapors of BTX in an activated carbon bed. *AIChE Journal,* 45**,** 751-760.

CHAPTER 2. LITERATURE REVIEW

2.1 Irreversible Adsorption and Conventional Regeneration Methods

Most studies on irreversible adsorption were completed in liquid phase, using phenolic compounds as adsorbate. Several factors play a role in the development of irreversible adsorption. Adsorption and regeneration temperature and atmosphere, the presence of functional groups on the surface of carbon, adsorbent porosity and physical properties of the adsorbate are important parameters which can affect irreversible adsorption.

2.1.1 Adsorption temperature

During adsorption of phenolic compounds from water, higher temperatures favor the polymerization of phenolic compounds on the surface of activated carbon (Li and Moe, 2005, Mattson et al., 1969). On the other hand, when two organic compounds (methyl ethyl ketone (MEK) and cyclohexanone) were adsorbed from air onto activated carbon, it was observed that by increasing the adsorption temperature, the irreversible adsorption on the surface of carbon also increased (Henning et al., 1989). Similar observation was also reported for adsorption of a mixture of VOCs from air on activated carbon (Lashaki et al., 2012).

2.1.2 Regeneration temperature and heating rate

Higher temperatures favor chemisorption because it provides the activation energy required for the formation of the adsorbate-adsorbent complex (Schnelle and Brown, 2002). During regeneration of carbon loaded with ortho and meta chlorophenol from water, it was observed that at a lower temperature (277 °C) the adsorbates reversibly adsorbed on the surface of carbon. At higher temperatures (800 °C), regeneration using high heating rates (as high as 40 °C /min) increased irreversible adsorption on carbon by converting physisorbed adsorbate into chemisorbed adsorbate (Ferro-Garcia et al., 1995, Ferro-Garcia et al., 1996). In another study, it

was observed that during regeneration of a mainly microporous (97% micropore volume) activated carbon fibre cloth loaded with 1,2,4-trimethylbenzene (TMB), higher heating rate (as high as 100 °C /min) favors coke formation (Niknaddaf et al., 2015). During regeneration of carbon loaded with a mixture of organic compounds, it was found that increasing regeneration temperature from 288 to 400 °C decreased the heel by as much as 61% (Lashaki et al., 2012).

2.1.3 The effect of adsorption and regeneration atmosphere

2.1.3.1 The effect of adsorption atmosphere

When phenolic compounds adsorbed from water onto activated carbon, the presence of molecular oxygen enhanced the irreversible adsorption and increased the adsorption capacity (De Jonge et al., 1996). The mechanism for irreversible adsorption is called oxidative coupling, which is a type of oligomerization. Oligomerization is a process in which phenolic compounds react with oxygen molecules to produce phenoxy radicals. When phenoxy radicals are attached, dimmers and trimmers form (Osei-Twum et al., 1996). Henning et al. (1989) found that the presence of oxygen could also improve the irreversible adsorption of organic compounds from air. Therefore, the presence of oxygen favors irreversible adsorption in both water and air as adsorption environments.

2.1.3.2 The effect of regeneration atmosphere

Thermal regeneration (at 850 °C) of activated carbon loaded with phenol from water was compared to ozone regeneration (at 25 °C) under the same conditions (Álvarez et al., 2004). It was observed that by using an inert atmosphere, the thermal regeneration was not successful in recovering the original adsorption capacity. However by using an oxidizing atmosphere (CO_2), higher regeneration efficiency (more than 90%) was obtained. During the ozonation of spent activated carbon at room temperature, the physisorbed and chemisorbed phenol on the carbon

was successfully removed, and most (80%) of adsorbent surface area was restored. At a low ratio of ozone to phenol (1.31 g O_3/g Phenol), phenol was not completely removed (64.8% regeneration) while at a high ratio of ozone to phenol (2.78 g O_3/g Phenol), ozone reacted with the surface functional groups on the carbon which prevented phenol adsorption and resulted in 58.1% regeneration efficiency. However for 1.71 g O_3/g Phenol, the regeneration was 74.8%.

In another study, activated carbon loaded with phenolic compounds went through pyrolysis and was oxidized with oxygen and steam at a high temperature (between 415 and 500 °C). It was observed that the rate of oxidation of the remaining residue after pyrolysis increased significantly (12-15 times), and that oxidation with oxygen (5-7.5% of nitrogen or helium used as carrier gas) improved the removal of residue (10-15% wt) (Harriott and Cheng, 1988).

By increasing the regeneration time and temperature, there was an increase in the portion of phenolic compounds that was chemisorbed onto activated carbon. It is possible to significantly reduce the chemisorption of phenol onto activated carbon and recover the original adsorption capacity. For this to happen, carbon must be slightly oxidized before adsorption, the time between the adsorption and regeneration processes must be reduced, and the regeneration temperature must be kept as low as possible (Magne and Walker Jr, 1986).

Jahandar Lashaki et al (2016) investigated the effect of oxygen content of regeneration purge gas on heel buildup during consecutive adsorption/regeneration of activated carbon loaded with VOCs. Performing regeneration using high oxygen content purge gas (625-10,000 ppm) resulted in shorter breakthrough time, larger loss of adsorption capacity, and greater cumulative heel accumulation compared to a low level of oxygen (≤5 ppm). When regeneration was performed using high oxygen content purge gas, chemisorption was the main heel buildup mechanism. Micropore surface analysis showed that chemisorption increased the diffusive

resistance in micropores. On the other hand, when low oxygen content purge gas was used for regeneration, the main heel buildup mechanism was physisorption.

2.1.4   The effect of functional groups on the surface of carbon

The surface oxides considerably affect the catalytic reactions and adsorption on the surface of activated carbon, and can be categorized into acidic and basic functional groups (Shen et al., 2008). The acidic functional groups on activated carbon increase metal adsorptive capacities but decrease organic adsorptive capacities (Gaur and Shankar, 2008).

During irreversible adsorption of phenolic compounds, adsorbate molecules chemically interact with oxygenated functional groups on the activated carbon surface (Grant and King, 1990). Surface functional groups (e.g., acidic and basic surface functional groups, metal and metal oxides complexes) catalyze the oligomerization process on the activated carbon surface (Lu and Sorial, 2009). When unsaturated groups such as carboxyl and nitro groups are present, the oxidation of adsorbates is less probable. However, the presence of saturated groups such as methyl groups increases the possibility for adsorbate oxidation (De Jonge et al., 1996). Acidic surface functional groups on the activated carbon can influence the adsorption of phenol in several ways: 1) decreasing the dispersive interactions of activated carbon with phenol during the removal of π-electrons from the carbon surface; 2) forming the water clusters which can block pores, keeping phenol from diffusing into them; 3) avoiding irreversible adsorption of phenol onto activated carbon under oxic conditions via oxidative coupling reactions; 4) chemisorption of phenol onto carbonyl groups through the donor-acceptor complex mechanism; and 5) chemisorption of phenol on carboxylic groups via ester formation (Álvarez et al., 2004).

2.1.5 The effect of adsorbate

As mentioned before, the main products of oxidative coupling of adsorbed phenol on the surface of carbon are dimmers and trimmers. One important factor in oligomerization is the level of critical oxidation potential (COP), which is the affinity of the adsorbate to undergo oxidative coupling on activated carbon. The presence of electron-withdrawing functional groups on phenol molecules (e.g., nitro and chloro) makes it harder for the phenolic compounds to lose a proton (i.e., those groups increase the level of COP). Therefore, as COP increases, the level of irreversible adsorption decreases. On the other hand, the presence of electron-donating groups, such as methyl and ethyl groups, enhances the oligomerization process. The order of irreversibility for different compounds is: p-methoxyphenol > 2,4-dimethylphenol = p-chlorophenol > phenol > aniline >p-nitrophenol = p-hydroxybenzaldehyde (Grant and King, 1990).

Rudling and Björkholm (1987) evaluated the irreversible adsorption of organic compounds onto activated carbon using organic solvent desorption. The adsorption of non-polar or weakly polar compounds (e.g. dioxane and octane) depicted low (3.8%) irreversibility, while alcohols and glycol ethers, which are polar compounds, depicted higher (9%) levels of irreversible adsorption. Calorimetric experiments showed that the heat of adsorption of butanol is higher for mesoporous carbon than microporous carbon.

As a general rule, the heat of desorption resulting from a physisorbed material is similar to or slightly more than the heat of vaporization (Popescu et al., 2003). Lukomskaya et al. (1986) explored gas phase adsorption of o-xylene on carbons and found that it was chemisorption, because the heat of adsorption (75 kJ/mol) was significantly greater than the characteristic values of the heats of physical adsorption (46 kJ/mole).

Liu et al. (1987) studied the thermal desorption behavior of organic compounds including alkanes, alkenes and aromatic hydrocarbons on granular activated carbon (GAC). The low molecular weight of the alkanes (up to C_8) was physically adsorbed; however, the heavier ones (greater than C_8) thermally decomposed on the surface of activated carbon. The desorption behavior of alkenes was similar to that of alkanes.

Organic adsorbates were categorized into three groups based on temperature-programmed pyrolysis of activated carbon samples, loaded by adsorption from aqueous phase: Group I mostly includes compounds which can be completely vaporized by heating; Group II mostly includes compounds that decomposed during a first-order kinetic and left some residue on the carbon; Group III mostly includes aromatic compounds (e.g., phenol, β-naphtol and lignin) and after regeneration about 60% of the adsorbed compounds are left on the carbon. The amount of irreversibly adsorbed compounds in this group changes with the type of carbon and with the pyrolysis process (Harriott and Cheng, 1988, Suzuki et al., 1978).

2.1.6 The effect of adsorbent and adsorbent pore size

GAC, beaded activated carbon (BAC), activated carbon fibre (ACF), activated carbon fibre cloth (ACFC) and activated carbon monolith are different forms of activated carbon that are typically used for adsorption of organic vapors (Águeda et al., 2011, Kim et al., 2001, Luo et al., 2006).

Pore size distribution (PSD) is an important factor in determining adsorption behavior of adsorbent (Chiang et al., 2006, Li et al., 2011). During regeneration of BAC saturated with a mixture of VOCs, most of heel was formed in the narrower micropores and the highest reduction in breakthrough time was observed after the first adsorption/regeneration cycle (Lashaki et al., 2012). On the other hand, it was found that ACF with the narrower pore width was more

effective in reducing the oligomerization of phenols than GAC with the wider PSD (Lu and Sorial, 2004b).

To investigate the effect of PSD on irreversible adsorption, Lu and Sorial (2004a) studied adsorption of two phenolic adsorbates (o-cresol and 2-ethylphenol) on four ACFs and one GAC with different PSDs. The experiments were completed under oxic and anoxic conditions. The highest regeneration efficiency was found for the adsorbent with smallest pore width, which was an activated carbon cloth (ACC-10). During another study, the effect of molecular oxygen on irreversible adsorption of several phenolic compounds (phenol, 2-methylphenol, 2-ethylphenol, 2-chlorophenol, 2-nitrophenol, 4-chlorophenol, and 4-nitrophenol) was studied. Similar to the previous study, four ACFs and a GAC with different PSDs were used as adsorbents. By changing adsorption condition from oxic to anoxic, the adsorption capacity for the adsorbent with the smallest pore width (ACC-10) did not change. The authors attributed this observation to the small size of the ACC-10 pores, which resulted in hampering irreversible adsorption (Lu and Sorial, 2007).

In another study, the effect of adsorbate COP and adsorbent PSD on irreversible adsorption of phenol on several adsorbents were investigated (Lu and Sorial, 2009). During this study, binary and ternary mixtures of phenolic compounds were used as adsorbate. It was observed that the adsorbent with the smallest pore width had the lowest oligomerization. Moreover, the oligomerization for ternary mixture was lower than for binary mixture, due to competitive adsorption between different components of the mixture.

2.2 Microwave Heating as an Alternative Regeneration Method

Microwave heating has been considered as an effective tool in environmental engineering and has been applied in several areas such as contaminated soil remediation, waste processing,

minerals processing and adsorbent regeneration (Jones et al., 2002). Microwave heating has recently been used for processing carbon with tailored properties. The processed carbon could be used to indirectly heat other materials or to act as catalyst and microwave receptor in reactions (Menéndez et al., 2010). Materials can be categorized into three groups depending on how they interact with the microwaves: conductors which reflect microwaves, insulators which are transparent to microwaves, and absorbers or dielectric materials which can absorb microwaves. The most important mechanism in microwave heating is polarization loss, in which the dipole moments of molecules rotate based on the electric field direction. During the rotation, some heat will be released (Bradshaw et al., 1997, Jones et al., 2002). Another mechanism is ionic conduction, where ions freely move through the material resulting in ohmic losses (Clark and Sutton, 1994). The interaction of materials with microwaves can be described using the material's complex permittivity or ε^*. This parameter is usually expressed by two terms: a real part (ε', dielectric constant) and an imaginary part (ε'', dielectric loss factor):

$$\varepsilon^* = \varepsilon' - \varepsilon'' j$$

The heating potential or average absorption of microwave power per unit volume is (Hashisho et al., 2005):

$$Q_{avg} = \omega \varepsilon_0 \varepsilon'' E_{rms}^2$$

Where Q_{avg} is the average absorption of microwave per unit volume in W/m^3; ω is the angular frequency in rd/s; ε_0 is the permittivity of free space, 8.85×10^{-12} F/m; ε'' is the loss factor of the heated material which is dimensionless; and E_{rms} is the root-mean-square electric field intensity in V/m. It can be observed that the loss factor plays an important role in microwave heating of materials.

The following sections discuss the investigations completed on microwave regeneration of activated carbon and molecular sieves loaded with organic compounds or water.

2.2.1 Microwave regeneration of loaded activated carbon

Activated carbon can be effectively heated by microwave energy due to the presence of delocalized π electrons. Therefore, microwave heating regeneration has been widely used for regeneration of loaded activated carbon (Çalişkan et al., 2012, Hashisho et al., 2009).

2.2.1.1 Regeneration of carbon loaded with VOCs

Fang and Peter (1996) applied microwave heating to regenerate powder activated carbon (PAC) loaded with acetone and ethanol. They suggested a 4-step mechanism to regenerate the PAC. Hashisho et al (2005) used microwave heating to regenerate ACFC, loaded with MEK, water vapor and tetrachloroethylene (PERC). They found that the difference in polarity of MEK and PERC didn't have a significant effect on the regeneration of activated carbon. The recovered adsorption capacity and recovered adsorbate for MEK was 74% and 40%, respectively. Thermal "runaway effect" or uncontrolled increase in adsorbent's temperature was not observed during heating.

During on-site regeneration of GAC, loaded with MEK, it was observed that using 200 W microwave power, desorption efficiency of 80% could be achieved in 4 min for 5 g MEK adsorbed on 5 g GAC, and in 6 min for 3 g MEK adsorbed on 5 g GAC. The variation in duration depends on amount of loading. Besides, the loaded adsorbent could be recovered to its original adsorption capacity (Tai and Lee, 2007). Cha and Charlisle (2001) used a pilot-scale microwave desorber to regenerate GAC loaded with VOCs, present in effluents from non-combustion sources such as paint booth ventilation streams. It was observed that the original adsorption capacity of adsorbent could be restored, however, after 20 successive

adsorption/regeneration cycles, the adsorption capacity decreased by 7% of the original capacity. In another study, a system containing an on-site adsorber/desorber, connected to a scrubber was used. The system was tested for adsorption and microwave regeneration of GAC and zeolites that were loaded with several adsorbates (e.g., toluene, ethyl acetate, methylene chloride and hydrochloric acid) (Cha et al., 2004). For each adsorbent-adsorbate pair, complete regeneration was achieved and the original adsorption capacity of adsorbent was restored after four adsorption/regeneration cycles. All hydrocarbons in the fume exhaust air were captured by GAC while, zeolite only captured hydrochloric acid. They also used an oxidizer to oxidize the concentrated paint solvent using a fixed bed of oxidation catalyst mixed with silicon carbide. An oxidation efficiency of 99% was achieved. Sometimes increase of dielectric properties of carbon with temperature results in failure of microwave regeneration. During microwave regeneration of activated carbon loaded with acetic acid or triethylamine, intense spark discharge was observed; consequently the efficiency for microwave regeneration of loaded carbon could not be assessed (Robers et al., 2005).

2.2.1.2 *Regeneration of carbon loaded with other organic compounds*

Ania et al. (2004) compared the performance of microwave heating and the thermal conductive heating method (electric furnace) for the regeneration of activated carbon loaded with phenol. It was observed that after several successive adsorption/regeneration cycles, the sample regenerated by microwave heating maintained its adsorption capacity compared to the original one. Compared to the thermal conductive heating method, microwave heating was much more energy efficient. The regeneration under the CO_2 atmosphere helped maintaining the porous structure of the loaded carbon because of partial gasification of the sample under oxidizing atmosphere. In another study, it was found that after successive adsorption and regeneration

20

cycles, the microporosity of activated carbon decreased in both microwave and thermal conductive heating cases (Ania et al., 2005). The reduction in the microporosity of adsorbent, however, is lower for microwave regeneration; because during microwave heating a temperature gradient was created in the sample, decreasing from the core towards the surface of the material. Therefore, before having any significant adsorbate decomposition and coke formation in the micropores, adsorbate molecules rapidly moved to the adsorbent surface. The adsorption capacity after six successive cycles decreased in both methods; however, the reduction was larger for the thermal conductive heating method.

Çalışkan et al. (2012) compared the performance of microwave and conductive heating (i.e., electric furnace) during regeneration of activated carbons loaded with a complex compound (promethazine which is a pharmaceutical compound). During regeneration of loaded carbon at 350 °C, incomplete regeneration were observed in both cases (conventional and microwave), however, higher regeneration efficiency was observed for microwave heating. Because direct heating during microwave heating resulted in desorption of both physisorbed and chemisorbed parts of adsorbate whereas during conductive heating only physisorbed part of adsorbate was desorbed. During regeneration at 500 °C, however, the regeneration efficiency for microwave heating was lower than that for regeneration in an electric furnace. The lower microwave regeneration efficiency is due to thermal cracking of the adsorbate inside the pores of the adsorbent. In another study completed using a pharmaceutical compound as adsorbate (salicylic acid), it was observed that using high temperature (850 °C) microwave regeneration under oxidizing carrier gas, high regeneration efficiency (>95%) could be obtained. The efficiency was obtained after 6 successive adsorption/regeneration cycles. It was also found that the adsorption capacity of the regenerated sample was higher than for the as-received samples, which is due to

changes in microporous structure of carbon during heating. Moreover, salicylic acid was desorbed in a molecular state and then partially decomposed in the gas phase, which decreased the formation of deposit in the pores and improved the performance of microwave regeneration over successive cycles (Ania et al., 2007).

Xin-hui et al. (2012) used response surface methodology technique (RSM) to optimize microwave regeneration of activated carbon loaded with HCl and SiO_2. The optimum regeneration temperature, time and flow rate were 950 °C, 60 min and 2.5 g/min, respectively. The carbon regenerated at optimum condition has iodine number of 1103 mg/g and a yield of 68.5%. Moreover, the regenerated carbon was 69.3% microporous and has a Brunauer Emmett Teller (BET) surface area and pore volume of 1302 m^2/g and 0.86 cm^3/g, respectively. Microwave regeneration of GAC, loaded with acid orang 7 was completed using a power of 850 W for 5 min (Quan et al., 2004). Then, the effect of successive adsorption/regeneration on the structural properties of the regenerated sample was studied. The regenerated sample had higher adsorption rate and capacity than the virgin sample. Moreover, PSD of the regenerated sample showed that it had higher mesoporosity than the virgin sample. In another study, optimum conditions for regeneration of PAC loaded during xylose decolourization process, were found (heating for 30 min, using power of 800 W) (Li et al., 2013). The methylene blue and iodine number for the regenerated carbon under optimum conditions were 16 cm^3/0.1 g and 1000.1 mg/g, respectively. Moreover, the BET surface area and pore volume for the regenerated sample were 1064 m^2/g and 1.18 ml/g, respectively. During microwave regeneration of 20 g GAC, loaded during treatment of an azo dye, Reactive Black 5, effective regeneration was obtained using power of 800W for 30 s. Chemical Oxygen Demand removal did not significantly decrease

after 7 successive adsorption/regeneration cycles, however, the adsorption capacity for removal of A265 (benzene-related groups) and toxicity decreased after 6th cycle (Chang et al., 2010).

Bradshaw et al. (1997) studied microwave regeneration of GAC loaded with dissolved gold during carbon-in-pulp process. The regeneration was completed at three temperatures (i.e., 650, 700 and 750 °C). Microwave regeneration until temperature reached 650 °C gave acceptable results which were an activity of 0.65, a loading capacity of 44.7 kg Au/ton carbon and an abrasion resistance factor of 96%, at a total electricity energy consumption of 1.47 kWh/kg. In their next study, it was found that after microwave regeneration at 750 °C for 15 min, the GAC activity was even higher than the original sample (106%). They also found that for 120 kg/h microwave unit, there is a return on investment of 12% (Bradshaw et al., 1998).

Prices and Schmidt (1998b) investigated several process configurations for fixed-bed microwave regeneration systems designed for VOC abatement and recovery of the condensed organic solvents. The important factors on the performance of different designs and economics were found as follows: adsorbent selection, regeneration purge method, column flow configuration, regeneration system pressure, and regeneration coverage. Polymeric adsorbent with low dielectric loss factor was reported as a favorable adsorbent in terms of economics and process. In their next study, they compared economics of the batch and continuous microwave regeneration systems with 10 different conventional VOC control systems. After analyzing the capital and operating costs, they found that depending on application, solvent properties and emission stream concentrations, microwave regeneration could be economically superior to other regeneration technologies.

Fu et al. (2012) studied the microwave regeneration of field–spent GAC from a power plant. The GAC was loaded with natural organic matters. It was observed that microwave

regeneration was able to recover the adsorption capacity of the adsorbent in a very short time and the adsorption capacity of the regenerated GAC was 9 times greater than that of the field-spent GAC. In addition, results confirmed that hydrochloric acid pre-treatment could improve regeneration efficiency by 99.6% and increase the iodine number by 859 mg/g. In fact, acid eliminated some of the inorganic matters adsorbed by the GAC.

2.2.2 Regeneration of loaded molecular sieve adsorbents

Depending on the structure, molecular sieve adsorbents have different dielectric properties and microwave absorption. For example DAY zeolite is a microwave transparent, while NaX zeolite could be effectively heated by microwave (Polaert et al., 2010). Low dielectric properties of microwave transparent adsorbents allows for energy efficient regeneration of microwave absorbing adsorbates such as water vapor or ethanol (Burkholder et al., 1986, Kubota et al., 2011).

2.2.2.1 *Regeneration of molecular sieves loaded with VOCs*

In microwave regeneration, dielectric properties of adsorbate relative to adsorbent could control microwave regeneration (Polaert et al., 2010). During microwave regeneration of a microwave transparent adsorbent loaded with a polar adsorbate (ethanol), ethanol was desorbed quickly and energy-efficiently by a combination of vaporization and expulsion mechanisms. The fast desorption was theoretically attributed to >3500 times faster temperature increase rate for ethanol in comparison to for the adsorbent. Microwave heating of a silicalite zeolite was investigated in another study, and it was observed that the part of adsorbent with silanol group could better absorb microwave and reach to higher temperature than the bulk adsorbent (Turner et al., 2000). Two zeolites (silicalite zeolite and dealuminized Y zeolite) were loaded with a polar (methanol) and a non-polar (cyclohexane) VOCs and regenerated using a constant microwave

power. It was observed that increasing power resulted in desorption of methanol and adsorption of cyclohexane in its place. Considering the lower heat of adsorption of methanol compared to that of cyclohexane, the opposite trend should have been observed if conventional heating was used. Therefore, it was concluded that microwave heating changed adsorption selectivity of adsorbates depending on their permittivities (Turner et al., 2000).

Di and Cheng (1996) investigated the feasibility of regenerating some microwave-transparent adsorbent saturated with isopropanol (as a VOC). The effect of several factors such as purge gas flow rate, humidification, microwave input power, and adsorbent types (zeolites and polymeric adsorbents) was evaluated. It was found that increasing microwave input power increased the regeneration efficiency. Similarly, increasing the humidity of purge gas improved the regeneration efficiency, especially for non-polar VOCs such as hexane. During the regeneration of two microwave transparent zeolites (4A and 13X) loaded with methanol, it was found that heating was applied uniformly through the bed. Also, the presence of methanol, which is a polar molecule, increased the loss factor dramatically (Weissenberger and Schmidt, 1994). Another study investigated microwave regeneration of several binary mixtures made from ethanol, toluene and water from two molecular sieves (microwave transparent and non-transparent). The choice of adsorbent and adsorbate greatly affected the desorption efficiency. For example, microwave regeneration of a transparent adsorbent loaded with a polar adsorbate is very efficient. Also during regeneration of a binary mixture made from a polar and non-polar adsorbate, the polar adsorbate was desorbed much better than the non-polar one (Reuß et al., 2002). Cherbański et al. (2011) compared hot purge gas (N_2) and microwave regeneration during regeneration of zeolite 13X loaded with acetone and toluene. It was found that microwave regeneration could regenerate the adsorbent to its original capacity in shorter time. Moreover,

during microwave regeneration, energy losses were much lower than when hot gas was used for regeneration and bed temperature in microwave regeneration was lower than for hot gas regeneration.

Most of studies on microwave regenerations were completed at bench scale. To study microwave regeneration in a larger scale, Meier et al. (2009) studied microwave regeneration of a 1 m column silicalite zeolite, loaded with methanol. They measured temperature at 5 axial and 3 radial positions throughout the bed. When the bed was loaded with an adsorbate with high dielectric properties, microwave energy was significantly attenuated. During microwave regeneration, some methanol reacted on the zeolite surface, forming dimethylether and water. Besides, some methanol methoxylated the zeolite surface. Therefore in some cases, microwave heating might change adsorbent/adsorbate characteristics and make them unrecoverable.

2.2.2.2 *Dehydration of molecular sieve adsorbents*

Roussy et al. (1984) found that the kinetic relationship for microwave regeneration of 13X, loaded with water is first order and independent of the temperature of solid. The suggested model for desorption shows the instantaneous dependence of desorption on the complex permittivity of the system. During microwave dehydration of zeolite NaX, it was found that independent of the purge gas flow rate, dehydration rates linearly changed with the absorbed power (Polaert et al., 2007). Microwave dehydration of molecular sieve could also depend on molecular structure of adsorbent, particularly on the quantity and position of the exchange cations. During microwave heating of dry zeolite NaX, it was observed that dielectric properties of NaX increased with temperature; as a result, with increase of temperature, microwave absorption for NaX increased. Conversely, the dielectric properties for NaY did not change with

temperature; therefore during regeneration of loaded NaY, the dielectric properties of water were the main contributors to microwave absorption (Polaert et al., 2010).

2.2.3 Microwave regeneration and decomposition

According to several studies, during regeneration of some VOCs and phenolic compounds, some adsorbates were decomposed by microwave irradiation. In microwave regeneration of GAC loaded with trichloroethylene, it was observed that the whole adsorbate was decomposed completely to CO_2 and HCl (Jou, 1998). In microwave regeneration of GAC loaded with phenol, it was observed that most of adsorbate decomposed during the process and the residual detected for a complete decomposition was only H_2O and CO_2 (Hua-Shan and Chih-Ju, 1999). In another study, it was observed that during microwave regeneration of GAC loaded with pentachlorophenol, most of the adsorbate decomposed to CO_2, H_2O and HCl. Also, after several adsorption and microwave regeneration cycles, adsorption capacity of GAC did not change (Liu et al., 2004).

2.3 Microwave Sensing

2.3.1 Introduction

The application of the electromagnetic waves for sensing has been widely researched for environmental engineering purposes (Bourgeois et al., 2003). Particularly, sensing technology has been applied for environmental monitoring of pollutant concentrations in water and treated wastewater quality, water level measurements, material moisture content, carbon level emission for continuous process monitoring of biogas plants and in the healthcare industry (Korostynska et al., 2012).

Microwave sensing is principally completed based on the interaction of the electromagnetic waves with the testing matter. During sensing, the test object alters the velocity

of the signal, attenuates or reflects it. These interactions result in frequency change or attenuation of the incident electromagnetic signal. The variations in transmitted (S_{21}) and reflected (S_{11}) microwave powers at different frequencies could be then linked to the composition of the object under test (Korostynska et al., 2014, Zarifi et al., 2015).

2.3.2 Microwave sensing application

2.3.2.1 Liquid phase concentration monitoring

Yunus (2011) used a planar meander and inter-digital electromagnetic sensors to monitor the concentration of contaminants in water sources. For this purpose, sodium nitrates and ammonium nitrates were mixed in various different ratios dissolved in 1L of distilled water and were used to monitor the response of the sensors. In the first phase of this study, the presence of two nitrates forms (sodium nitrates and ammonium nitrates) could be monitored even at very low concentrations. In the next stage, the levels of contaminants in water samples, taken from different sources were measured using the sensor. There was very good agreement between the sensing results and those measured by nuclear magnetic resonance technique. In the next study, the results from sensor measurements were validated by simulation (Md Yunus and Mukhopadhyay, 2011). Microwave sensors have also been used for phosphorus detection in wastewater treatment industries (Al-Dasoqi et al., 2011).

2.3.2.2 Multiphase flow rate monitoring

Monitoring fluid flow in a dynamic pipeline is an important problem in the oil industry. For managing oil field wells efficiently, the oil industry needs accurate online sensors to monitor the oil, gas, and water flow in the production pipelines (Al-Hajeri et al., 2009). Al-Kizwini et al. (2013) used an electromagnetic wave cavity resonator for a real-time monitoring of multiphase fluid flow in a dynamic pipeline. The percentage volume of each phase (oil or water) was

determined using the resonance frequency shifts, occurring within the resonator. There was good agreement between the theoretical model and the experimental results. Ashton et al. (1994) developed a microwave and gamma-ray multiphase flow meter to measure oil, water and gas flow rates on production pipeline. The oil and water flow rates were determined with errors of 5.4 and 5.9%, respectively.

2.3.2.3 *Gas phase concentration monitoring*

Bernou et al. (2000) developed a gas sensor, using the change in the electromagnetic properties of some sensitive materials in the presence humidity at ultrahigh frequencies. The measurements were in good agreement with the previsions on the detection principle. Moreover, the sensor showed high sensitivity to humidity and good reversibility. de Fonseca et al. (2014) used microwave sensor based on zeolite layers to measure toluene concentration. The developed sensor showed promising possibilities for the detection of toluene concentration lower than 50 ppm. Barochi et al. (2011) used a coplanar grounded wave guide with a gas sensing material to study the sensor sensitivity to ammonia in argon flux. During this study the effect of sensitive material on the response of the microwave sensor, in presence of ammonia gas was investigated. It was found that there is a correlation between ammonia gas concentration and the reflected microwave power (S_{11}).

2.3.2.4 *Residual life of adsorbent monitoring*

Mason et al. (2014) used a microwave cavity resonator to measure the residual lifetime of activated carbon exposed to water vapor. For this purpose they exposed two batches of activated carbon to relative humidity of 80% for 7 months. Two regions in the microwave spectra (7500 and 8595 MHz) were identified to represent similar transmitted signal attenuation: 0.25 dBm/month and 0.35 dBm/month, respectively. For each carbon a calibration curve was

developed to predict its residual life. In another study, it was shown that a resistor-capacitor circuit, connected to a dielectric cavity could be used to measure the capacitance of GAC by monitoring the voltage change across a charging-discharging capacitor. During this study, electrical theory for the time-dependent voltage was used to determine capacitor capacitance from the decay rate of the discharging voltage cycle. It was observed that by increasing the dew point of air blowing on GAC, the capacitance increased as water adsorption increased. Conversely, with decrease of dew point the carbon capacitance decreased.

2.4 References

ÁGUEDA, V. I., CRITTENDEN, B. D., DELGADO, J. A. & TENNISON, S. R. 2011. Effect of channel geometry, degree of activation, relative humidity and temperature on the performance of binderless activated carbon monoliths in the removal of dichloromethane from air. *Separation and Purification Technology,* 78**,** 154-163.

AL-DASOQI, N., MASON, A., ALKHADDAR, R. & AL-SHAMMA'A, A. Use of sensors in wastewater quality monitoring - A review of available technologies. World Environmental and Water Resources Congress 2011: Bearing Knowledge for Sustainability - Proceedings of the 2011 World Environmental and Water Resources Congress, 2011. 3379-3388.

AL-HAJERI, S., WYLIE, S. R., SHAW, A. & AL-SHAMMA'A, A. I. 2009. Real time em waves monitoring system for oil industry three phase flow measurement. *Journal of Physics: Conference Series,* 178.

AL-KIZWINI, M. A., WYLIE, S. R., AL-KHAFAJI, D. A. & AL-SHAMMA'A, A. I. 2013. The monitoring of the two phase flow-annular flow type regime using microwave sensor technique. *Measurement: Journal of the International Measurement Confederation,* 46**,** 45-51.

ÁLVAREZ, P. M., BELTRÁN, F. J., GÓMEZ-SERRANO, V., JARAMILLO, J. & RODRIGUEZ, E. M. 2004. Comparison between thermal and ozone regenerations of spent activated carbon exhausted with phenol. *Water Research,* 38**,** 2155-2165.

ANIA, C. O., MENÉNDEZ, J. A., PARRA, J. B. & PIS, J. J. 2004. Microwave-induced regeneration of activated carbons polluted with phenol. A comparison with conventional thermal regeneration. *Carbon,* 42**,** 1377-1381.

ANIA, C. O., PARRA, J. B., MENÉNDEZ, J. A. & PIS, J. J. 2005. Effect of microwave and conventional regeneration on the microporous and mesoporous network and on the adsorptive capacity of activated carbons. *Microporous and Mesoporous Materials,* 85**,** 7-15.

ANIA, C. O., PARRA, J. B., MENÉNDEZ, J. A. & PIS, J. J. 2007. Microwave-assisted regeneration of activated carbons loaded with pharmaceuticals. *Water Research,* 41**,** 3299-3306.

ASHTON, S. L., CUTMORE, N. G., ROACH, G. J., WATT, J. S., ZASTAWNY, H. W. & MCEWAN, A. J. Development and trial of microwave techniques for measurement of multiphase flow of oil, water and gas. SPE - Asia Pacific Oil & Gas Conference, 1994. 681-689.

BAROCHI, G., ROSSIGNOL, J. & BOUVET, M. 2011. Development of microwave gas sensors. *Sensors and Actuators, B: Chemical,* 157**,** 374-379.

BERNOU, C., REBIÈRE, D. & PISTRÉ, J. 2000. Microwave sensors: a new sensing principle. Application to humidity detection. *Sensors and Actuators, B: Chemical,* 68**,** 88-93.

BOURGEOIS, W., ROMAIN, A. C., NICOLAS, J. & STUETZ, R. M. 2003. The use of sensor arrays for environmental monitoring: Interests and limitations. *Journal of Environmental Monitoring,* 5**,** 852-860.

BRADSHAW, S. M., VAN WYK, E. J. & DE SWARDT, J. B. 1997. Preliminary economic assessment of microwave regeneration of activated carbon for the carbon in pulp process. *Journal of Microwave Power and Electromagnetic Energy,* 32**,** 131-144.

BRADSHAW, S. M., VAN WYK, E. J. & DE SWARDT, J. B. 1998. Microwave heating principles and the application to the regeneration of granular activated carbon. *Journal of The South African Institute of Mining and Metallurgy,* 98**,** 201-210.

BURKHOLDER, H. R., FANSLOW, G. E. & BLUHM, D. D. 1986. Recovery of ethanol from a molecular sieve by using dielectric heating. *Industrial and Engineering Chemistry Fundamentals,* 25**,** 414-416.

ÇALIŞKAN, E., BERMÚDEZ, J. M., PARRA, J. B., MENÉNDEZ, J. A., MAHRAMANLIOĜLU, M. & ANIA, C. O. 2012. Low temperature regeneration of activated carbons using microwaves: Revising conventional wisdom. *Journal of Environmental Management,* 102**,** 134-140.

CHA, C. Y., WALLACE, S., GEORGE, A. H. & ROGERS, S. 2004. Microwave technology for treatment of fume hood exhaust. *Journal of Environmental Engineering,* 130**,** 338-348.

CHANG, S. H., WANG, K. S., LIANG, H. H., CHEN, H. Y., LI, H. C., PENG, T. H., SU, Y. C. & CHANG, C. Y. 2010. Treatment of Reactive Black 5 by combined electrocoagulation-granular activated carbon adsorption-microwave regeneration process. *Journal of Hazardous Materials,* 175**,** 850-857.

CHANG YUL, C. & CARLISLE, C. T. 2001. Microwave process for volatile organic compound abatement. *Journal of the Air and Waste Management Association,* 51**,** 1628-1641.

CHERBAŃSKI, R., KOMOROWSKA-DURKA, M., STEFANIDIS, G. D. & STANKIEWICZ, A. I. 2011. Microwave swing regeneration Vs temperature swing regeneration - Comparison of desorption kinetics. *Industrial and Engineering Chemistry Research,* 50**,** 8632-8644.

CHIANG, Y. C., LEE, C. C. & SU, W. P. 2006. Adsorption behaviors of activated carbons for the exhaust from spray painting booths in vehicle surface coating. *Toxicological and Environmental Chemistry,* 88**,** 453-467.

CLARK, D. F. & SUTTON, W. H. 1994. *Microwave Processing of Materials*, The National Academies Press.

DE FONSECA, B., ROSSIGNOL, J., BEZVERKHYY, I., BELLAT, J. P., STUERGA, D. & PRIBETICH, P. 2014. VOCs Detection by Microwave Transduction Using Zeolites as Sensitive Material. *Procedia Engineering,* 87**,** 1019-1022.

DE JONGE, R. J., BREURE, A. M. & VAN ANDEL, J. G. 1996. Reversibility of adsorption of aromatic compounds onto powdered activated carbon (PAC). *Water Research,* 30**,** 883-892.

DI, P. & CHANG, D. P. Microwave regeneration of volatile organic compounds (VOC) adsorbents. Presented at 89th Annual Conference & Exhibition of A&WMA, Nashville, TN, 1996.

FANG, C. S. & LAI, P. M. C. 1996. Microwave regeneration of spent powder activated carbon. *Chemical Engineering Communications,* 147**,** 17-27.

FERRO-GARCIA, M. A., JOLY, J. P., RIVERA-UTRILLA, J. & MORENO-CASTILLA, C. 1995. Thermal desorption of chlorophenols from activated carbons with different porosity. *Langmuir,* 11**,** 2648-2651.

FERRO-GARCIA, M. A., RIVERA-UTRILLA, J., BAUTISTA-TOLEDO, I. & MORENO-CASTILLA, C. 1996. Chemical and thermal regeneration of an activated carbon saturated with chlorophenols. *Journal of Chemical Technology & Biotechnology,* 67**,** 183-189.

FU, Y., WANG, L. & ZHOU, Z. 2012 Microwave regeneration of field-spent granular activated carbon from power plants. *Advanced Materials Research.*

GAUR, V. & SHANKAR, P. A. 2008. Surface modification of activated Carbon for the Removal of water impurities. *Water Conditioning & Purification*.

GRANT, T. M. & KING, C. J. 1990. Mechanism of irreversible adsorption of phenolic compounds by activated carbons. *Industrial and Engineering Chemistry Research,* 29**,** 264-271.

HARRIOTT, P. & CHENG, A. T.-Y. 1988. KINETICS OF SPENT ACTIVATED CARBON REGENERATION. *AIChE Journal,* 34**,** 1656-1662.

HASHISHO, Z., ROOD, M. & BOTICH, L. 2005. Microwave-swing adsorption to capture and recover vapors from air streams with activated carbon fiber cloth. *Environmental Science and Technology,* 39**,** 6851-6859.

HASHISHO, Z., ROOD, M. J., BAROT, S. & BERNHARD, J. 2009. Role of functional groups on the microwave attenuation and electric resistivity of activated carbon fiber cloth. *Carbon,* 47**,** 1814-1823.

HENNING, K. D., BONGARTZ, W. & DEGEL, J. Adsorptive Recovery of Problematic Solvents. Paper presented at the Meeting of the Nineteenth Biennial Conference on Carbon 1989 Pennsylvania State University, USA.

HUA-SHAN, T. & CHIH-JU, G. J. 1999. Application of granular activated carbon packed-bed reactor in microwave radiation field to treat phenol. *Chemosphere,* 38**,** 2667-2680.

JAHANDAR LASHAKI, M., ATKINSON, J. D., HASHISHO, Z., PHILLIPS, J. H., ANDERSON, J. E., NICHOLS, M. & MISOVSKI, T. 2016. Effect of desorption purge gas oxygen impurity on irreversible adsorption of organic vapors. *Carbon,* 99**,** 310-317.

JONES, D. A., LELYVELD, T. P., MAVROFIDIS, S. D., KINGMAN, S. W. & MILES, N. J. 2002. Microwave heating applications in environmental engineering - A review. *Resources, Conservation and Recycling,* 34**,** 75-90.

JOU, G. C.-J. 1998. Application of activated carbon in a microwave radiation field to treat trichloroethylene. *Carbon,* 36**,** 1643-1648.

KIM, J. H., RYU, Y. K., HAAM, S., LEE, C. H. & KIM, W. S. 2001. Adsorption and steam regeneration of n-hexane, MEK, and toluene on activated carbon fiber. *Separation Science and Technology,* 36**,** 263-281.

KOROSTYNSKA, O., MASON, A. & AL-SHAMMA'A, A. 2012. Monitoring of nitrates and phosphates in wastewater: Current technologies and further challenges. *International Journal on Smart Sensing and Intelligent Systems,* 5**,** 149-176.

KOROSTYNSKA, O., MASON, A. & AL-SHAMMA'A, A. 2014. Microwave sensors for the non-invasive monitoring of industrial and medical applications. *Sensor Review,* 34**,** 182-191.

KUBOTA, M., HANADA, T., YABE, S., KUCHAR, D. & MATSUDA, H. 2011. Water desorption behavior of desiccant rotor under microwave irradiation. *Applied Thermal Engineering,* 31**,** 1482-1486.

LASHAKI, M. J., FAYAZ, M., WANG, H., HASHISHO, Z., PHILIPS, J. H., ANDERSON, J. E. & NICHOLS, M. 2012. Effect of adsorption and regeneration temperature on irreversible adsorption of organic vapors on beaded activated carbon. *Environmental Science and Technology,* 46**,** 4083-4090.

LI, C. & MOE, W. M. 2005. Activated carbon load equalization of discontinuously generated acetone and toluene mixtures treated by biofiltration. *Environmental Science and Technology,* 39**,** 2349-2356.

LI, L., LIU, S. & LIU, J. 2011. Surface modification of coconut shell based activated carbon for the improvement of hydrophobic VOC removal. *Journal of Hazardous Materials,* 192**,** 683-690.

LI, W., WANG, X. & PENG, J. 2013. Effects of microwave heating on porous structure of regenerated powdered activated carbon used in xylose. *Environmental Technology (United Kingdom),* 34**,** 2917-2925.

LIU, P. K. T., FELTCH, S. M. & WAGNER, N. J. 1987. Thermal desorption behavior of aliphatic and aromatic hydrocarbons loaded on activated carbon. *Industrial and Engineering Chemistry Research,* 26**,** 1540-1545.

LIU, X., QUAN, X., BO, L., CHEN, S. & ZHAO, Y. 2004. Simultaneous pentachlorophenol decomposition and granular activated carbon regeneration assisted by microwave irradiation. *Carbon,* 42**,** 415-422.

LU, Q. & SORIAL, G. A. 2004a. Adsorption of phenolics on activated carbon - Impact of pore size and molecular oxygen. *Chemosphere,* 55**,** 671-679.

LU, Q. & SORIAL, G. A. 2007. The effect of functional groups on oligomerization of phenolics on activated carbon. *Journal of Hazardous Materials,* 148**,** 436-445.

LU, Q. & SORIAL, G. A. 2009. A comparative study of multicomponent adsorption of phenolic compounds on GAC and ACFs. *Journal of Hazardous Materials,* 167**,** 89-96.

LU, Q. L. & SORIAL, G. A. 2004b. The role of adsorbent pore size distribution in multicomponent adsorption on activated carbon. *Carbon,* 42**,** 3133-3142.

LUKOMSKAYA, A. Y., TARKOVSKAYA, I. A. & STRELKO, V. V. 1986. Chemisorption of o-xylene on activated carbons. *Theoretical and Experimental Chemistry,* 22**,** 357-360.

LUO, L., RAMIREZ, D., ROOD, M. J., GREVILLOT, G., HAY, K. J. & THURSTON, D. L. 2006. Adsorption and electrothermal desorption of organic vapors using activated carbon adsorbents with novel morphologies. *Carbon,* 44**,** 2715-2723.

MAGNE, P. & WALKER JR, P. L. 1986. Phenol adsorption on activated carbons: Application to the regeneration of activated carbons polluted with phenol. *Carbon,* 24**,** 101-107.

MASON, A., KOROSTYNSKA, O., WYLIE, S. & AL-SHAMMA'A, A. I. 2014. Non-destructive evaluation of an activated carbon using microwaves to determine residual life. *Carbon,* 67**,** 1-9.

MATTSON, J. A., MARK JR, H. B., MALBIN, M. D., WEBER JR, W. J. & CRITTENDEN, J. C. 1969. Surface chemistry of active carbon: Specific adsorption of phenols. *Journal of Colloid and Interface Science,* 31**,** 116-130.

MD YUNUS, M. A. & MUKHOPADHYAY, S. C. 2011. Planar electromagnetic sensor for the detection of nitrate and contamination in natural water sources using electrochemical impedance spectroscopy approach. *Lecture Notes in Electrical Engineering.*

MEIER, M., TURNER, M., VALLEE, S., CONNER, W. C., LEE, K. H. & YNGVESSON, K. S. 2009. Microwave regeneration of zeolites in a 1 meter column. *AIChE Journal,* 55**,** 1906-1913.

MENÉNDEZ, J. A., ARENILLAS, A., FIDALGO, B., FERNÁNDEZ, Y., ZUBIZARRETA, L., CALVO, E. G. & BERMÚDEZ, J. M. 2010. Microwave heating processes involving carbon materials. *Fuel Processing Technology,* 91**,** 1-8.

NIKNADDAF, S., ATKINSON, J. D., SHARIATY, P., LASHAKI, M. J., HASHISHO, Z., PHILIPS, J. H., ANDERSON, J. E. & NICHOLS, M. 2015. Heel Formation during

Volatile Organic Compound Desorption from Activated Carbon Fiber Cloth. *Carbon,* 196, 131-138.

OSEI-TWUM, E. Y., ABUZAID, N. S. & NAHKLA, G. 1996. Carbon-catalyzed oxidative coupling of phenolic compounds. *Bulletin of Environmental Contamination and Toxicology,* 56**,** 513-519.

POLAERT, I., ESTEL, L., HUYGHE, R. & THOMAS, M. 2010. Adsorbents regeneration under microwave irradiation for dehydration and volatile organic compounds gas treatment. *Chemical Engineering Journal,* 162**,** 941-948.

POLAERT, I., LEDOUX, A., ESTEL, L., HUYGHE, R. & THOMAS, M. 2007. Microwave assisted regeneration of zeolite. *International Journal of Chemical Reactor Engineering,* 5.

POPESCU, M., JOLY, J. P., CARRÉ, J. & DANATOIU, C. 2003. Dynamical adsorption and temperature-programmed desorption of VOCs (toluene, butyl acetate and butanol) on activated carbons. *Carbon,* 41**,** 739-748.

PRICE, D. W. & SCHMIDT, P. S. 1998a. VOC recovery through microwave regeneration of adsorbents: Comparative economic feasibility studies. *Journal of the Air and Waste Management Association,* 48**,** 1146-1155.

PRICE, D. W. & SCHMIDT, P. S. 1998b. VOC recovery through microwave regeneration of adsorbents: Process design studies. *Journal of the Air and Waste Management Association,* 48**,** 1135-1145.

QUAN, X., LIU, X., BO, L., CHEN, S., ZHAO, Y. & CUI, X. 2004. Regeneration of acid orange 7-exhausted granular activated carbons with microwave irradiation. *Water Research,* 38**,** 4484-4490.

REUß, J., BATHEN, D. & SCHMIDT-TRAUB, H. 2002. Desorption by microwaves: Mechanisms of multicomponent mixtures. *Chemical Engineering and Technology,* 25**,** 381-384.

ROBERS, A., FIGURA, M., THIESEN, P. H. & NIEMEYER, B. 2005. Desorption of odor-active compounds by microwaves, ultrasound, and water. *AIChE Journal,* 51**,** 502-510.

ROUSSY, G., ZOULALIAN, A., CHARREYRE, M. & THIEBAUT, J. M. 1984. How microwaves dehydrate zeolites. *The Journal of Physical Chemistry,* 88**,** 5702-5708.

RUDLING, J. & BJÖRKHOLM, E. 1987. Irreversibility effects in liquid desorption of organic solvents from activated carbon. *Journal of Chromatography A,* 392**,** 239-248.

SCHNELLE, K. B. J. & BROWN, C. A. 2002. Air pollution control technology handbook.

SHEN, W., LI, Z. & LIU, Y. 2008. Surface Chemical Functional Groups Modification of Porous Carbon. *Recent Patents on Chemical Engineering,* 1**,** 27-40.

SUZUKI, M., MISIC, D. M., KOYAMA, O. & KAWAZOE, K. 1978. Study of thermal regeneration of spent activated carbons: Thermogravimetric measurement of various single component organics loaded on activated carbons. *Chemical Engineering Science,* 33**,** 271-279.

TAI, H. S. & LEE, C. L. 2007. Desorption of methy-ethyl-ketone from granular activated carbon with microwave radiation. *Environmental Progress,* 26**,** 299-303.

TURNER, M. D., LAURENCE, R. L., CONNER, W. C. & YNGVESSON, K. S. 2000. Microwave radiation's influence on sorption and competitive sorption in zeolites. *AIChE Journal,* 46**,** 758-768.

WEISSENBERGER, A. P. & SCHMIDT, P. S. 1994. Microwave Enhanced Regeneration of Adsorbents. *MRS Proceedings,* 347.

XIN-HUI, D., SRINIVASAKANNAN, C., QU, W. W., XIN, W., JIN-HUI, P. & LI-BO, Z. 2012. Regeneration of microwave assisted spent activated carbon: Process optimization, adsorption isotherms and kinetics. *Chemical Engineering and Processing: Process Intensification,* 53**,** 53-62.

YUNUS, M. A. M. & MUKHOPADHYAY, S. C. 2011. Novel planar electromagnetic sensors for detection of nitrates and contamination in natural water sources. *IEEE Sensors Journal,* 11**,** 1440-1447.

ZARIFI, M. H., FAYAZ, M., GOLDTHORP, J., ABDOLRAZZAGHI, M., HASHISHO, Z. & DANESHMAND, M. 2015. Microbead-assisted high resolution microwave planar ring resonator for organic-vapor sensing. *Applied Physics Letters,* 106.

CHAPTER 3. ACCUMULATION OF ADSORBED ORGANIC VAPORS FROM AUTOMOBILE PAINTING OPERATIONS ON BEAD ACTIVATED CARBON

3.1 Introduction

Adsorption is widely used for controlling volatile organic compounds (VOCs) typically produced during automobile painting operation (Chatzopoulos et al., 1993). After adsorption the loaded adsorbent should be regenerated to recover adsorption capacity of adsorbent and reuse the adsorbent for the subsequent adsorption regeneration cycles. The accumulation of non-desorbed adsorbate in the pores, known as heel formation, reduces adsorption capacity of adsorbent and increased the operational cost of capturing VOCs (Lashaki et al., 2012).

Adsorption can be divided into physical adsorption and chemical adsorption or chemisorption. In physical adsorption, physical forces such as Van der Waals' force and interaction between adsorbate molecules and adsorbent surface are responsible for the process. Typically, physical adsorption can occur at temperatures lower than chemisorption. In chemisorption adsorbate molecules chemically react on the adsorbent surface and chemical bonds between those molecules and adsorbent are formed. Both physical adsorption and chemisorption are exothermic processes. Due to the formation of chemical bonds, the heat of adsorption in chemisorption is high and close to the heat of formation of chemical bonds. So, adsorption heat in chemisorption is higher than the one for physical adsorption (Lowell and Shields, 1991). In contrast to physical adsorption, chemisorption is difficult to reverse which results in the decrease in the adsorption capacity of the adsorbent. Chemisorption is caused or resulted by two mechanisms: formation of permanent bond between adsorbate molecules and

adsorbent surface, and chemical conversion of adsorbate molecules through chemical reactions catalyzed by adsorbent surface (Chatzopoulos et al., 1993). Activated carbon adsorption can be specified by parameters such as specific surface area, pore structure, and surface chemical functional group (Gaur and Shankar, 2008). Typically, surface functional groups can be formed during activation process, heat treatment, and post activation chemical treatment. They can also be derived from precursor material. There are some parameters by which the surface area and pore structure of porous carbon can be controlled: activation conditions (activation agent, temperature and time), and template and precursor materials. The surface functional groups are formed by heteroatoms (specifically oxygen, nitrogen, hydrogen and halogen). Those atoms are bonded to the edge of the carbon layers. Some of the functional groups which provide catalytic characteristics of activated carbon and found on activated carbon are oxygen-containing functional groups or surface oxides.

Functional groups such as carbonyl, carboxyl, phenolic, hydroxyl, lactone and quinine can be included in acidic surface functional groups. On the other hand, chromene and pyrone-like groups are typically considered as basic functional groups (Tamon and Okazaki, 1996). There are several methods by which surface functional groups can be identified: neutralization and titration reaction, thermal desorption, and infrared spectroscopy (Bansal and Goyal, 2005).

There are different factors that might affect the chemisorption intensity. One of the studies showed that during regeneration of phenolic compounds, higher temperatures favor chemisorption. In this example, the activation energy needed for the adsorbate-adsorbent complex to be formed can be provided (Schnelle and Brown, 2002). Álvarez et al. (2004) found that thermal regeneration under an oxidizing atmosphere such as carbon dioxide is more efficient than under an inert atmosphere such as nitrogen. According to several studies, the presence of

molecular oxygen improves oxidative coupling and consequently increases irreversible adsorption of organic compounds onto activated carbon (Chatzopoulos et al., 1993, De Jonge et al., 1996, Henning et al., 1989). Henning et al. (1989) showed that when adsorption is completed at a higher temperature, the level of chemisorption increases. On the other hand, adsorbate characteristics can be effective in chemisorption. Studies have shown that phenol and some other aromatic compounds irreversibly adsorb on activated carbon.

Since heel buildup, which could be formed due to chemisorption or physisorption, decreases the adsorption capacity of adsorbent, it reduces regeneration productivity which is undesirable. The hypothesis of this study is that VOCs with higher boiling points and molecular weights have larger contribution to heel formation. In this paper, several organic compounds commonly generated during automobile painting operation were screened for heel buildup, by conducting 5 consecutive adsorption/regeneration cycles.

3.2 Experimental

3.2.1 Adsorbent and adsorbates

The adsorbent used in this research was microporous beaded activated carbon (BAC) (Kureha Corporation). The BAC adsorbent has a mean diameter of 0.71 mm with a narrow particle size distribution (99.5% of the beads have diameter between 0.60 and 0.84 mm). The Brunauer Emmett Teller (BET) surface area, total pore volume, and micropore volume of the BAC were 1371 m^2/g, 0.55 cm^3/g, and 0.50 cm^3/g, respectively. These properties were determined by a micropore surface analysis system (IQ2MP, Quantachrome) with nitrogen testing gas at 77 K. Before starting adsorption experiments, BAC was dried using a laboratory oven at 150 °C for 24 h and then stored in a desiccator. The adsorbates used in this study as well as their physical properties and molecular structures are listed in Table 3-1.

3.2.2 Experimental setup

All adsorption and regeneration cycles for each adsorbate were completed in a stainless steel adsorption tube. The outer diameter of the adsorption tube was 1.90 cmand its length was 15.24 cm. The adsorption tube was filled with BAC.

To provide organic vapor for the adsorption test, a syringe pump (KD Scientific) was used to inject liquid into a stream of dry air. The flow rate of air was controlled with a 0-20 standard liter per minute (SLPM) mass flow controller (Alicat Scientific). Typically, the flow rate of air used in adsorption tests was set at 10 SLMP and the flow rate of nitrogen used in regeneration tests was set at 1 SLPM. Based on the density of the organic solvent and air flow rate, the inlet concentration of organic vapor entering the adsorption tube was determined. The gas detection system consisted of a photoionization detector (PID, Minirae 2000, Rae Systems), which was calibrated before each test using the adsorbate stream generated with the vapor generation system. Before starting adsorption the inlet concentration was measured using a PID to make sure the inlet concentration is equal to the desired concentration.

During all adsorption experiments, the concentration at the adsorption tube outlet was measured by PID. The outlet concentration for high boiling point compounds was measured intermittently to avoid condensation of the adsorbate inside the PID.

After reaching saturation, adsorption was stopped and regeneration was started. During electrothermal regeneration, a heating tape (Omega) was wrapped around the adsorption tube. In order to prevent heat loss during the regeneration experiment, an insulator tape was wrapped around the heating tape. During initial experiments heating rate was controlled by a variac (Staco), while for other tests a data acquisition and control (DAC) system consisted of a Labview program (National Instruments) and a data logger (National Instruments, Compact DAQ)

equipped with an analog input and output module used for controlling the temperature. During regeneration, DAC recorded the regeneration temperature measured by a 1/16" (i.e., 0.16 mm) outer diameter thermocouple type K and controlled the temperature by changing the applied power rate. Also, a mass flow controller (Alicat Scientific) was used to provide a 1 SLPM of nitrogen stream in order to purge oxygen from the adsorption tube. The regeneration tests were completed at 288 ºC. Figure 3-1 illustrates a simple sketch of the setup.
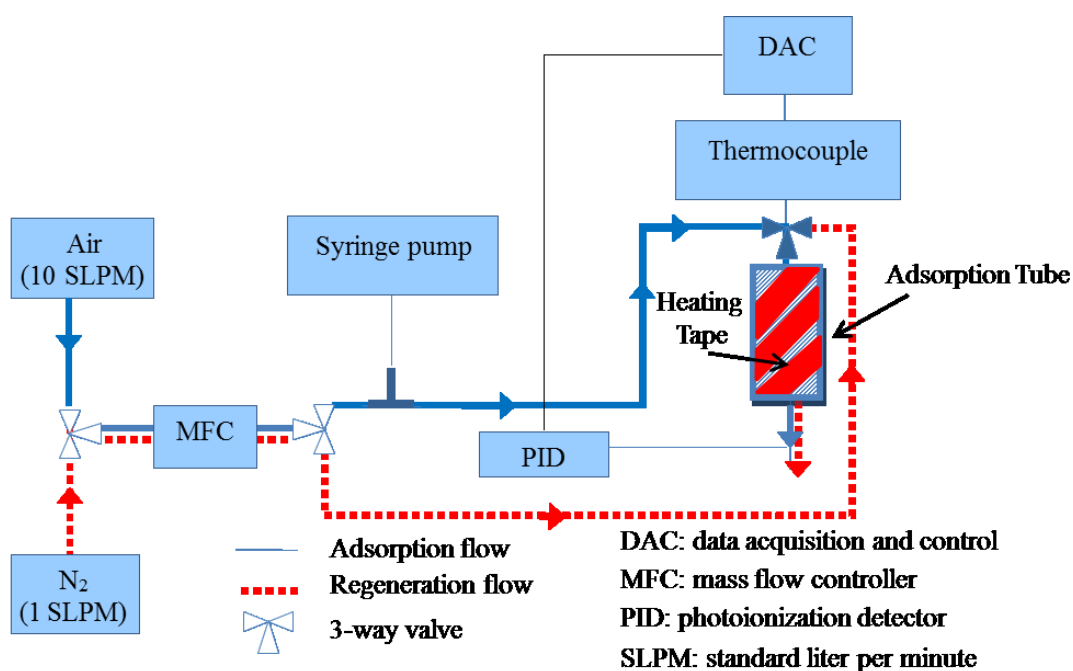
Figure 3-1 Diagram of the adsorption /regeneration setups

3.2.2.1 *Methodology*

During calibration, organic vapor bypassed the adsorption tube till it reached the desired and steady concentration. At this point, the gas stream was directed into the adsorption tube and adsorption started. The outlet concentration was constantly measured till it reached the inlet concentration value. At this point, adsorption was completed since the BAC inside the adsorption

tube had reached saturation. After BAC saturation, adsorption capacity was determined using Equation (1).

$$\text{Adsorption capacity (g/g)} = \frac{W_{AA} - W_{BA}}{W_{BA}} \quad \text{Eq. (1)}$$

where W_{AA} is the BAC weight after adsorption, and W_{BA} is the BAC weight before adsorption.

Typically each adsorption tube went through 5 consecutive adsorption and regeneration cycles. The regenerated carbon was then used for the next adsorption cycle of the same adsorbate.

At the end of the last regeneration cycle, cumulative heel percentage on the BAC was calculated using Equation (2):

$$\text{Cumulative heel percentage (\%)} = \frac{W_{AR} - W_{BA}}{W_{BA}} \times 100 \quad \text{Eq. (2)}$$
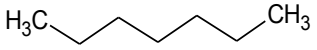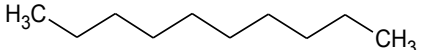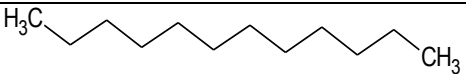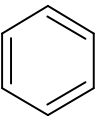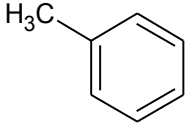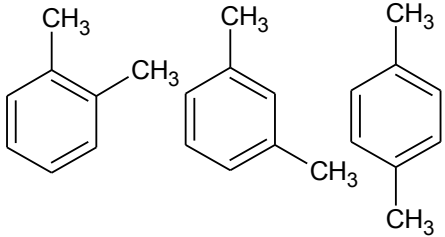
where W_{AR} is the BAC weight after last cycle regeneration, and W_{BA} is the BAC weight before the first cycle adsorption.
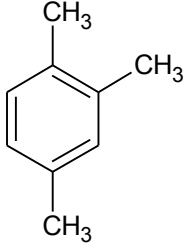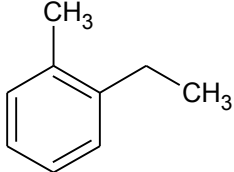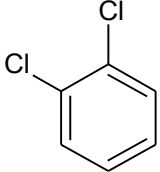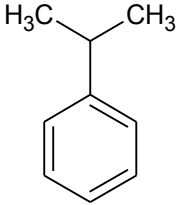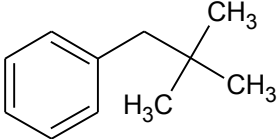
To investigate if adsorption of air on BAC has any contribution in heel formation, 5 consecutive adsorption/regeneration cycles were performed on BAC using pure air containing no VOC. It was observed that no heel was produced over the cycles. Therefore air has no contribution in heel formation. As it can be seen in Table 3-1, the 2,2,4-Trimethyl-1,3-Pentaediol Diisobutyrate (TXIB) and both of the amine compounds have very low vapor pressure; hence producing the organic vapors of those compounds at room temperature was not feasible. Therefore, they were dissolved in tetrahydrofuran (THF) which has very high vapor pressure. According to the Table 3-1, THF provided no heel so all provided heel by those binary mixtures could be attributed to the other compound. The total concentration of all binary mixtures was 500 ppm and the concentration of heavier compounds in each of them was 45 ppm.
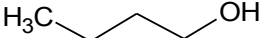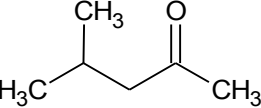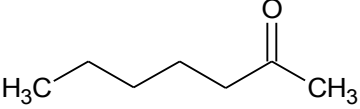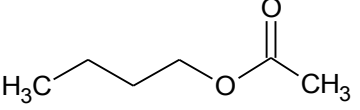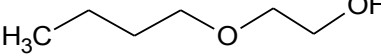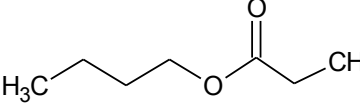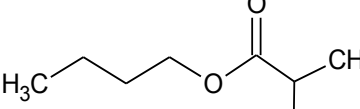
3.3 Results and Discussion

Table 3-1 lists the physical properties of each adsorbate (i.e., molecular weight, boiling point and vapor pressure) as well as the cumulative heel depicted by each compound after 5 successive adsorption and regeneration cycles. The adsorbates are categorized in five groups: aliphatic hydrocarbons, benzene and alkyl benzene, oxygenated compounds, polyaromatic hydrocarbons and amines.

Table 3-1: Physical properties and the cumulative heel percentage of adsorbates

Name	Structure	Molecular weight (g/mol)	Boiling point (°C)	Vapor pressure (mmHg)	Inlet Concentration (ppm$_v$)	Cumulative Heel (%)
n-Heptane		100	99	45	1,610	-0.4
Decane		142	174	1.3	791	1.2
Dodecane		170	216	0.1	100	5.0
Benzene		78	80	95	500	0.1
Toluene		92	110	28	500	0.3
Xylene		106	138	8.3	1,900	0.3

Name	Structure	Molecular weight (g/mol)	Boiling point (°C)	Vapor pressure (mmHg)	Inlet Concentration (ppm$_v$)	Cumulative Heel (%)
1,2,4-Trimethyl benzene		120	170	2.0	500	1.1
1-Ethyl-2-Methylbenzene		120	165	2.9	583	2.1
Dichlrobenzene		147	174	1.8	500	-0.4
Isopropylbenzene		120	152	4.6	600	-0.1
2,2-Dimethyl-Propylbenzene		148	186	0.3	500	1.4

Name	Structure	Molecular weight (g/mol)	Boiling point (°C)	Vapor pressure (mmHg)	Inlet Concentration (ppm$_v$)	Cumulative Heel (%)
n-Butanol		74	117	6.2	1,800	-0.2
Methylisobutylketone		100	117	20.1	1,900	-0.3
2-Heptanone		114	151	2.9	490	0
n-Butyl Acetate		116	126	11.2	1,800	-0.7
Tetrahydrofuran		72	66	162	1,900	-0.1
2-butoxyethanol		118	171	0.8	520	-0.1
Propanoic acid		130	145	4.2	1,125	-0.3
Butyl Isobutyrate		144	155	2.9	1,000	-0.1

Name	Structure	Molecular weight (g/mol)	Boiling point (°C)	Vapor pressure (mmHg)	Inlet Concentration (ppm$_v$)	Cumulative Heel (%)
2,2,4-Trimethyl-1,3-Pentaediol Diisobutyrate (dissolved in THF)		286	280	0.0	500	15.6
Indan		116	176	1.5	500	1.4
Diethanolamine (dissolved in THF)		105	269	0.0	500	3.1
Methyldiethanolamine (dissolved in THF)		119	247	0.0	500	3.4

Figure 3-2 and Figure 3-3 depict the variation of cumulative heel buildup on the BAC with the boiling point and molecular weight of the adsorbates. In general, as the boiling point and molecular weight increase, the level of heel buildup on the BAC increases. While previous research indicated that compounds with oxygen functional groups can increase irreversible adsorption, it was observed that other than TXIB, which has very low vapor pressure, no heel buildup depicted by other oxygenated compounds (Rudling and Björkholm, 1987). The results are consistent with previous reports that adsorbates with molecular weights higher than 130 g/mole cannot be easily desorbed (EPA, 1993).
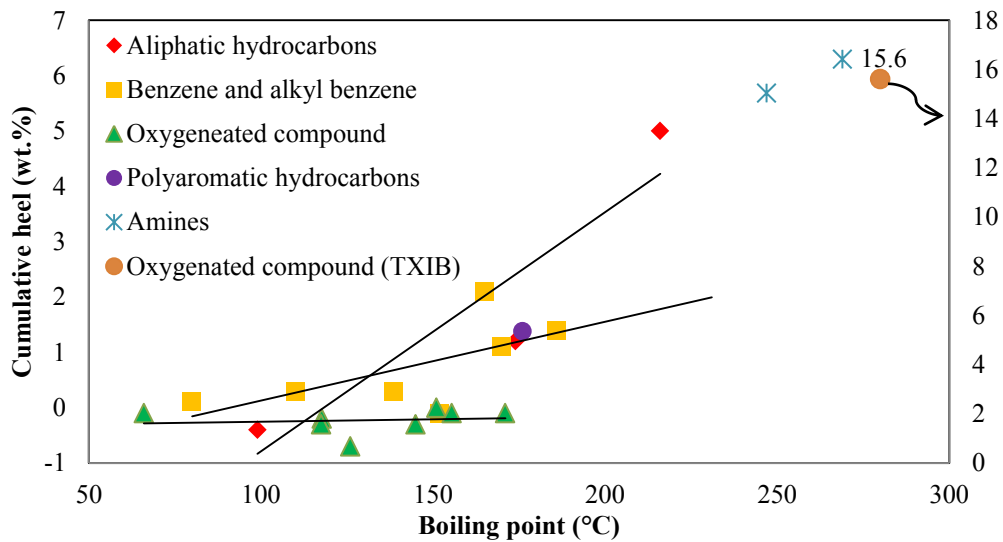
Figure 3-2 Variations of cumulative heel percentage with boiling point of adsorbates
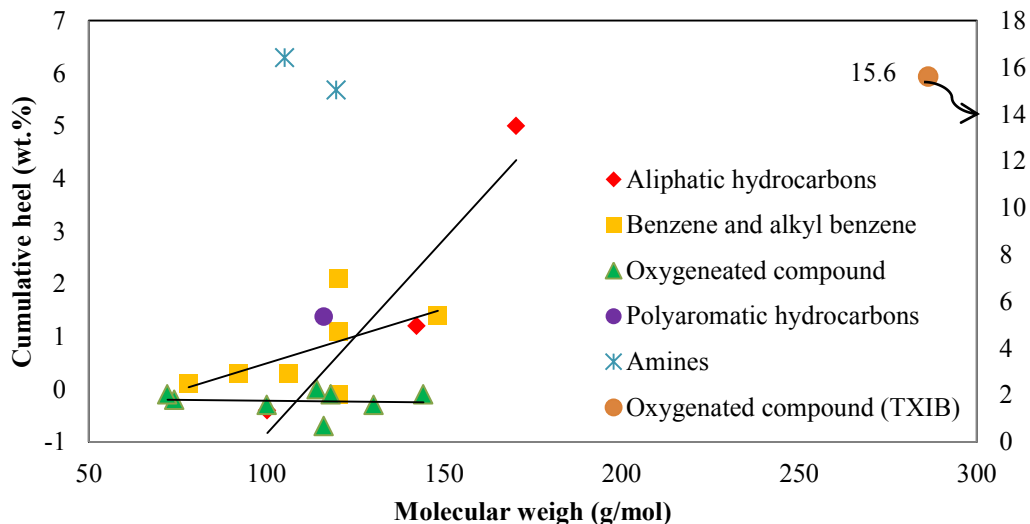
Figure 3-3 Variations of cumulative heel percentage with molecular weight of adsorbates

Vapor pressures for all compounds were calculated using the Antoine equation. Compounds with lower vapor pressure tend to stay in the liquid phase and are more difficult to desorb than compounds with higher vapor pressure. Figure 3-4 illustrates the cumulative heel percentage versus the vapor pressure of adsorbates. According to Figure 3-4, as vapor pressure increased, the cumulative heel buildup dramatically decreased. Adsorbates with very low vapor pressure, such as diethanolamine and methyldiethanolamine, showed a significant heel buildup. The negligible vapor pressure for TXIB is consistent with the a significant heel buildup (15.6 wt.%).
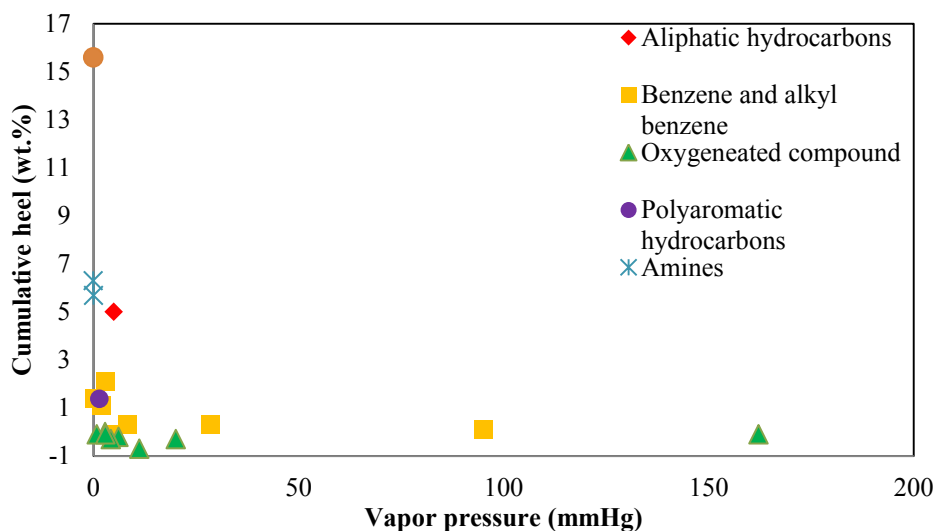
Figure 3-4 Variations of cumulative heel percentage versus with vapor pressure of adsorbates

According to several studies, phenolics and some other aromatic compounds (e.g., o-cresol) irreversibly adsorb onto activated carbon (De Jonge et al., 1996, Ferro-Garca et al., 1995, Grant and King, 1990, Lu and Sorial, 2007, Lu and Sorial, 2009, Vidic et al., 1994). In fact phenolic compounds irreversibly react with surface functional groups on activated carbon (Grant and King, 1990). Surface functional groups catalyze this irreversible process called oligomerization (Lu and Sorial, 2009). According to X-ray photoelectron spectroscopy (XPS) analysis of virgin and used bead activated carbon, some surface functional groups were detected (e.g. C-O, O-C=O, C=O, O-H, C-O-C, O-C=O). In this case, chemisoprtion can be expected. During the oligomerization process, phenolic compounds lose one proton and transfer phenoxy radicals. After coupling those radicals, dimmers and trimmers are formed. One of the major factors which play an important role in oligomerization is the critical oxidation potential (COP). It shows the tendency of adsorbate to react on activated carbon through oxidative coupling. So the presence of electron donating groups such as methyl and ethyl on the aromatic molecule; improves the oxidative coupling process (Osei-Twum et al.,

1996). In Table 3-1, it can be observed that toluene and xylene with one and two methyl groups, respectively, have lower cumulative heel than 1,2,4-trimethyl benzene (TMB). TMB has three methyl groups which causes it to have more cumulative heel. The presence of one ethyl and one methyl group results in higher cumulative heel. However for pentamethylbenzene with five methyl groups, the cumulative heel is the highest. As the number of electron donating group increases, the amount of cumulative heel increases. This trend is shown in Figure 3-5.
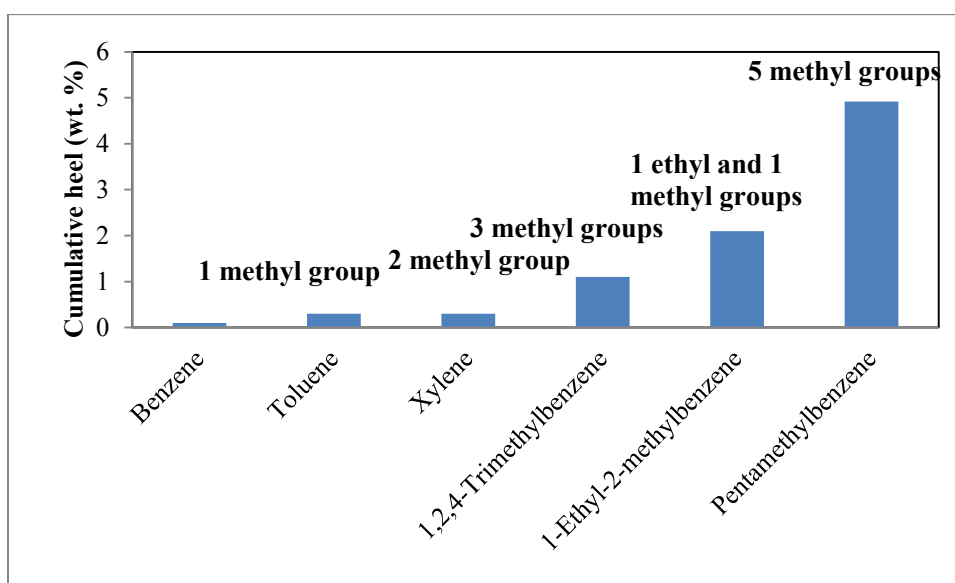
Figure 3-5 : Cumulative heel percentage for four aromatic compounds

It has been observed that adsorbate with molecular weights higher than 130 g/mole cannot be easily desorbed (EPA, 1993). In the aliphatic group, n-dodecane, having a relatively high boiling point produced more heel. Except for TXIB, other oxygenated compounds are light, have low boiling point and depicted low buildup of heel after going through several cycles. TXIB has a very high molecular weight and boiling point, and depicted high heel buildup. Moreover, the relatively high heel values for amine compounds (e.g., diethanolamine and methyldiethanolamine) can be attributed to their high molecular weights and boiling

points. Furthermore both of these compounds have low vapor pressure. Therefore a significant heel buildup for those chemicals is reasonable or predictable.

3.4 Conclusions

Incomplete desorption of several adsorbed adsorbates commonly found in painting booths have been studied through consecutive adsorption and regeneration tests. For benzene and alkyl benzene groups, it was observed that molecules with more electron donating groups have higher amount of heel buildup. The results indicated that the levels of heel buildup for compounds with higher boiling points are substantially high. Except for TXIB, the rest of the tested oxygenated compounds have low molecular weight and boiling point and depicted small buildup of heel. Amine compounds such as diethanolamine and methyl diethanol amine have high molecular weight and boiling point. Additionally, both of them are very viscous which means that producing significant heel was expected. These results are in agreement with the hypothesis proposed in this study that VOCs with higher boiling points have larger contribution to heel formation.

3.5   References

ÁLVAREZ, P. M., BELTRÁN, F. J., GÓMEZ-SERRANO, V., JARAMILLO, J. & RODRIGUEZ, E. M. 2004. Comparison between thermal and ozone regenerations of spent activated carbon exhausted with phenol. *Water Research,* 38**,** 2155-2165.

BANSAL, R. C. & GOYAL, M. 2005. *Activated carbon adsorption,* Boca Raton, Taylor & Francis.

CHATZOPOULOS, D., VARMA, A. & IRVINE, R. L. 1993. Activated carbon adsorption and desorption of toluene in the aqueous phase. *AIChE Journal,* 39**,** 2027-2041.

CHIANG, Y. C., LEE, C. C. & SU, W. P. 2006. Adsorption behaviors of activated carbons for the exhaust from spray painting booths in vehicle surface coating. *Toxicological and Environmental Chemistry,* 88**,** 453-467.

DE JONGE, R. J., BREURE, A. M. & VAN ANDEL, J. G. 1996. Reversibility of adsorption of aromatic compounds onto powdered activated carbon (PAC). *Water Research,* 30**,** 883-892.

EPA, U. 1993. Control of Volatile Organic Compound Emissions from Reactor Processes and Distillation Operations Processes in the Synthetic Organic Chemical Manufacturing Industry. *Guideline series*.

FERRO-GARCA, M. A., JOLY, J. P., RIVERA-UTRILLA, J. & MORENO-CASTILLA, C. 1995. Thermal desorption of chlorophenols from activated carbons with different porosity. *Langmuir,* 11**,** 2648-2651.

GAUR, V. & SHANKAR, P. A. 2008. Surface modification of activated Carbon for the Removal of water impurities. *Water conditioning and purification*.

GRANT, T. M. & KING, C. J. 1990. Mechanism of irreversible adsorption of phenolic compounds by activated carbons. *Industrial and Engineering Chemistry Research,* 29**,** 264-271.

HENNING, K. D., BONGARTZ, W. & DEGEL, J. Adsorptive Recovery of Problematic Solvents. Paper presented at the Meeting of the Nineteenth Biennial Conference on Carbon 1989 Pennsylvania State University, USA.

LASHAKI, M. J., FAYAZ, M., WANG, H., HASHISHO, Z., PHILIPS, J. H., ANDERSON, J. E. & NICHOLS, M. 2012. Effect of adsorption and regeneration temperature on

irreversible adsorption of organic vapors on beaded activated carbon. *Environmental Science & Technology,* 46, 4083-4090.

LOWELL, S. & SHIELDS, J. E. 1991. *Powder surface area and porosity,* London ; New York, Chapman & Hall.

LU, Q. & SORIAL, G. A. 2007. The effect of functional groups on oligomerization of phenolics on activated carbon. *Journal of Hazardous Materials,* 148**,** 436-445.

LU, Q. & SORIAL, G. A. 2009. A comparative study of multicomponent adsorption of phenolic compounds on GAC and ACFs. *Journal of Hazardous Materials,* 167**,** 89-96.

OSEI-TWUM, E. Y., ABUZAID, N. S. & NAHKLA, G. 1996. Carbon-catalyzed oxidative coupling of phenolic compounds. *Bulletin of Environmental Contamination and Toxicology,* 56**,** 513-519.

SCHNELLE, K. B. J. & BROWN, C. A. 2002. Air pollution control technology handbook.

TAMON, H. & OKAZAKI, M. 1996. Influence of acidic surface oxides of activated carbon on gas adsorption characteristics. *Carbon,* 34**,** 741-746.

CHAPTER 4. USING MICROWAVE HEATING TO IMPROVE THE DESORPTION EFFICIENCY OF HIGH MOLECULAR WEIGHT VOC FROM BAC [1]

4.1 Introduction

Adsorption with activated carbon is widely applied for controlling low concentration volatile organic compounds (VOCs) because it is cost-effective and has high removal efficiency (Lashaki et al., 2012). Typically, adsorption is followed by regeneration to allow for adsorbent reuse and adsorbate recovery or concentration (Weissenberger and Schmidt, 1994). One associated challenge is heel buildup which is defined as non-desorbed adsorbate remained in adsorbent pores after regeneration. Heel buildup decreases the working capacity and lifespan of the adsorbent. For gas phase adsorption applications, VOC molecules can be retained on the adsorbent through chemisorption or strong physisorption (Popescu et al., 2003).

Previous studies showed that regeneration conditions and heating method can impact heel buildup on activated carbon (Lashaki et al., 2012). Conductive heating, hot gas purging, or steam heating are typically used to regenerate adsorbents. Drawbacks associated with these techniques include long duration, high energy consumption due to heat losses (to surrounding equipment, adsorbent, and concentrated VOC gas stream), and potential changes to the

---

adsorbent's physical and chemical properties (Ania et al., 2004, Ania et al., 2005, Burkholder et al., 1986, Cherbański and Molga, 2009, Cherbański et al., 2011, Di and Chang, 1996).

Microwave heating provides volumetric heating (Cherbański et al., 2011, Di and Chang, 1996), fast heating rates (Jones et al., 2002), no contact between heating source and adsorbent (Hua-Shan and Chih-Ju, 1999, Jones et al., 2002), and selective heating (Weissenberger and Schmidt, 1994). The performance of microwave heating regeneration depends on dielectric properties of adsorbent/adsorbate. Dielectric properties of materials include dielectric constant (ε'), which describes a material's ability to be polarized by an electromagnetic field, and loss factor (ε"), which describes a material's ability to convert absorbed energy into heat (Cherbański and Molga, 2009). Activated carbon with high dielectric properties can be effectively heated by microwaves since delocalized π electrons allow for high microwave absorbance and correspondingly fast heating rates (Çalışkan et al., 2012, Hashisho et al., 2009). These advantages indicate that microwave heating requires lower energy consumption compared to conventional heating techniques. Furthermore, for microwave heating, mass and heat transfer can proceed in the same direction to improve desorption efficiencies (Ania et al., 2004, Ania et al., 2005, Bouraoui, 1991, Legras et al., 2012, Miura et al., 2004). Direct adsorbate heating by microwaves may further improve desorption efficiency and decrease desorption diffusion resistance (Di and Chang, 1996).

Optimal regeneration techniques allow for complete recovery of adsorption capacity, require low energy consumption and short regeneration times, cause negligible changes to the adsorbent's physical/chemical properties, and do not adversely affect the adsorbate. Ania et al (Ania et al., 2004) compared the performance of microwave and conductive heating for regenerating activated carbon loaded with phenol (aqueous phase). Because phenol

oligomerization necessitates the use of high regeneration temperatures, the authors consistently experienced pore blockage and corresponding decreases in adsorption capacity during subsequent use, attributed to phenol decomposition during regeneration. For gas phase studies, non-destructive regeneration using microwave heating has been shown, but only for low molecular weight, low boiling point adsorbates (e.g., methane, ethane, ethylene, methyl ethyl ketone, water) (Burkholder et al., 1986, Coss and Cha, 2000, Hashisho et al., 2007, Hashisho et al., 2008, Hashisho et al., 2005, Price and Schmidt, 1997, Robers et al., 2005). For many industrial applications, however, heavy compounds (e.g., n-dodecane, ethylbenzene, and 1,2,4-trimethylbenzene) are present in the gaseous VOC mixtures and often have high affinity for the adsorbent, requiring more intense regeneration conditions (i.e., higher temperature, longer times) for complete regeneration (Demir and Saral, 2013). It would be beneficial to evaluate whether microwave regeneration can be similarly efficient and non-destructive when desorbing high molecular weight, high boiling point contaminants. Current information available in the literature describing high boiling point VOC regeneration from activated carbon uses hot air regeneration or solvent extraction techniques, but microwave regeneration has not been reported (Fabrizi et al., 2013, Popescu et al., 2003).

The hypothesis of this study is that microwave heating is able to regenerate an adsorbent loaded with a high boiling point VOC in an energy-efficient and non-destructive way. The objective of this research, therefore, is to demonstrate the performance of microwave heating for regenerating activated carbon loaded with a high boiling point and low loss tangent VOC. Accordingly, n-dodecane, a nonpolar VOC with high boiling point (216 $^{\circ}$C), was used as the test adsorbate (Hsieh et al., 2012). The absence of functional groups negates chemisorption. The non-polarity of n-dodecane suggests low microwave absorption

and is used as a challenge for microwave regeneration (Reuß et al., 2002). Although n-dodecane has a high molecular weight (170 g/mol), its small kinetic diameter (4.3 Å) permits penetration into micropores (Breck, 1974). This creates a challenging scenario in which a heavy compound with a high boiling point must be desorbed from narrow, high energy micropores. In this case, heel buildup can only be attributed to diffusive mass transfer resistance, particularly in micropores with pore size close to the kinetic diameter of n-dodecane (Rodrı´guez-Mirasol et al., 2005). Regeneration of carbon adsorbents loaded with n-dodecane is accomplished using microwave heating, and the desorption efficiency, energy consumption, and adsorbent/adsorbate properties are monitored. These results are compared with a more conventional heating technique, conductive heating, to benchmark the performance of microwave regeneration. Results presented herein are expected to expand the industrial relevance of microwave heating to use with high boiling point contaminants.

4.2 Experimental

4.2.1 Adsorbent and adsorbate

The adsorbent used was microporous beaded activated carbon (BAC, Kureha Corporation). The BAC has a mean particle diameter of 0.71 mm with a narrow particle size distribution (99.5% of the beads have diameter between 0.60 and 0.84 mm) (Lashaki et al., 2012). Bulk and particle density of BAC are 606 and 982 kg/m^3, respectively. Complete physical properties of the BAC can be found elsewhere (Tefera et al., 2013). Before adsorption experiments, BAC was dried in air at 150 °C for 24 h and then stored in a desiccator.

n-dodecane (99%, Acros Organics) was used as the adsorbate for all tests described herein, except for blanks tests. Five-cycle adsorption-desorption blank tests were completed

under the same conditions and duration described below except no adsorbate was injected during the adsorption cycles.

4.2.2   Experimental setup and methods

4.2.2.1   Adsorption

The adsorption setup consisted of an adsorption tube, adsorbate vapor generation system, gas detection system, and data acquisition and control (DAC) system (Figure 4-1). The tube was made of quartz (2.2 cm inner diameter, 35.6 cm length) for microwave heating regeneration and stainless steel (2.1 cm inner diameter, 15 cm length) for conductive heating regeneration. Note that different adsorption tube materials were used to allow the lowest energy requirement for each regeneration technique. Each was filled with 5.3 ± 0.1 g of dry, virgin BAC resulting in a bed height of approximately 2.5 cm. For the quartz tube, a fritted glass disk held the BAC bed in place. For the stainless steel tube, glass-wool was used at the top and bottom of the adsorbent bed to retain the BAC. The adsorbate vapor generation system consisted of a syringe pump (KD Scientific, KDS-220) that injected liquid n-dodecane into a dry, 10 standard liter per minute (SLPM, measured at 25 °C and 1 atm) air stream to achieve a concentration of 100 ppm$_v$. The air flow rate was set using a mass flow controller (Alicat Scientific). The gas detection system consisted of a photoionization detector (PID, Minirae 2000, Rae Systems), which was calibrated before each test using the adsorbate stream generated with the vapor generation system. Before starting adsorption the inlet concentration was measured by PID to make sure the inlet concentration is equal to the desired concentration. Moreover, during adsorption PID monitored VOC concentration at the tube's outlet. When the outlet concentration matched the inlet concentration, the adsorbent was considered to be saturated with the adsorbate. The BAC was fully loaded during all

adsorption experiments, requiring 440 min of exposure to the 10 SLPM, 100 ppm$_v$ gas stream. The DAC system consisted of a LabVIEW program (National Instruments) and a data logger (National Instruments, Compact DAC) equipped with analog input and output modules for recording temperature and outlet VOC concentration. After BAC saturation, adsorption capacity was determined using Equation (1).

$$\text{Adsorption capacity (g/g)} = \frac{W_{AA} - W_{BA}}{W_{BA}} \quad \text{Eq. (1)}$$

where W_{AA} is the BAC weight after adsorption, and W_{BA} is the BAC weight before adsorption
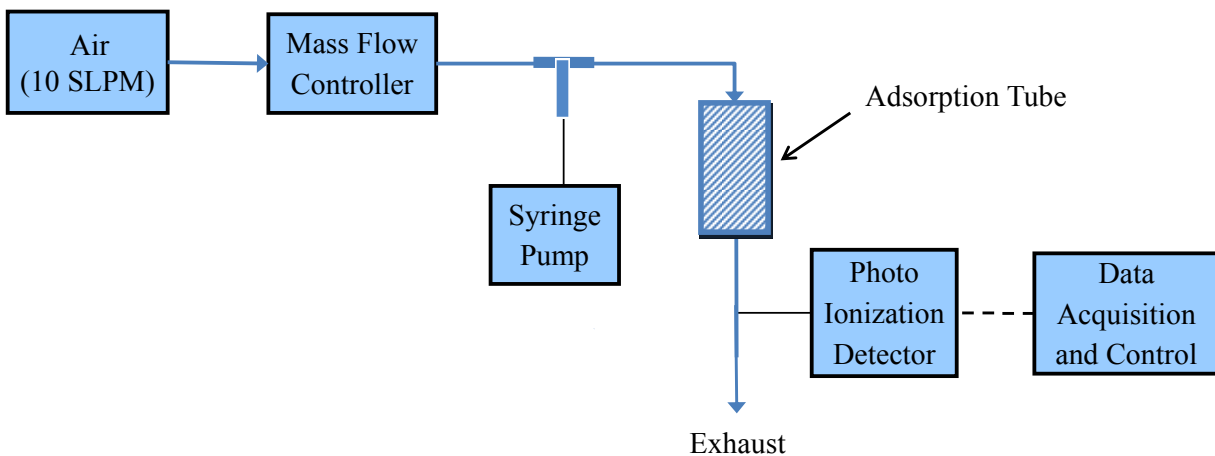
Figure 4-1 Block diagram of adsorption setup

4.2.2.2 *Microwave heating regeneration*

After BAC saturation, the tube was transferred to a microwave applicator for regeneration. The microwave regeneration set-up was similar to one described elsewhere (Figure 4-2a) (Chowdhury et al., 2012). It consisted of a 2 kW switch-mode power supply (SM745G.1, Alter), a 2 kW microwave source (MH2.0W-S, National Electronics) with a 2.45 GHz magnetron, an isolator (National Electronics), a three stub tuner (National Electronics),

and a waveguide applicator connected to a sliding short. Power was monitored using a dual directional coupler with 60 db attenuation (Mega Industries), two power sensors (8481 A, Agilent), and a dual channel microwave power meter (E44119B, Agilent). Microwave power values reported throughout the manuscript represent the incident, or forward, power delivered by the microwave generator. The power supply and power meter were interfaced to the DAC system to record the applied power. The regeneration temperature was measured immediately after microwave generation was stopped by inserting a type K thermocouple into the center of the adsorbent bed. BAC was heated in a flow of nitrogen (0.3 SLPM) during microwave regeneration and then cooled for 10 min while continuing the nitrogen purge. Regeneration times (4.2 − 8.8 min) and powers (105 − 215 W) varied, but the most common conditions were 5 min and 180 W. Microwave heating during 5-cycle adsorption/desorption testing was completed using these conditions. Desorption efficiency was calculated using Equation (2)

$$\text{Desorption efficiency } (\%) = \left(\frac{W_{AA} - W_{AR}}{W_{AA} - W_{BA}} \right) \times 100 \quad \text{Eq. (2)}$$

where W_{AR} is the BAC weight after regeneration

(a)

(b)
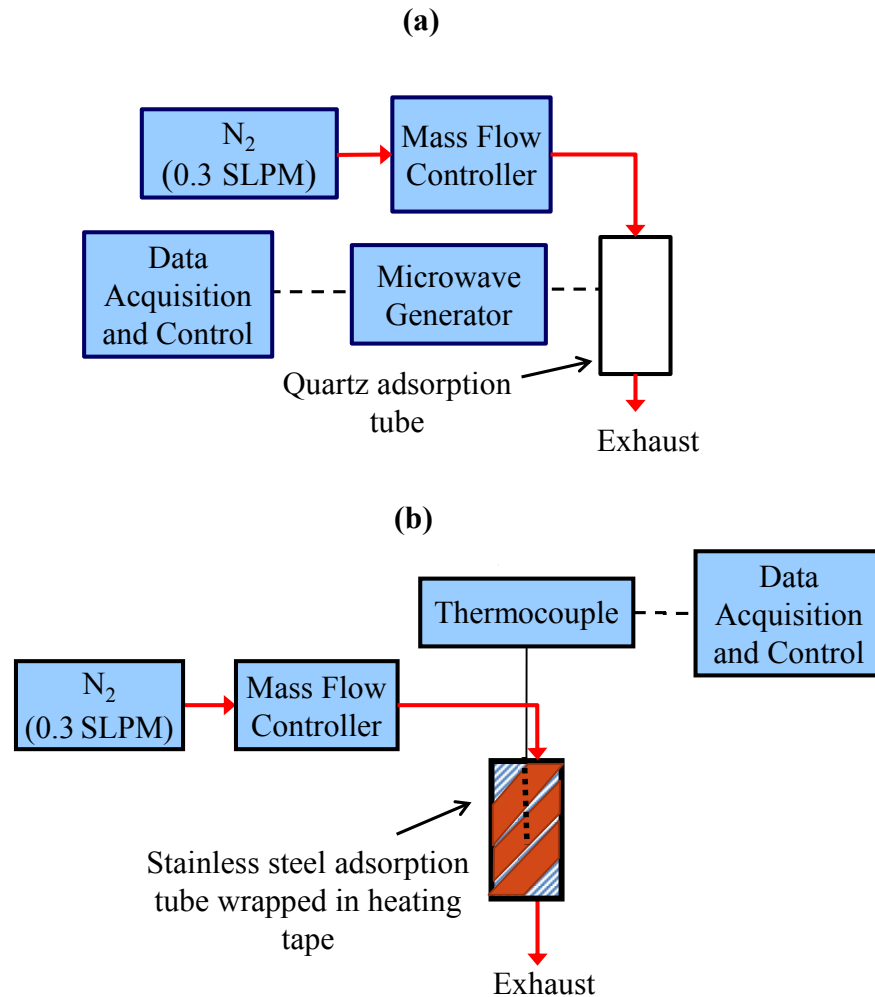
Figure 4-2 Block diagram of (a) microwave heating and (b) conductive heating regeneration set ups

4.2.2.3 *Conductive heating regeneration*

For conductive heating regeneration, the tube was wrapped with heating and insulation tapes (Omega) after BAC loading (Figure 4-2b) and voltage was applied by a Variac (Staco). A thermocouple measured the temperature at the center of the carbon bed. The voltage and current applied were measured with a true RMS multimeter (Omega) and a clamp ammeter (Fluke), respectively. BAC was heated in a flow of nitrogen (0.3 SLPM) and then cooled for 50 min while continuing the nitrogen purge. Regeneration times (4 – 162 min) and powers

64

(100 – 180 W) varied, but the most common conditions were 90 min and 180 W. Conductive heating during 5-cycle adsorption/desorption cycles was completed using these conditions. Desorption efficiency (%) was calculated using Equation 2.

4.2.3   Characterization tests

4.2.3.1   Micropore surface analysis

Brunner Emmett Teller (BET) surface area and pore size distribution (PSD) of the virgin, blank, and regenerated samples were determined using a micropore surface analysis system (iQ2MP, Quantachrome) with nitrogen as the probe molecule at relative pressures from 10^{-7} to 1 and at 77 K. BAC samples of 30 to 50 mg were first degassed under vacuum at 120 $^{\circ}$C for 5 h to remove moisture. The relative pressure ranges used for determining BET surface area and micropore volume were 0.01 to 0.07 and 0.2 to 0.4, respectively. The V-t model was used for determining micropore volume. PSDs were obtained from nitrogen adsorption/desorption isotherms by applying the non-linear density functional theory (NLDFT) model for slit-shaped pores (Olivier, 1998).

4.2.3.2   XPS analysis

Surface elemental composition (C, O) of select samples was determined with X-ray photoelectron spectroscopy (XPS, Kratos Analytical). XPS provided the elemental composition of activated carbon samples at depths < 60Å (Briggs and Seah, 1983). The C1s peak was adjusted to 285 eV before determining the relative amounts of C and O using CasaXPS Software.

4.2.3.3 GC-FID analysis

During regeneration, desorbed compounds condensed at the tube outlet without any ancillary cooling. The condensed desorbate was collected during the first 60 min of regeneration and then diluted to 25 vol% using n-hexane (Fischer Scientific, used for calibration). The diluted sample was analyzed with a gas chromatography with flame ionization detector (GC-FID, Agilent Technologies, model 7890A). The GC was equipped with a 15 m long, 0.25 mm diameter, and 0.25 μm film thickness DB-5ms Ultra Inert column (Agilent). The injection port temperature was 300 ^{o}C, helium was the carrier gas (25 mL/min), and the injection volume was 1 μL. After sample injection, the oven temperature was maintained at 50 ^{o}C for 2 min and then ramped to 320 ^{o}C in 5 min and held at that temperature for up to 5 min.

4.3 Results and Discussion

4.3.1 Effect of applied energy on desorption efficiency

To evaluate the effect of applied energy on regeneration by microwave and conductive heating, constant power (180 W) was applied for different times, resulting in different applied energies. Figure 4-3 shows desorption efficiency improvements with increasing heating time, for both heating methods. In every case, energy required to attain equal desorption efficiencies was lower for microwave heating. Hence, compared to conductive heating, energy consumption in microwave regeneration was much lower, as has been reported for low molecular weight adsorbates (Chowdhury et al., 2012). Higher heat losses during conductive heating is one reason for this difference (Di and Chang, 1996). To achieve complete n-dodecane desorption from BAC (100% desorption efficiency), microwave heating required 6% of the energy consumed during conductive heating. Previous researchers reported microwave regeneration requiring < 50% of

the energy needed for conventional regeneration processes (including resistive heating and steam stripping) (Turner et al., 2000). The results presented here buildup on this early estimate, showing that complete regeneration of activated carbon saturated with n-dodecane can be achieved with < 10% of the energy consumption by using microwave heating instead of conductive heating. Similarly, complete regeneration by microwave heating was achieved in 6% of the time required for conductive heating (5 min vs. 90 min).
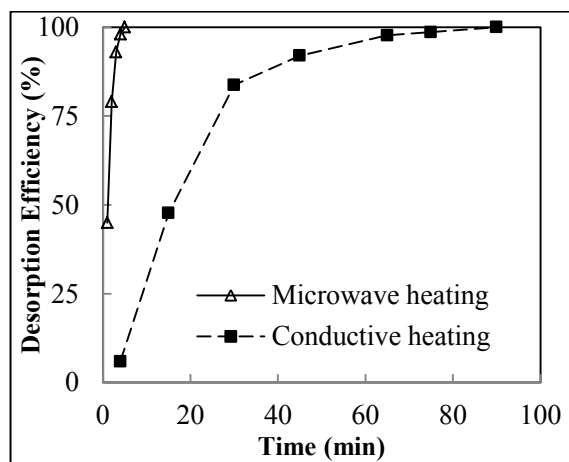
Figure 4-3 Desorption efficiency as a function of time for constant power (180 W) microwave and conductive heating of BAC loaded with n-dodecane

4.3.2   Effect of applied power on regeneration

Using an applied power of 180 W (Figure 4-4), the total energy needed for complete regeneration with microwave and conductive heating was 56 and 972 kJ, respectively. The effect of applied power was evaluated using different combinations of power and duration that maintained the same total applied energy for the corresponding technique (Figure 4-4). For microwave heating, applying 56 kJ of energy with power ranging from 100 W to 220 W consistently resulted in complete regeneration. For conductive heating; however, decreasing the power (and increasing time) with 972 kJ of total energy resulted in progressively lower regeneration efficiencies.
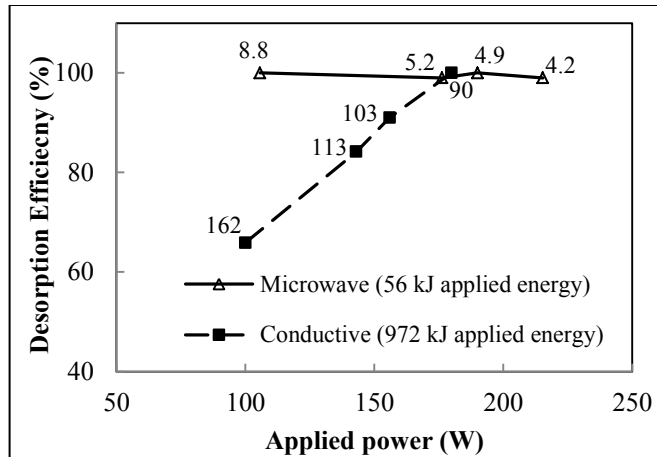
Figure 4-4 Variation of desorption efficiency with combinations of applied power and duration that provide equal total applied energy. Labeled regeneration durations are presented in min next to the datapoints.

Figure 4-5 shows the final regeneration temperatures measured for the conditions described in Figure 4-4. Since Knudsen diffusion and molecular diffusion coefficients depend on temperature ($T^{1.5}$ and $T^{0.5}$, respectively) (Youngquist, 1970), increasing the regeneration temperature increases diffusive mass transfer and improves desorption (Adu and Otten, 1993, Price and Schmidt, 1997, Roussy et al., 1984, Weissenberger and Schmidt, 1994). For microwave heating, the amount of power applied did not impact the final temperature achieved because the duration was adjusted so that the same total amount of energy was applied in all scenarios. Temperature and desorption efficiency are essentially unchanged for microwave heating with constant applied power, suggesting minimal energy losses. On the other hand, for conductive heating, decreasing the applied power while increasing duration resulted in decreased regeneration temperature and, correspondingly, decreased desorption efficiency. Since the duration was longer, more of the input energy was lost to the surrounding equipment and carrier gas, and lower temperatures were achieved. These results highlight aspects of the energy efficiency of microwave heating resulting from fast heat transfer over a range of applied powers.

68

During microwave regeneration, the BAC is heated volumetrically, and the temperature gradient is from inside to outside of adsorbent (highest temperature inside). Previous studies showed that during regeneration of loaded carbon, heat and mass transfer could be in the same direction (Ania et al., 2005). This, along with a small contribution from direct heating of the non-polar, non-functionalized adsorbate, reduces energy lost to unproductive heating of other system components or the sweep gas. Shorter regeneration times and the tube configuration (embedded in the microwave applicator) may also lower energy lost by free convection. The same cannot be said of conductive heating systems where energy losses to surrounding equipment and gases are prominent.
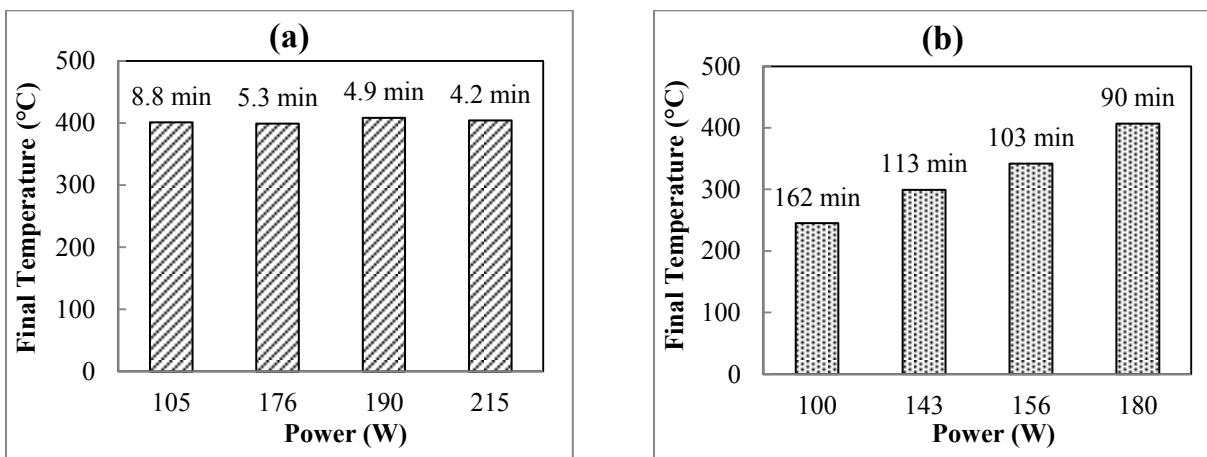
Figure 4-5 Final temperature as a function of power (and duration) in combinations that provide equal total applied energy: a) microwave heating using 56 kJ of applied energy, and b) conductive heating using 972 kJ of applied energy.

4.3.3   Impact of regeneration method on BAC physical and chemical properties

Previous studies reported pore blockage associated with microwave heating for activated carbon regeneration (Ania et al., 2004, Ania et al., 2005). As such, it is important to identify potential changes to the physical properties of the adsorbent when desorbing n-dodecane with microwave heating. To observe these effects, five adsorption/desorption cycles (180 W for 5 min

with microwave heating and 180 W for 90 min with conductive heating) were completed with both heating techniques (Figure 4-6). Since sufficient energy for complete regeneration was provided by both regeneration methods, as described earlier, n-dodecane adsorption capacity did not change throughout the cycle experiments. Unchanged breakthrough times for each adsorption cycle support this observation (Figure 4-6).
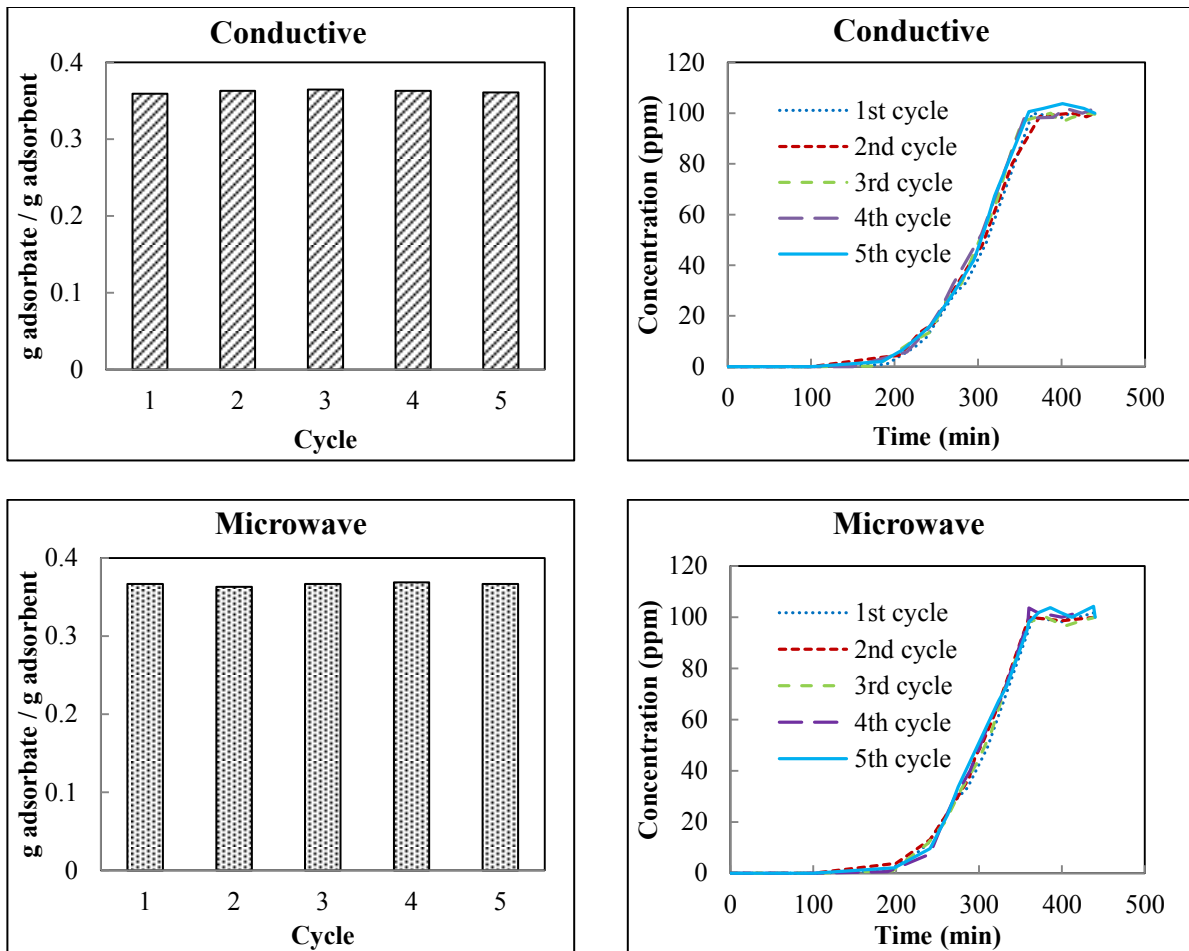
Figure 4-6 BAC adsorption capacities and adsorption breakthrough curves for five consecutive adsorption / desorption cycles. Desorption was completed with 180 W of applied power for 5 min of microwave heating and 180 W of applied power for 90 min of conductive heating

Physical properties for BAC samples (i.e., BET surface area and PSD, measured with nitrogen adsorption) after five adsorption/desorption cycles were obtained and compared to the virgin and loaded BACs. Comparisons to blank BAC samples that also underwent five cycles of exposure to air under the same adsorption conditions (but without any adsorbate) followed by desorption with identical regeneration conditions were also made (Table 4-1).

Table 4-1 Physical and surface properties of virgin, spent, and regenerated BAC samples

Sample	BET Surface Area (m^2/g)	Micropore Volume (cm^3/g)	Meso/Macro Pore Volume (cm^3/g)	Pore Volume (cm^3/g)	Carbon Content (%)[a]	Oxygen Content (%)[a]
Virgin	1371±21	0.50±0.01	0.05±0.01	0.55±0.01	92.4±0.1	7.6±0.1
Loaded	341	0.09	0.10	0.19	-	-
5-Cycle, Conductive	1312	0.47	0.07	0.54	93.6±0.8	7. ±0.8
5-Cycle, Microwave	1320	0.47	0.07	0.54	92.9±0.8	7.1±0.8
5-Cycle, Conductive (Blank)	1357	0.49	0.06	0.55	93.9±0.2	6.1±0.2
5-Cycle, Microwave (Blank)	1366	0.49	0.06	0.55	94.0±0.7	7.0±0.7

[a] Relative percentages (%C + %O = 100%); other possible elements (e.g., hydrogen, nitrogen, sulfur) are assumed negligible

Table 4-1 shows that BAC after five cycles of adsorption/desorption using conductive heating or microwave heating have relatively unchanged micropore volume (within 6% of virgin sample), total pore volume (within 2% of virgin sample), and BET surface area (within 5% of virgin sample). Blank samples for each regeneration method also have similar physical properties (all within 2% of virgin sample), showing that the heating technique has minimal impact on the pore structure of the adsorbent. The loss in micropore volume (> 80%) for the loaded BAC

(Table 4-1) confirms that n-dodecane adsorption primarily occurs in BAC micropores. The structure of n-dodecane is linear without branching, so while it has a high molecular weight, it also has a small kinetic diameter (4.3 Å). This allows for penetration into BAC's most narrow micropores (5 – 6 Å, Figure 4-7) where physical adsorption affinity is high due to overlapping energy fields of neighbouring pore walls (Rodrı´guez-Mirasol et al., 2005). Minimal differences between the physical properties of the virgin and 5-cycle samples confirm that both heating methods are sufficient for recovering the micropore volume. Figure 4-7 shows that micropore size distributions for all three samples are nearly identical, with the only discernable differences being in the very narrow pore widths (< 6 Å). Adsorbate decomposition during microwave application, postulated to cause pore blockage in previous studies (Ania et al., 2005, Çalışkan et al., 2012), was not observed.
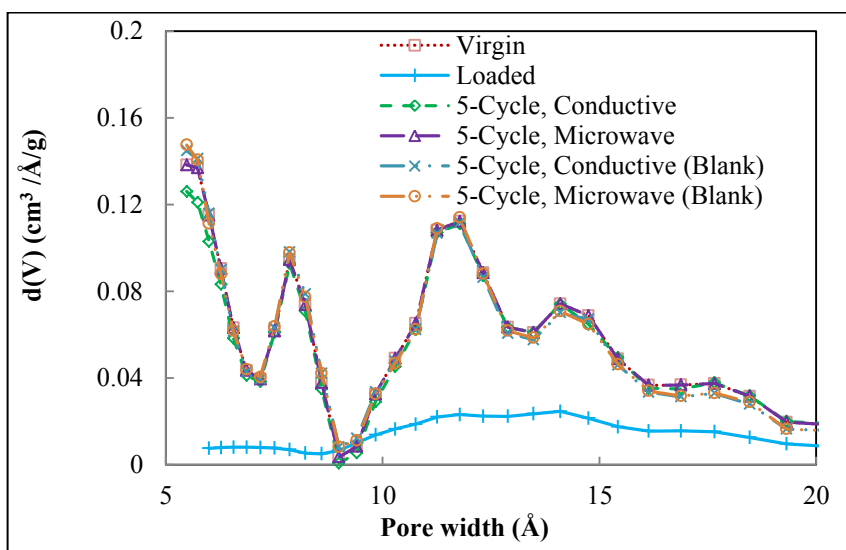
Figure 4-7. Micropore size distributions of BAC samples

In terms of BAC surface chemical properties, XPS identified a decrease in surface oxygen content for both 5-cycle blank and 5-cycle regenerated samples, independent of regeneration technique (Table 4-1). Lower oxygen content for regenerated samples compared to

virgin samples could be due to partial desorption of surface oxygen functionalities during microwave or conductive heating, independent of the presence of adsorbate. Based on similar PSDs for all samples and no change in adsorption capacities after regeneration, this oxygen loss apparently had no impact on the physical properties or adsorption performance of the BACs.

4.3.4 Impact of regeneration method on adsorbate properties

Since VOC recovery for possible reuse is an important aspect of adsorbent regeneration, the potential for adsorbate decomposition during microwave and conductive heating regeneration methods was assessed. According to previous reports, microwave regeneration of carbon can cause a portion of the organic adsorbate (e.g., phenol, pentachlorophenol, trichloroethylene) to decompose, also impacting the PSD of the regenerated adsorbent (Jou, 1998, Hua-Shan and Chih-Ju, 1999, Liu et al., 2004, Ania et al., 2004, Ania et al., 2005). This may be partially attributed to rapid microwave heating rates, which could expose the adsorbate and desorbate to high temperatures. However, the effect of microwave heating on the chemical structure of straight-chain organic molecules has not been previously described. Microwave impacts on chemical reactions can be attributed to either thermal or non-thermal effects. Thermal effects include overheating, hot spots, and selective heating, while non-thermal effects include molecular mobility and field stabilization (De La Hoz et al., 2005). To observe if decomposition occurred as a result of each regeneration technique, GC-FID analysis was completed on desorbate collected during constant power regeneration (180 W for 5 min of microwave heating and 180 W for 90 min of conductive heating) and compared to a n-dodecane standard (in hexane) (Figure 4-8). The GC-FID profiles for the three samples were nearly identical, including two peaks attributed to the hexane solvent and the n-dodecane solute. No other peaks or shifts in peak retention times

were observed that would indicate adsorbate decomposition as a result of the two heating methods. Non-catalyzed n-dodecane decomposition is not expected at 400 $^{\circ}$C (Liu et al., 1987) and the absence of polar functional groups makes direct microwave heating of the adsorbate less effective, also decreasing the tendency for adsorbate decomposition. This research illustrates that microwave heating can be used for effective and energy efficient regeneration of activated carbon loaded with high boiling point VOCs, without negatively altering the adsorbate or the adsorbent.
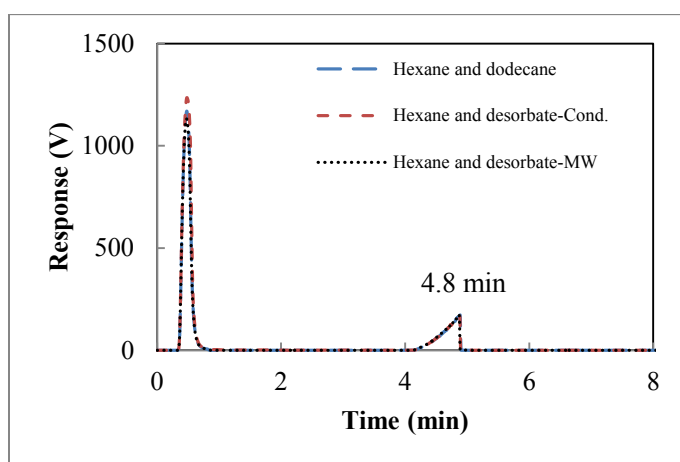
Figure 4-8 Chromatograms of n-dodecane (4.8 min) standard and desorbate collected during microwave (MW) and conductive (Cond.) heating regenerations

4.4 Conclusion

This study investigated the performance of microwave heating method during regeneration of adsorbents loaded with high molecular weight VOCs, in terms of regeneration efficiency and energy consumption. A microporous adsorbent was loaded with n-dodecnae and regenerated using conductive and microwave heating under different applied powers and energies. It was found that the minimum energy required to completely regenerate the adsorbent (100% desorption efficiency) using microwave regeneration was 6% of that needed with conductive heating regeneration. According to micropore surface analysis and XPS

results, neither heating method changed the physical/chemical properties of BAC. Additionally, gas chromatography (with flame ionization detector) confirmed that neither regeneration method detectably altered the adsorbate composition during desorption. These results confirmed the hypothesis proposed in this study that microwave heating regeneration is an energy-efficient technique for non-destructive regeneration of adsorbents loaded with high boiling point VOCs. Improvements in energy consumption and desorption efficiency and stable adsorbate and adsorbent properties make microwave heating an attractive method for activated carbon regeneration particularly when high-affinity VOC adsorbates are present.

4.5 References

ADU, B. & OTTEN, L. 1993. Simultaneous microwave heat and mass transfer characteristics of porous hygroscopic solids. *Journal of Microwave Power and Electromagnetic Energy,* 28**,** 41.

ANIA, C. O., MENÉNDEZ, J. A., PARRA, J. B. & PIS, J. J. 2004. Microwave-induced regeneration of activated carbons polluted with phenol. A comparison with conventional thermal regeneration. *Carbon,* 42**,** 1377-1381.

ANIA, C. O., PARRA, J. B., MENÉNDEZ, J. A. & PIS, J. J. 2005. Effect of microwave and conventional regeneration on the microporous and mesoporous network and on the adsorptive capacity of activated carbons. *Microporous and Mesoporous Materials,* 85**,** 7-15.

BOURAOUI, M. M. 1991. *Microwave and convective drying of potato slices.* M.Sc. Dissertation, The University of British Columbia.

BRECK, D. W. 1974. *Zeolites molecular sieves: structure chemistry and use,* New York, Wiley.

BRIGGS, D. & SEAH, M. P. 1983. *Practical surface analysis: By auger and x-ray photoelectron spectroscopy,* New York, USA, Wiley: Chichester.

BURKHOLDER, H. R., FANSLOW, G. E. & BLUHM, D. D. 1986. Recovery of ethanol from a molecular sieve by using dielectric heating. *Industrial and Engineering Chemistry Fundamentals,* 25**,** 414-416.

ÇALIŞKAN, E., BERMÚDEZ, J. M., PARRA, J. B., MENÉNDEZ, J. A., MAHRAMANLIOĞLU, M. & ANIA, C. O. 2012. Low temperature regeneration of activated carbons using microwaves: Revising conventional wisdom. *Journal of Environmental Management,* 102**,** 134-140.

CHERBAŃSKI, R. & MOLGA, E. 2009. Intensification of desorption processes by use of microwaves-An overview of possible applications and industrial perspectives. *Chemical Engineering and Processing: Process Intensification,* 48**,** 48-58.

CHERBAŃSKI, S., R., KOMOROWSKA-DURKA, M., STEFANIDIS, G. D. & STANKIEWICZ, A. I. 2011. Microwave swing regeneration vs temperature swing regeneration - Comparison of desorption kinetics. *Industrial and Engineering Chemistry Research,* 50**,** 8632-8644.

CHOWDHURY, T., SHI, M., HASHISHO, Z., SAWADA, J. A. & KUZNICKI, S. M. 2012. Regeneration of Na-ETS-10 using microwave and conductive heating. *Chemical Engineering Science,* 75**,** 282-288.

COSS, P. M. & CHA, C. Y. 2000. Microwave regeneration of activated carbon used for removal of solvents from vented air. *Journal of Air & Waste Management Association,* 50**,** 529-535.

DE LA HOZ, A., Dı́AZ-ORTIZ, A. & MORENO, A. 2005. Microwaves in organic synthesis. Thermal and non-thermal microwave effects. *Chemical Society Reviews,* 34**,** 164-178.

DEMIR, S. & SARAL, A. 2013. Identification and apportionment of sources of ozone-forming potential for proper reduction strategies. *Clean - Soil, Air, Water,* 41**,** 107-112.

DI, P. & CHANG, D. P. Microwave regeneration of volatile organic compounds (VOC) adsorbents. Presented in 89th Annual Conference & Exhibition of A&WMA, Nashville, TN, 1996.

FABRIZI, G., FIORETTI, M. & MAINERO ROCCA, L. 2013. Occupational exposure to complex mixtures of volatile organic compounds in ambient air: Desorption from activated charcoal using accelerated solvent extraction can replace carbon disulfide? *Analytical and Bioanalytical Chemistry,* 405**,** 961-976.

HASHISHO, Z., EMAMIPOUR, H., CEVALLOS, D., ROOD, M. J., HAY, K. J. & KIM, B. J. 2007. Rapid response concentration-controlled desorption of activated carbon to dampen concentration fluctuations. *Environmental Science and Technology,* 41**,** 1753-1758.

HASHISHO, Z., EMAMIPOUR, H., ROOD, M. J., HAY, K. J., KIM, B. J. & THURSTON, D. 2008. Concomitant adsorption and desorption of organic vapor in dry and humid air streams using microwave and direct electrothermal swing adsorption. *Environmental Science and Technology,* 42**,** 9317-9322.

HASHISHO, Z., ROOD, M. & BOTICH, L. 2005. Microwave-swing adsorption to capture and recover vapors from air streams with activated carbon fiber cloth. *Environmental Science and Technology,* 39**,** 6851-6859.

HASHISHO, Z., ROOD, M. J., BAROT, S. & BERNHARD, J. 2009. Role of functional groups on the microwave attenuation and electric resistivity of activated carbon fiber cloth. *Carbon,* 47, 1814-1823.

HSIEH, L., YANG, H., LIN, Y. & TSAI, C. 2012. Levels and composition of volatile organic compounds from the electric oven during roasting pork activities. *Sustainable environment research,* 22, 7.

HUA-SHAN, T. & CHIH-JU, G. J. 1999. Application of granular activated carbon packed-bed reactor in microwave radiation field to treat phenol. *Chemosphere,* 38, 2667-2680.

JONES, D. A., LELYVELD, T. P., MAVROFIDIS, S. D., KINGMAN, S. W. & MILES, N. J. 2002. Microwave heating applications in environmental engineering-a review. *Resources, Conservation and Recycling,* 34, 75-90.

JOU, G. C.-J. 1998. Application of activated carbon in a microwave radiation field to treat trichloroethylene. *Carbon,* 36, 1643-1648.

LASHAKI, M. J., FAYAZ, M., WANG, H., HASHISHO, Z., PHILIPS, J. H., ANDERSON, J. E. & NICHOLS, M. 2012. Effect of adsorption and regeneration temperature on irreversible adsorption of organic vapors on beaded activated carbon. *Environmental Science & Technology,* 46, 4083-4090.

LEGRAS, B., POLAERT, I., THOMAS, M. & ESTEL, L. 2013. About using microwave irradiation in competitive adsorption processes. *Applied Thermal Engineering,* 164–171.

LIU, P. K. T., FELTCH, S. M. & WAGNER, N. J. 1987. Thermal desorption behavior of aliphatic and aromatic hydrocarbons loaded on activated carbon. *Industrial and Engineering Chemistry Research,* 26, 1540-1545.

LIU, X., QUAN, X., BO, L., CHEN, S. & ZHAO, Y. 2004. Simultaneous pentachlorophenol decomposition and granular activated carbon regeneration assisted by microwave irradiation. *Carbon,* 42, 415-422.

MIURA, M., KAGA, H., SAKURAI, A., KAKUCHI, T. & TAKAHASHI, K. 2004. Rapid pyrolysis of wood block by microwave heating. *Journal of Analytical and Applied Pyrolysis,* 71, 187-199.

OLIVIER, J. P. 1998. Improving the models used for calculating the size distribution of micropore volume of activated carbons from adsorption data. *Carbon,* 36, 1469-1472.

POPESCU, M., JOLY, J. P., CARRÉ, J. & DANATOIU, C. 2003. Dynamical adsorption and temperature-programmed desorption of VOCs (toluene, butyl acetate and butanol) on activated carbons. *Carbon,* 41, 739-748.

PRICE, D. W. & SCHMIDT, P. S. 1997. Microwave regeneration of adsorbents at low pressure: Experimental kinetics studies. *Journal of Microwave Power & Electromagnetic Energy,* 32, 145-154.

REUß, J., BATHEN, D. & SCHMIDT-TRAUB, H. 2002. Desorption by microwaves: Mechanisms of multicomponent mixtures. *Chemical Engineering and Technology,* 25, 381-384.

ROBERS, A., FIGURA, M., THIESEN, P. H. & NIEMEYER, B. 2005. Desorption of odor-active compounds by microwaves, ultrasound, and water. *AlChE Journal ,* 51, 502-510.

RODRı´GUEZ-MIRASOL, J., BEDIA, J. & CORDERO, C. 2005. Influence of water vapor on the adsorption of VOCs on lignin-based activated carbons. *Separation Science and Technology,* 40, 3113–3135.

ROUSSY, G., ZOULALIAN, A., CHARREYRE, M. & THIEBAUT, J. M. 1984. How microwaves dehydrate zeolites. *Journal of Physical Chemistry,* 88, 5702-5708.

TEFERA, D. T., JAHANDAR LASHAKI, M., FAYAZ, M., HASHISHO, Z., PHILIPS, J. H., ANDERSON, J. E. & NICHOLS, M. 2013. Two-dimensional modeling of volatile organic compounds adsorption onto beaded activated carbon. *Environmental Science and Technology,* 47, 11700-11710.

TURNER, M. D., LAURENCE, R. L., CONNER, W. C. & YNGVESSON, K. S. 2000. Microwave radiation's influence on sorption and competitive sorption in zeolites. *AIChE Journal,* 46, 758-768.

WEISSENBERGER, A. P. & SCHMIDT, P. S. 1994. Microwave enhanced regeneration of adsorbents. *MRS Proceedings,* 347, 383-394.

YOUNGQUIST, G. R. 1970. Diffusion and flow of gases in porous solids. *Industrial and Engineering Chemistry Research,* 62, 52-63.

CHAPTER 5. INVESTIGATION OF THE EFFECT OF REGENERATION TEMPERATURE, HEATING RATE AND ADSORBENT POROSITY ON HEEL FORMATION

5.1 Introduction

Volatile organic compounds (VOCs) are generated from many industrial activities such as painting operations (Chang Yul and Carlisle, 2001, Kim et al., 2001). When adsorption is used as the control technique, adsorbent regeneration becomes an important step in terms of the economic and technical feasibility of the abatement process (Nigar et al., 2015). Conductive heating, steam regeneration, and hot gas purging are typically used for adsorbent regeneration (Di and Chang, 1996). While each is widely applied industrially, drawbacks including long regeneration times and high energy consumption are problematic (Adu and Otten, 1993, Di and Chang, 1996). Microwave heating, an alternative to conventional regeneration techniques, provides rapid, scaleable, and selective volumetric heating (Cherbański et al., 2011, Di and Chang, 1996, Fayaz et al., 2015a, Hua-Shan and Chih-Ju, 1999, Jones et al., 2002, Weissenberger and Schmidt, 1994). During microwave heating adsorbent/adsorbate convert microwave energy into thermal energy depending on their dielectric materials, including dielectric constant (ε') and loss factor (ε"). The dielectric constant describes a material's ability to be polarized by an electromagnetic field, and loss factor describes a material's ability to convert absorbed energy into heat (Cherbański and Molga, 2009).

One challenge in regeneration step is accumulation of non-desorbed adsorbate in the adsorbent pores which is defined as heel build. Heel buildup reduces the adsorbent working

capacity and lifetime (Lashaki et al., 2012). Heel buildup has been attributed to non-desorbable physical adsorption, oligomerization, chemical adsorption, and coke formation resulted by adsorbate decomposition (Ania et al., 2004, Ania et al., 2005, Çalişkan et al., 2012, Ha and Vinitnantharat, 2000, Thakkar and Manes, 1987). Previous studies showed that regeneration temperature impacts heel formation (Lashaki et al., 2012). Jahandar Lashaki et al. found that for conductive heating regeneration of a beaded activated carbon (BAC) loaded with a VOC mixture, increasing the regeneration temperature from 288 to 400 °C reduced the heel by up to 61% (Lashaki et al., 2012). Similar results were observed for regeneration via microwave heating. Fayaz et al. (2015) showed that for conductive and microwave regeneration of activated carbon loaded with n-dodecane, complete regeneration was only obtained at a temperature of 400 °C, notably higher than the adsorbate's boiling point (216 °C) (Fayaz et al., 2015). Niknaddaf et al. investigated heel formation on three activated carbon fibre cloths (ACFC10, ACFC15, and ACFC20, with increasing pore widths and volumes) after cyclic adsorption/resistive heating regeneration using 1,2,4-trimethylbenzene (TMB). Interestingly, increasing the regeneration temperature from 288 to 400 °C increased heel buildup for ACFC-10, ACFC-15 and ACFC-20 by 5.7, 153, and 350%, respectively (Niknaddaf et al., 2015). This counter-intuitive result was attributed to adsorbate decomposition due to exposure to high temperature (400 °C) in the adsorbent pores, triggering coking reactions.

None of the above mentioned studies considered the effect of regeneration heating rate on heel formation. A faster heating rate shortens regeneration duration and reduces energy consumption, which is desirable. However, fast heating rate might also result in unwanted challenges. Limited information is available in the literature about the effect of heating rate on

irreversible adsorption of organic compounds. During high temperature (800 °C) regeneration of mesoporous activated carbon loaded with chlorophenols via aqueous-phase adsorption, it was observed that high heating rates (as high as 40 °C /min) increased irreversible adsorption on carbon by converting physisorbed adsorbate into chemisorbed adsorbate (Ferro-Garcia et al., 1995, Ferro-Garcia et al., 1996). Another study showed that during regeneration of a mainly microporous (97% micropore volume) ACFC loaded with TMB, higher heating rate (as high as 100 °C /min) favors coke formation. All of these studies, however, were completed at a single regeneration temperature (800 °C (Ferro-Garcia et al., 1995, Ferro-Garcia et al., 1996) or 400 °C (Niknaddaf et al., 2016)); the combined effect of regeneration temperature and regeneration heating rate on heel formation was not considered.

Adsorbent porosity can also affect irreversible adsorption (Lu and Sorial, 2004). During regeneration of BAC saturated with a mixture of gas-phase VOCs, the heel mainly accumulated in narrow micropores (pore width < 8 Å) of the adsorbent (Lashaki et al., 2012). It was also found that adsorbents with higher microporosity turn a greater portion of adsorbed species into heel due to higher share of high energy adsorption sites in their structure (Jahandar Lashaki et al., 2016a). In another study of the aqueous-phase adsorption of phenols, it was found that the ACFC with the narrowest pore width was more effective in reducing irreversible adsorption (from oligomerization) of phenols relative to granular activated carbon and ACFCs with larger pores (Lu and Sorial, 2004). No studies, however, investigated the combined effect of regeneration heating rate and adsorbent porosity on heel buildup.

The first hypothesis of this study is that compared to micropores, mesopores have lower diffusive mass transfer resistance, therefore, it is expected that mesopores have less contribution in heel formation compared to micropores. The second hypothesis of this study is

that using a high heating rate during regeneration may increase heel formation; therefore, to improve regeneration performance, heating rate should be optimized while considering the regeneration temperature. The objective of this study, therefore, is to elucidate the effect of regeneration heating rate on heel formation during regeneration of activated carbons with different pore size distributions at different regeneration temperatures. For this purpose, two BACs with different porosities (mainly microporous versus partially microporous) were loaded with TMB. Loaded adsorbents were regenerated at 288 and 400 °C using microwave heating. Heating rates from 25 to 150 °C/min were applied during regeneration. Adsorbents were characterized before and, in some cases, after 5 successive adsorption/regeneration cycles using micropore surface analysis, X-ray photoelectron spectroscopy (XPS), and derivative thermogravimetry (DTG) analysis to assess changes in the adsorbents' properties.

5.2   Experimental

5.2.1   Adsorbents and adsorbate

A mainly microporous BAC (G-70R; Kureha Corporation, 88% microporous, referred to as BAC-50-07 hereafter) and a partially microporous BAC (B101412; Blucher GmbH, 46% microporous, referred to as BAC-52-66 hereafter) were studied. The sample naming convention, BAC-X-Y, indicates the micropore volume (X) and mesopore volume (Y) of the samples in $cm^3/g \times 100$, respectively. For each sample, the sum of micropore and mesopore volume gives total pore volume. The mean particle diameter of BAC-50-07 and BAC-52-66 are 0.70 mm (99% by mass between 0.60 and 0.84 mm) and 0.56 mm (97.5% by mass between 0.50 and 0.71 mm) respectively (Lashaki et al., 2012). Before adsorption, virgin samples were heated in air at 150 °C for 24 h to remove impurities and were then stored in a desiccator before use. TMB (98%, Sigma Aldrich) was used as adsorbate in all experiments.

TMB is an aromatic VOC with bulky molecular structure and high boiling point (171 °C), which makes it susceptible for heel buildup (Fayaz et al., 2011).

5.2.2 Experimental setup and methods

5.2.2.1 *Adsorption*

The adsorption setup included an adsorption tube, a vapor generation system, a vapor detection system, and a data acquisition and control (DAC) system (Figure 5-1). The adsorption tube was made of quartz (2.2 cm inner diameter, 35.6 cm length) and filled with 5.1 g BAC-50-07 or 3.3 g BAC-52-66, resulting in a bed height of 2.5 cm for both cases. A fritted glass disc in the middle of the tube supported the BACs. To generate the vapor stream, a syringe pump (KD Scientific, KDS-220) injected liquid TMB into a 10 standard liter per minute (SLPM) dry air stream to provide 500 ppm$_v$. A mass flow controller (Alicat Scientific) controlled the air flow rate. To monitor VOC concentrations at the influent and effluent of the adsorbent bed, a photoionization detector (PID) (Rae System, Minirae 2000) was used. PID was calibrated before each test using the adsorbate stream generated with the vapor generation system. Before starting adsorption the inlet concentration was measured by PID to make sure the inlet concentration is equal to 500ppm$_v$.

The DAC system consisted of a LabVIEW program (National Instruments) and a data logger (National Instruments, Compact DAC) equipped with analog input and output modules for recording temperature and outlet VOC concentration. Before adsorption, the PID was calibrated using the generated vapor stream. Adsorption started by directing the gas stream with stable TMB concentration to the bed. During adsorption, the outlet concentration was continually recorded by the DAC system. Adsorption continued until adsorbent saturation, identified when the outlet TMB concentration reached 500 ppm$_v$. The total adsorption time for both adsorbents

was 135 min. Breakthrough time is defined as the time when the effluent concentration was 5% of the influent concentration.
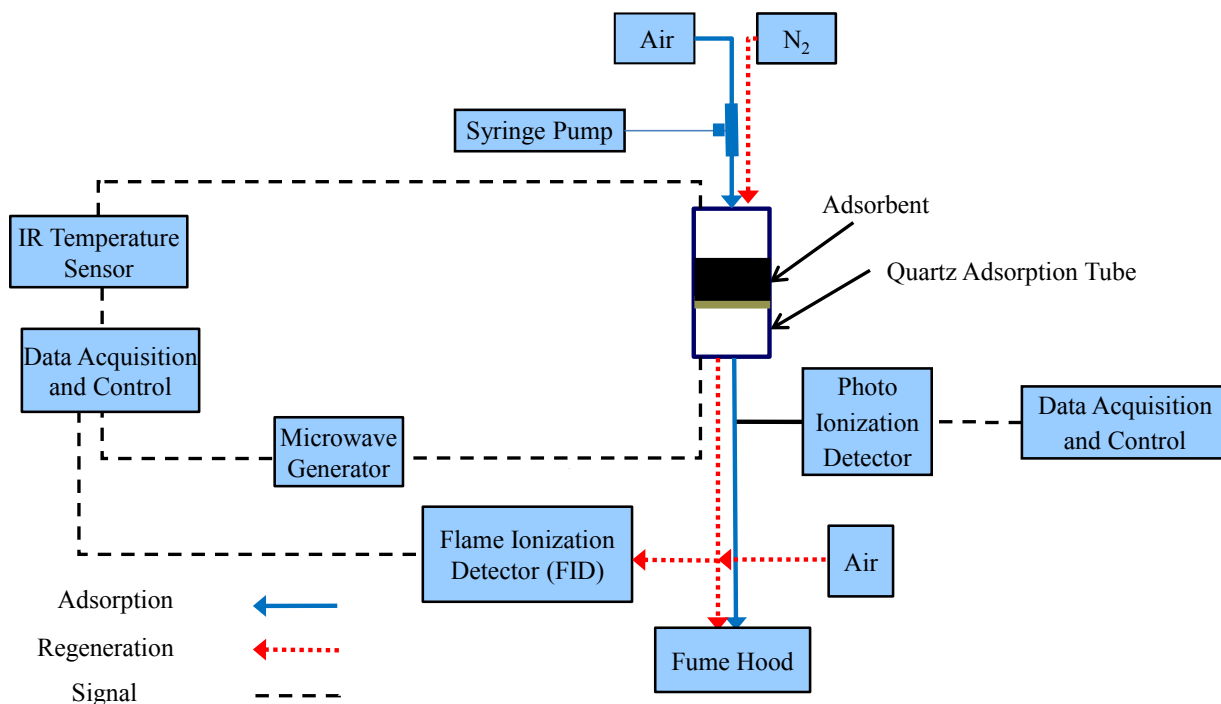
Figure 5-1. Block diagram of adsorption/regeneration setup

Microwave heating regeneration

The tube containing the loaded BAC was transferred to a microwave applicator for regeneration. The microwave regeneration setup (Figure 5-1) was similar to the one described by Fayaz et al. (2015) and Chowdhury et al. (2012), and included a 2 kW switch-mode power supply (Alter, SM745G.1), a 2 kW microwave source (National Electronics, MH2.0W-S) with a 2.45 GHz magnetron, an isolator (National Electronics), and a waveguide applicator with a sliding short. Forward and reverse (reflected) power was monitored through a dual directional coupler with 60 db attenuation (Mega Industries), two power sensors (Agilent, 8481 A), and a dual channel microwave power meter (Agilent, E44119B). The temperature of the bed was monitored using an infrared (IR) sensor (Process Sensor, PSC-SSS). The IR sensor, power meter,

and power supply were connected to the DAC system to record data and control power application. During regeneration, a LabVIEW program controlled the applied power to control the heating rate and maintain a target temperature. Desorption consisted of heating the BAC to the target temperature (288 or 400 °C) for 180 min while purging with high purity N_2 (99.9984%; 0.1 SLPM) followed by cooling for 10 min while continuing the N_2 purge.

To measure effluent VOC concentrations during regeneration, the effluent stream during desorption was diluted with air, and a flame ionization detector (FID, Baseline-Mocon, series 9000) sampled the diluted stream at a rate of 12 cm^3/min. The FID was operated using 175 cm^3/min of air and 35 cm^3/min of hydrogen. Dilution ratios of 35 and 40 were used for regeneration temperatures of 288 and 400 °C, respectively. At the end of the last regeneration cycle, mass balance cumulative heel percentage on the BAC was calculated as follows:

$$\text{Mass balance Cumulative heel percentage (\%)} = \frac{W_{AR} - W_{BA}}{W_{BA}} \times 100$$

where W_{AR} is the BAC weight after last cycle regeneration, and W_{BA} is the BAC weight before the first cycle adsorption.

5.2.2.2 BAC characterization

Physical properties of virgin and regenerated samples were characterized using micropore surface analysis (Quantachrome, iQ2MP). Before analysis, samples were degassed for 5 h at 120 °C. Nitrogen adsorption was completed at -196 °C. Specific surface area was calculated using the Brunauer Emmett Teller (BET) method (Brunauer et al., 1938) at relative pressure between 0.01 and 0.07, allowing for high coefficient of determination (R^2) values and a positive BET constant (C). Total pore volume was recorded at $P/P_0 = 0.975$. Pore sieze distributions (PSDs) were obtained using the quench solid density functional theory (QSDFT) method and the V-t method provided micropore volume.

XPS (AXIS 165 spectrometer, Kratos Analytical) was used to determine surface elemental composition (C, O, N) of virgin BACs at depths < 60 Å using survey scans analyzed by CasaXPS Software (Briggs and Seah, 1983). Survey scans were collected for binding energy spanning from 1100 eV to 0 with analyzer pass energy of 160 eV and a step of 0.4 eV.

To assess the thermal stability of heel accumulated on the samples as a function of temperature, DTG analysis (TGA/DSC 1, Mettler Toledo) was completed. Samples were heated from 25 to 800 °C at 2 °C/min in N_2 (50 standard cm^3/min) and heel desorption percentages during heating were calculated. Heel desorption percentage is defined as the fraction of total heel removed during thermogravimetry analysis (TGA) as the temperature ramped up to 800 °C. To calculate heel desorption percentage, the cumulative weight loss at a given temperature (800 °C) was corrected according to the weight loss of the corresponding virgin BAC and was then divided by the mass balance cumulative heel (Jahandar Lashaki et al., 2016b). All adsorption/regeneration tests were completed in duplicate and average values were reported herein.

5.3 Results and Discussion

5.3.1 Characterization of virgin BACs

Virgin adsorbents were characterized prior to cyclic adsorption/regeneration experiments (Table 5-1). Both samples have high micropore volume, suggesting their ability to adsorb low concentration VOCs (Jahandar Lashaki et al., 2016a, Jahandar Lashaki et al., 2012). Although micropore volumes for both samples are similar, BAC-52-66 has an order of magnitude higher mesopore volume relative to BAC-50-07, which results in 207% more total pore volume (and a lower micropore percentage of total porosity), but only 21% more BET

surface area. Surface elemental compositions (93-94% carbon, 6-7% oxygen, negligible nitrogen) for the two BACs are also similar. Thus, the two carbons have different pore size distribution but have similar elemental composition.

Table 5-1 Physical and chemical properties of virgin adsorbents

Adsorbent	Physical Properties				Surface Composition by XPS		
	BET Surface Area (m^2/g)	Micropore Volume (cm^3/g)	Mesopore Volume (cm^3/g)	Total pore Volume (cm^3/g)	C $(\%)^a$	O $(\%)^a$	N $(\%)^a$
Virgin BAC-50-07	1371	0.50	0.07	0.57	93.0	7.0	No peak
Virgin BAC-52-66	1658	0.52	0.66	1.66	93.9	6.1	

[a] Relative atomic percentages (%C + %O + %N = 100); Other elements were not considered in surface composition

5.3.2 Adsorption/regeneration cycles

Figure 5-2a shows the breakthrough time reduction percentage over 5 consecutive adsorption/regeneration cycles (BTR%) for BACs regenerated at 288 or 400 °C, using different heating rates (25, 50, 100 and 150 °C/min). Sample breakthrough curves for the experiments completed using 25 °C/min and 150 °C/min are provided in the Figure A-1. Breakthrough times gradually decreased due to heel buildup. For regeneration at 288 °C, increasing the heating rate had minimal impact on breakthrough time for both BACs; increasing heating rate from 25 to 150 °C/min did not change BTR% for either BAC (BAC-50-07: 9.2% to 8.5 % and BAC-52-66: 11.8% to 12.8%). Conversely, for regeneration at 400 °C, increasing heating rate from 25 to 150 °C/min did increase BTR% for both BACs (BAC-50-07: 4.7% to 12.6 % and BAC-52-66: 7.9% to 18.5%). Therefore, two different trends were observed for BTR% as regeneration temperatures were increased from 288 to 400 °C. For low

heating rates (e.g., 25 °C/min), the higher regeneration temperature resulted in lower BTR%. This is consistent with our previous study that showed increasing the regeneration temperature from 288 to 400 °C using a low heating rate (< 10 °C/min) resulted in 47% lower BTR% (Lashaki et al., 2012). For higher heating rates (e.g., 150 °C/min), however, the higher regeneration temperature caused a greater BTR%.
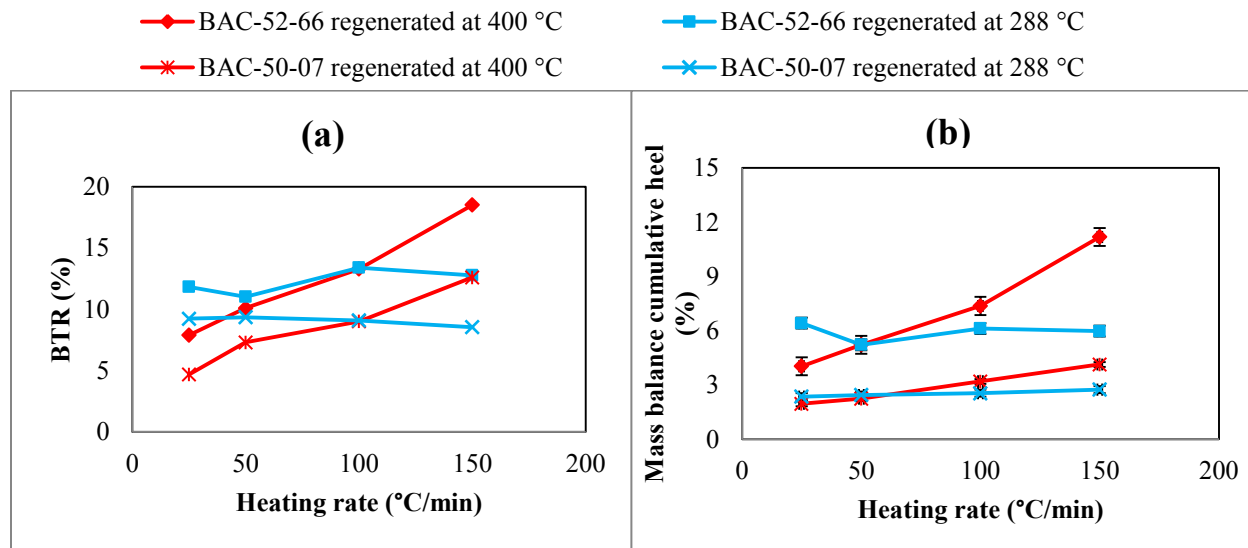
Figure 5-2 (a) BTR%, and (b) Cumulative heel for two BACs regenerated at 400 or 288 °C using different heating rates

Progressive reductions in breakthrough times were previously attributed to heel formation during adsorption/regeneration cycles (Lashaki et al., 2012). Accordingly, 5-cycle mass balance cumulative heel buildup was quantified for all considered conditions (Figure 5-2b). For regeneration at 288 °C, changing heating rate from 25 °C/min to 150 °C/min did not noticeably change heel formation after 5 cycles (<16% for BAC-50-07 and <10% for BAC-52-66). For regeneration at 400 °C, however, this increasing heating rate increased mass balance cumulative heel buildup after 5 cycles (by 92% for BAC-50-07 and 169% for BAC-52-66). For the high heating rate (150 °C/min), increasing regeneration

temperature increased heel by as much as 40% and 83% for BAC-50-07 and BAC-52-66, respectively. When a low heating rate (25 °C/min) was used, however, increasing regeneration temperature from 288 °C to 400 °C decreased heel by as much as 16% and 38% for BAC-50-07 and BAC-52-66, respectively. This is consistent with the previous work showing that an increase in regeneration temperature at a low heating rate (<10 °C/min) decreased heel buildup by up to 61% (Lashaki et al., 2012). These results suggest that regeneration conditions such as temperature and heating rate may increase or decrease heel buildup. Therefore, heel buildup can be minimized by optimizing the regeneration heating rate and temperature.

To characterize the type of heel present on regenerated samples, DTG analysis was used (Figure 5-3). For the samples regenerated at 288 °C (Figure 5-3a and Figure 5-3c), a single peak was observed at moderate DTG temperatures (280-340 °C), showing that physisorption is contributing to heel buildup (Jahandar Lashaki et al., 2016b). While changing the heating rate did not change the mass balance cumulative heel for these samples (Figure 5-2b), the DTG peaks have different amplitudes, showing that the heel consists of at least two parts: a physisorbed portion and a stable portion (likely coke) that could not be removed even at DTG temperatures as high as 800 °C. For both BAC samples, the amplitudes of the DTG peaks are inversely proportional to heating rate, indicating that the physisorbed portion was progressively less for higher heating rates. For the samples regenerated at 400 °C (Figure 5-3b and Figure 5-3d), no DTG peaks were observed, even at elevated temperatures, although these samples generally showed higher heel compared to samples regenerated at 288 °C. This suggests that the heel is solely non-desorbable; particularly since it could not be removed even at temperatures higher than 600 °C.
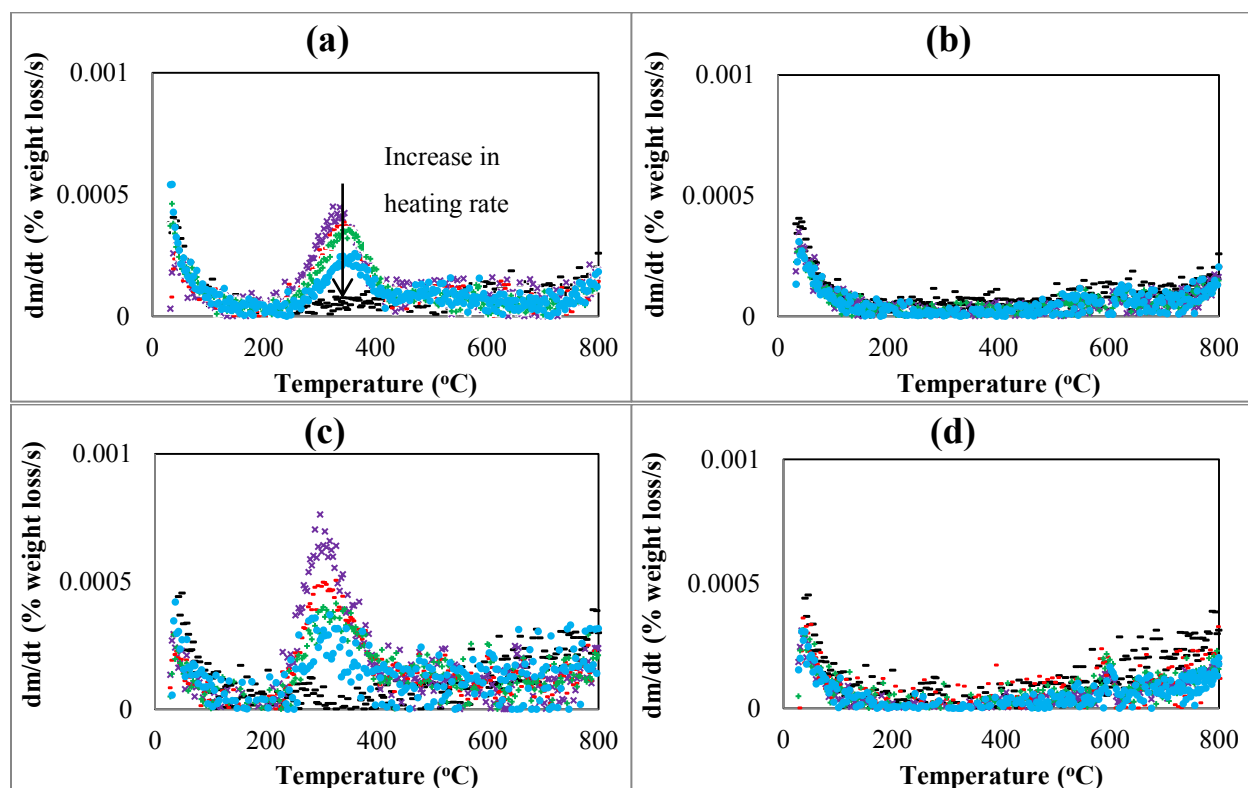
Figure 5-3 DTG curves for BAC-50-07 regenerated at (a) 288 °C and (b) 400 °C, and BAC-52-66 regenerated at (c) 288 °C and (d) 400 °C

For samples regenerated at 288 °C, the DTG-desorbed fraction after heating up to 800 °C was as high as 28.5% of the total heel (Figure 5-4). Therefore, for these samples, non-desorbable heel was dominant. For all samples regenerated at 400 °C, negative values were obtained for the desorbable heel percentage, i.e., greater DTG mass loss by virgin BAC samples than by BAC samples seeing TMB adsorption/desorption. This implies greater overall thermal stability of the TMB-exposed BAC samples relative to virgin BAC (Niknaddaf et al., 2015), possibly through removal of less stable carbon in the virgin BAC and/or deposition of more stable carbon from TMB during adsorption/desorption cycling. One possible mechanism for formation of non-desorbable heel is through desorbate decomposition (i.e., pyrolysis reaction), which deposits coke on the adsorbent surface. In this case, the

92

resulting heel cannot be removed unless exposed to oxidizing environments with temperatures > 600 °C (Álvarez et al., 2004, Ania et al., 2007). This hypothesis will be discussed in details in subsequent sections.
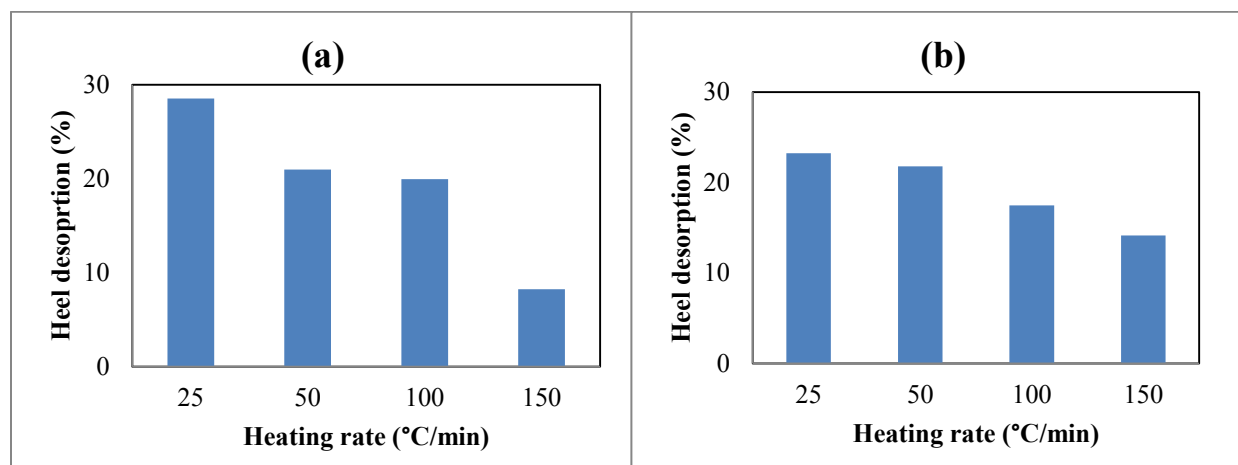
Figure 5-4 Heel desorption percentage for (a) BAC-50-07 and (b) BAC-52-66 regenerated at 288 °C using different heating rates.

For each regeneration test, most of the adsorbate was desorbed during temperature ramp up to the target regeneration temperature, highlighting the importance of heating rate in this study. Exposure of desorbate molecules to a sufficiently high temperature (e.g., 288 or 400 °C) could result in pyrolysis of the desorbate or coke formation on the carbon (Niknaddaf et al., 2015). In addition to regeneration temperature, the level of coke formation also depends on the yield of pyrolysis reaction, which is a function of the concentration of the participating organic compounds and their exposure time (i.e., time that adsorbate molecules in the pores were exposed to the high temperatures) inside the pores (Ancheyta, 2013, Basu, 2013, Moldoveanu, 2009). Therefore, it is expected that a higher heating rate could provide an initially higher concentration desorbate stream and higher exposure time of desorbate at high temperature, which may subsequently result in higher coke formation. To confirm this hypothesis, TMB effluent concentration during desorption after the first adsorption cycle were

measured (Figure 5-5). Although this concentration differs from the pore's concentration, it is a good indication of pore's concentration trend at different conditions. For all cases, the effluent concentration initially increased (up to 230 times higher than the inlet concentration during adsorption) and then dropped until reaching a plateau after approximately 15 min. Although both adsorbents had the same amount of TMB adsorbed, concentration peaks were slightly higher and sharper for BAC-52-66 than BAC-50-07, attributed to differences in porosity and mass transfer rates. Compared to BAC-50-07, BAC-52-66 has larger mesopore volume (0.66 versus 0.07 cm^3/g). Therefore, for BAC-52-66, desorption should be less restricted by diffusive mass transfer (Gritti and Guiochon, 2015). As a result, irrespective of regeneration temperature, desorption of adsorbate is faster in BAC-52-66 than BAC-50-07 (Jahandar Lashaki et al., 2016a). In addition, BAC-52-66 had smaller particle size relative to BAC-50-07 (i.e., 0.56 versus 0.70 mm) which might also contribute to the difference in diffusive mass transfer of the adsorbents (Tefera et al., 2013). With higher heating rates, the magnitude of the desorption concentration peak increased and the peak occurred at higher temperature (Figure 5-6b). For regeneration at 288 or 400 °C, having more TMB exposed to higher temperature may result in more coke formation. However a regeneration temperature of 288 °C may not suffice for triggering extensive coking reaction relative to 400 °C due to the endothermic nature of the reaction and coke formation is not detectable (Niknaddaf et al., 2015). Therefore, regeneration at higher temperature could result in higher coke formation. As mentioned earlier, higher concentration favors coking reactions. For each regeneration temperature, the desorption concentration for BAC-52-66 samples were higher than for BAC-50-07 samples, resulting in higher heel buildup (C.Moldoveanu, 2009).
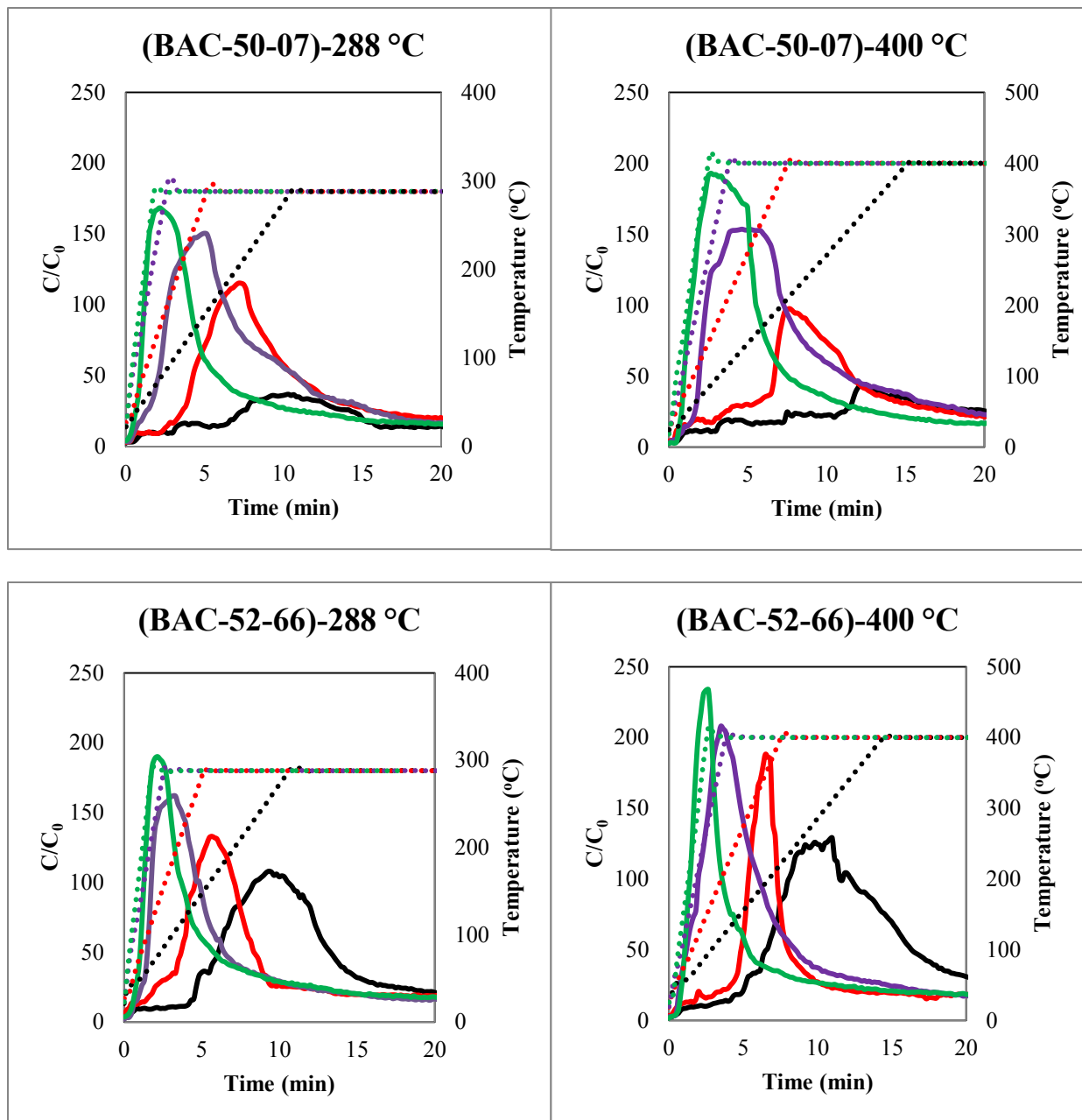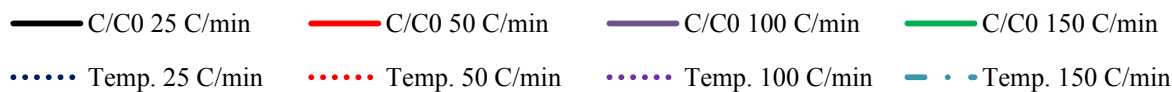
Figure 5-5 Outlet concentration during desorption and temperature profiles for BAC-50-07 and BAC-52-66 regenerated at 288 and 400 °C using various heating rates. Panels titles indicate adsorbent type and regeneration temperature.

A greater mass balance cumulative heel was observed for BAC with a higher pore's concentration (as indicated by the outlet concentration during desorption) after ramping to 400 °C (Figure 5-6a). However, this was not true for higher pore's concentration after ramping to 288 °C, but appeared to result in greater conversion of physisorbed heel into coke (Figure 5-4). The residual TMB amounts during first regeneration cycle were calculated and provided as Supporting Information (Figure A-2). When the temperature reached the target temperature, the residual TMB concentration is higher for the faster heating rates (Figure 5-6b). For each adsorbent, higher residual TMB at constant purge flow rate implies higher exposure time of TMB inside the pores, and consequently higher coke formation. Comparing residual TMB for both adsorbents at the same conditions indicated that BAC-50-07 has higher residual TMB than BAC-52-66 (Figure 5-6b), however higher TMB concentration of BAC-52-66 (Figure 5-5) resulted in higher mass balance cumulative heel (Figure 5-2b). These results indicated that higher TMB concentration and residual TMB (exposure time) both increase adsorbate decomposition but with different order of contribution and when they are against each other, the parameter with higher contribution determines the trend of adsorbate decomposition. However, specifying contribution of concentration and exposure time in adsorbate decomposition reaction requires a comprehensive kinetic study that is beyond the focus of this study.
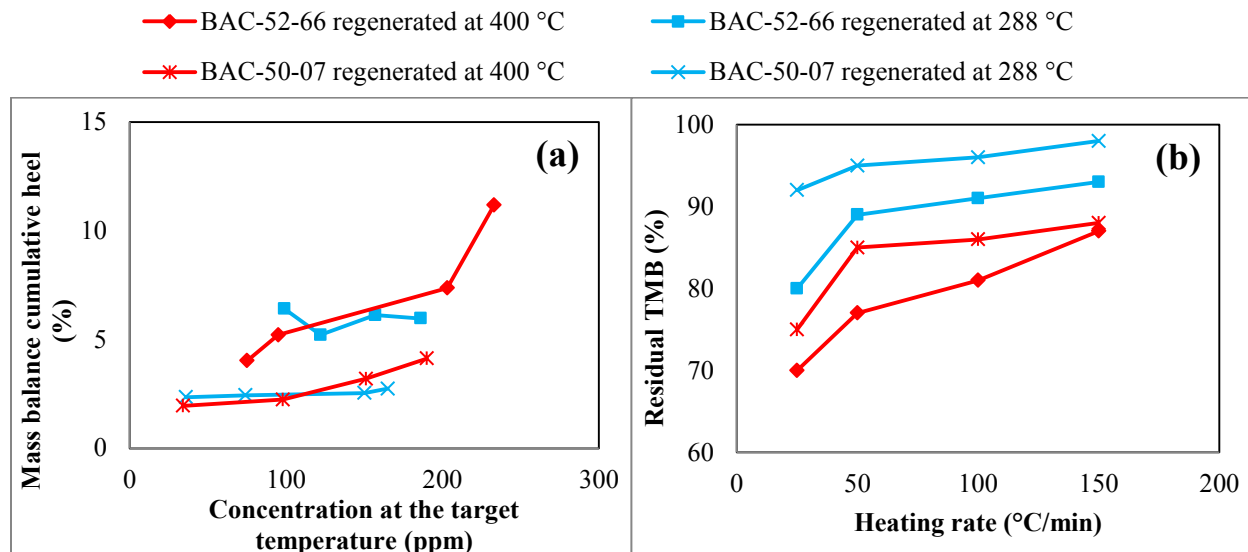
Figure 5-6 (a) Mass balance cumulative heel versus desorption concentration when the regeneration temperature reached the target temperature of 288 °C or 400 °C. For each set of data, the heating rate increased from left to right (i.e., 25, 50, 100 and 150 °C/min, correspondingly) (b) Residual TMB percentage for different samples exposed to the target temperatures

Figure 5-7 shows variation in BET surface area and pore volume for virgin and regenerated BACs. For all regeneration scenarios, independent of heel type (i.e., physisorption or coking), BET surface area, micropore volume, and total pore volume linearly decreased with heel formation. For each adsorbent, BAC regenerated at 400 °C has larger reduction in these properties because it has more heel than its 288 °C counterparts. This is consistent with previous work for BAC-50-07 that showed a proportional reduction in BET surface area and pore volume with accumulated heel (Lashaki et al., 2012b). During regeneration of BAC-52-66, heel formation also occurs in mesopore volume as evidenced by linear reduction of mesopore volume with heel. For BAC-52-66, heel buildup linearly reduces mesopore volume. For BAC-50-07, however, heel buildup did not affect mesopore volume. The different trends could be, at least in part, due to a measurement artifact associated with the significantly

smaller mesopore volume of BAC-50-07 relative to BAC-52-66, since mesopore volume is measured as the difference between total pore and micropore volumes.

Figure 5-7 Variation of BET surface area, micropore volume, mesopore volume, and total pore volume with mass balance cumulative heel for BAC-50-07 and BAC-52-66 regenerated at 288 and 400 $^\circ$C using various heating rates. Panels titles indicate adsorbent type and regeneration temperature.

To identify pore sizes contributing to heel formation, PSDs for regenerated samples were obtained (Figure 5-8). For BAC-50-07 samples regenerated at 288 or 400 °C, heel formation occurred in narrow micropores (<8 Å) and had no discernable impact on larger micropores (8-20 Å) and mesopores. For BAC-52-66, heel formation reduced larger micropores (8-20 Å) and midsize mesopores (40-130 Å). For each sample, the reduction in the volume of aforementioned pore size range/ranges increased with increase in heel formation.
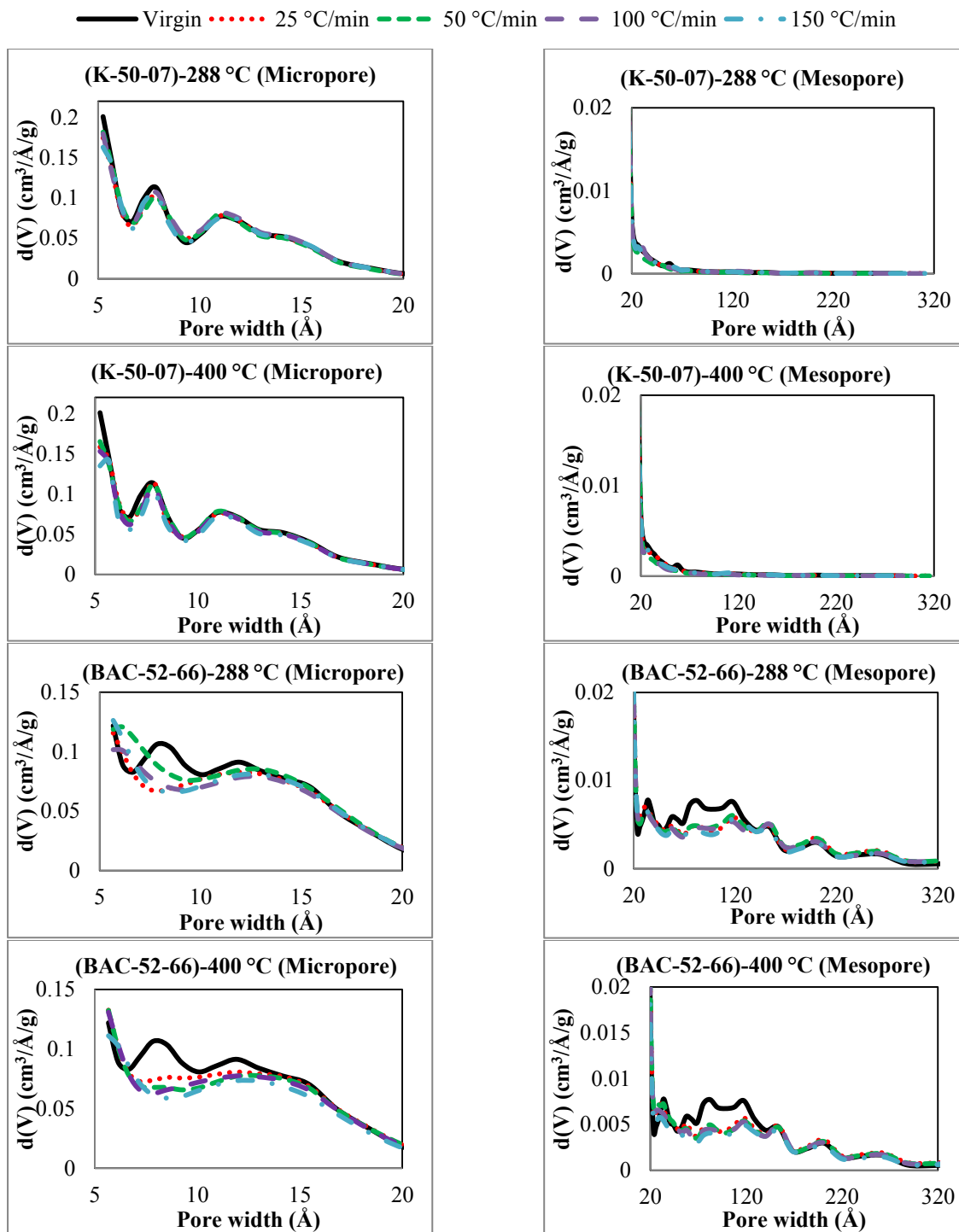
Figure 5-8 Micropore and mesopore size distribution for BAC-50-07 and BAC-52-66 regenerated at 288 and 400 °C using various heating rates. Panels titles indicate adsorbent type and regeneration temperature.

5.4 Conclusions

This study investigated the effect of activated carbon regeneration temperature, heating rate, and adsorbent porosity on heel formation. Two adsorbents with similar micropore volume but different mesopore volume were subjected to five successive adsorption/ regeneration cycles. For both regeneration temperatures, increasing the heating rate increased coke formation on the BACs. When a low heating rate was used, increasing the regeneration temperature decreased heel buildup. Conversely, when high heating rate was used, increasing the regeneration temperature increased heel buildup. Thermal analysis identified a combination of coke formation and physisorption as heel formation mechanisms for regeneration at 288 °C and solely coke formation at 400 °C. The results also showed that heel buildup occurred in the narrow micropores for the mainly microporous adsorbent, and in midsized micropores and mesopores for the partially microporous adsorbent. Contrary to the first proposed hypothesis of this study, the results suggest that for regeneration at high temperature, using a mainly microporous adsorbent resulted in lower heel buildup as compared to a mesoporous/microporous adsorbent, particularly in case of higher heating rates. The results from this study, however, confirmed the second proposed hypothesis of this study that using a fast heating rate during regeneration may negatively affect heel formation; therefore, to improve regeneration performance, heating rate should be optimized while considering the regeneration temperature and other system parameters. Although the purge gas flow rate was constant for all the experiments completed in this study, it can potentially affect heel formation along with other studied system parameters, demanding further studies to include the effect of purge gas flow rate variation.

5.5 References

ADU, B. & OTTEN, L. 1993. Simultaneous microwave heat and mass transfer characteristics of porous hygroscopic solids. *Microwave Power and Electromagnetic Engineering.,* 28**,** 41.

ÁLVAREZ, P. M., BELTRÁN, F. J., GÓMEZ-SERRANO, V., JARAMILLO, J. & RODRIGUEZ, E. M. 2004. Comparison between thermal and ozone regenerations of spent activated carbon exhausted with phenol. *Water Research,* 38**,** 2155-2165.

ANCHEYTA, J. 2013. *Modeling of Processes and Reactors for Upgrading of Heavy Petroleum*, CRC Press.

ANIA, C. O., MENÉNDEZ, J. A., PARRA, J. B. & PIS, J. J. 2004. Microwave-induced regeneration of activated carbons polluted with phenol. A comparison with conventional thermal regeneration. *Carbon,* 42**,** 1377-1381.

ANIA, C. O., PARRA, J. B., MENÉNDEZ, J. A. & PIS, J. J. 2005. Effect of microwave and conventional regeneration on the microporous and mesoporous network and on the adsorptive capacity of activated carbons. *Microporous and Mesoporous Materials,* 85**,** 7-15.

ANIA, C. O., PARRA, J. B., MENÉNDEZ, J. A. & PIS, J. J. 2007. Microwave-assisted regeneration of activated carbons loaded with pharmaceuticals. *Water Research,* 41**,** 3299-3306.

BASU, P. 2013. *Biomass Gasification, Pyrolysis and Torrefaction: Practical Design and Theory*, Elsevier Science.

BRIGGS, D. & SEAH, M. P. 1983. *Practical surface analysis: By auger and x-ray photoelectron spectroscopy,* New York, USA, Wiley: Chichester.

BRUNAUER, S., EMMETT, P. H. & TELLER, E. 1938. Adsorption of gases in multimolecular layers. *Journal of the American Chemical Society,* 60**,** 309-319.

C.MOLDOVEANU, S. 2009. *Pyrolysis of Organic Molecules Applications to Health and Environmental Issues,* Winston-Salem, NC, USA.

ÇALIŞKAN, E., BERMÚDEZ, J. M., PARRA, J. B., MENÉNDEZ, J. A., MAHRAMANLIOĜLU, M. & ANIA, C. O. 2012. Low temperature regeneration of

activated carbons using microwaves: Revising conventional wisdom. *Journal of Environmental Management,* 102**,** 134-140.

CHANG YUL, C. & CARLISLE, C. T. 2001. Microwave process for volatile organic compound abatement. *Journal of the Air and Waste Management Association,* 51**,** 1628-1641.

CHERBAŃSKI, S., R., KOMOROWSKA-DURKA, M., STEFANIDIS, G. D. & STANKIEWICZ, A. I. 2011. Microwave swing regeneration vs temperature swing regeneration - Comparison of desorption kinetics. *Industrial and Engineering Chemistry Research ,* 50**,** 8632-8644.

CHERBAŃSKI, R. & MOLGA, E. 2009. Intensification of desorption processes by use of microwaves-An overview of possible applications and industrial perspectives. *Chemical Engineering and Processing: Process Intensification,* 48**,** 48-58.

CHOWDHURY, T., SHI, M., HASHISHO, Z., SAWADA, J. A. & KUZNICKI, S. M. 2012. Regeneration of Na-ETS-10 using microwave and conductive heating. *Chemical Engineering Science,* 75**,** 282-288.

DI, P. & CHANG, D. P. Microwave regeneration of volatile organic compounds (VOC) adsorbents. 89th Annual Conference & Exhibition of A&WMA, Nashville, TN, 1996.

FAYAZ, M., SHARIATY, P., ATKINSON, J. D., HASHISHO, Z., PHILLIPS, J. H., ANDERSON, J. E. & NICHOLS, M. 2015a. Using microwave heating to improve the desorption efficiency of high molecular weight VOC from beaded activated carbon. *Environmental Science and Technology,* 49**,** 4536-4542.

FAYAZ, M., SHARIATY, P., ATKINSON, J. D., HASHISHO, Z., PHILLIPS, J. H., ANDERSON, J. E. & NICHOLS, M. 2015b. Using Microwave Heating To Improve the Desorption Efficiency of High Molecular Weight VOC from Beaded Activated Carbon. *Environmental Science and Technology,* 49**,** 4536–4542.

FAYAZ, M., WANG, H., JAHANDAR LASHAKI, M., HASHISHO, Z., PHILIPS, J. H. & ANDERSON, J. E. 2011. Accumulation of adsorbed of organic vapors from automobile painting operations on bead activated carbon. *Proceedings of the Air and Waste Management Association's Annual Conference and Exhibition, Orlando, FL.*

FERRO-GARCIA, M. A., JOLY, J. P., RIVERA-UTRILLA, J. & MORENO-CASTILLA, C. 1995. Thermal Desorption of Chlorophenols from Activated Carbons with Different Porosity. *Langmuir,* 11**,** 2648-2651.

FERRO-GARCIA, M. A., RIVERA-UTRILLA, J., BAUTISTA-TOLEDO, I. & MORENO-CASTILLA, C. 1996. Chemical and thermal regeneration of an activated carbon saturated with chlorophenols. *Journal of Chemical Technology & Biotechnology,* 67**,** 183-189.

GRITTI, F. & GUIOCHON, G. 2015. The quantitative impact of the mesopore size on the mass transfer mechanism of the new 1.9 μm fully porous Titan-C18 particles. I: Analysis of small molecules. *Journal of Chromatography A,* 1384**,** 76-87.

HA, S. R. & VINITNANTHARAT, S. 2000. Competitive removal of phenol and 2,4-dichlorophenol in biological activated carbon system. *Environmental Technology,* 21**,** 387-396.

HUA-SHAN, T. & CHIH-JU, G. J. 1999. Application of granular activated carbon packed-bed reactor in microwave radiation field to treat phenol. *Chemosphere,* 38**,** 2667-2680.

JAHANDAR LASHAKI, M., ATKINSON, J. D., HASHISHO, Z., PHILLIPS, J. H., ANDERSON, J. E. & NICHOLS, M. 2016a. The role of beaded activated carbon's pore size distribution on heel formation during cyclic adsorption/desorption of organic vapors. *Journal of Hazardous Materials,* 315**,** 42-51.

JAHANDAR LASHAKI, M., ATKINSON, J. D., HASHISHO, Z., PHILLIPS, J. H., ANDERSON, J. E., NICHOLS, M. & MISOVSKI, T. 2016b. Effect of desorption purge gas oxygen impurity on irreversible adsorption of organic vapors. *Carbon,* 99**,** 310-317.

JAHANDAR LASHAKI, M., FAYAZ, M., NIKNADDAF, S. & HASHISHO, Z. 2012. Effect of the adsorbate kinetic diameter on the accuracy of the Dubinin–Radushkevich equation for modeling adsorption of organic vapors on activated carbon. *Journal of Hazardous Materials,* 241–242**,** 154-163.

JONES, D. A., LELYVELD, T. P., MAVROFIDIS, S. D., KINGMAN, S. W. & MILES, N. J. 2002. Microwave heating applications in environmental engineering-a review. *Resources, Conservation and Recycling,* 34**,** 75-90.

KIM, B. R., KALIS, E. M. & ADAMS, J. A. 2001. Integrated emissions management for automotive painting operations. *Pure and Applied Chemistry,* 73**,** 1277-1280.

LASHAKI, M. J., FAYAZ, M., WANG, H., HASHISHO, Z., PHILIPS, J. H., ANDERSON, J. E. & NICHOLS, M. 2012a. Effect of adsorption and regeneration temperature on irreversible adsorption of organic vapors on beaded activated carbon. *Environmental Science and Technology,* 46**,** 4083-4090.

LU, Q. & SORIAL, G. A. 2004. Adsorption of phenolics on activated carbon - Impact of pore size and molecular oxygen. *Chemosphere,* 55**,** 671-679.

MOLDOVEANU, S. C. 2009. *Pyrolysis of Organic Molecules: Applications to Health and Environmental Issues*, Elsevier Science.

NIGAR, H., NAVASCUÉS, N., DE LA IGLESIA, O., MALLADA, R. & SANTAMARÍA, J. 2015. Removal of VOCs at trace concentration levels from humid air by Microwave Swing Adsorption, kinetics and proper sorbent selection. *Separation and Purification Technology,* 151**,** 193-200.

NIKNADDAF, S., ALAM, M., GHOLIDOUST, G., MOHAMMADREZA, F., ATKINSON, J. D., HASHISHO, Z., PHILIPS, J. H., ANDERSON, J. E. & NICHOLS, M. EFFECT OF DESORPTION CONDITIONS AND ADSORBATE PROPERTIES ON HEEL FORMATION DURING REGENERATION OF ACTIVATED CARBON FIBER CLOTH Conference on Carbon, 2016 Pennsylvania State University, USA.

NIKNADDAF, S., ATKINSON, J. D., SHARIATY, P., LASHAKI, M. J., HASHISHO, Z., PHILIPS, J. H., ANDERSON, J. E. & NICHOLS, M. 2015. Heel Formation during Volatile Organic Compound Desorption from Activated Carbon Fiber Cloth. *Carbon*, 196, 131-138.

Quantachrome Autosorb 1 Operating Manual, 2006

TEFERA, D. T., JAHANDAR LASHAKI, M., FAYAZ, M., HASHISHO, Z., PHILIPS, J. H., ANDERSON, J. E. & NICHOLS, M. 2013. Two-dimensional modeling of volatile organic compounds adsorption onto beaded activated carbon. *Environmental Science and Technology,* 47**,** 11700-11710.

THAKKAR, S. & MANES, M. 1987. Adsorptive displacement analysis of many-component priority pollutants on activated carbon. *Environmental science and technology,* 21**,** 546-549.

WEISSENBERGER, A. P. & SCHMIDT, P. S. 1994. Microwave Enhanced Regeneration of

Adsorbents. *MRS Proceedings,* 347

CHAPTER 6. MICROWAVE REGENERATION OF CARBONACEOUS AND POLYMERIC ADSORBENTS LOADED WITH VOCS

6.1 Introduction

During automobile painting operations, a wide range of volatile organic compounds (VOCs) are used. Many of these VOCs, such as 1,2,4-trimethylbenzene (TMB, 171 °C) and 2-butoxyethanol (BE, 171 °C) have high boiling points and usually have high affinity for the adsorbent, demanding higher temperature for efficient regeneration (Kim, 2011, Wang et al., 2013). Adsorption is widely used for controlling low concentration VOCs because of its high removal efficiency and cost-effectiveness (Bansode et al., 2003, Khan and Kr. Ghoshal, 2000, Lashaki et al., 2012, Weissenberger and Schmidt, 1994). A loaded adsorbent should be regenerated for adsorbent reuse and adsorbate recovery (Weissenberger and Schmidt, 1994). Steam or hot gas purging are conventionally used for regeneration (Di and Chang, 1996). For these heating methods, energy is transferred to the adsorbent by convection, conduction, and/or radiation of heat (Kuo, 2008). These techniques require long process duration, high energy consumption, and high volume of purge gas (Ania et al., 2007, Cherbański et al., 2011, Price and Schmidt, 1997).

Microwave heating is an alternative adsorbent regeneration technique. Microwave heating provides energy directly to the adsorbent and/or adsorbate via molecular interaction with the electromagnetic field (Chowdhury et al., 2012, Coss and Cha, 2000, Polaert et al., 2010, Reuß et al., 2002). Direct heating minimizes energy losses to the surroundings, allowing for shorter processing times, improved mass transfer, and easier adsorbate recovery (Adu and

Otten, 1993). These unique features of microwave heating can however compensate for the higher capital cost of a full-scale microwave system compared to systems using steam or hot inert gas, particularly when recovering valuable solvents (Cherbański and Molga, 2009).

The ability of a material to convert microwave energy into thermal energy is related to its dielectric properties, including dielectric constant (ε') and loss factor (ε''). The dielectric constant describes a material's ability to be polarized by an electromagnetic field, and loss factor describes a material's ability to convert absorbed energy into heat (Cherbański and Molga, 2009). For the same applied power, systems involving microwave absorbing adsorbents (e.g., activated carbon) and adsorbates (e.g., polar compounds such as water) absorb more total power and can achieve higher temperatures than microwave transparent adsorbents (e.g., silica gel and zeolite) loaded with non-polar adsorbates (e.g., toluene) (Polaert et al., 2010, Reuß et al., 2002). These results are expected, but power absorption does not necessarily control the regeneration efficiency of a given adsorbent/adsorbate system, as has been reported before (Shariaty et al., 2013).

Reuβ et al. (2012) showed that, with constant applied power, a microwave transparent adsorbent with a polar adsorbate can be regenerated effectively and completely. Based on heat transfer and microwave absorption model, the temperature increase for a polar adsorbate was significantly higher than that for a microwave transparent adsorbent, allowing for high regeneration efficiency (Burkholder et al., 1986). Other researchers have identified a linear relationship between desorption percentage and absorbed power in microwave transparent adsorbent with polar or non-polar adsorbate (Polaert et al., 2010).

Researchers also investigated the application of microwave heating at constant temperature. Chowdhury et al. (2012) compared the performance of conductive and

microwave heating methods during regeneration of a zeolite, Na-ETS-10, loaded with two binary mixtures (i.e., C_2H_4/C_2H_6 and CO_2/CH_4). While the required energy for microwave regeneration was 9% of that for conductive heating regeneration, gas recovery for C_2H_4/C_2H_6 and CO_2/CH_4 were 24 and 19% higher for microwave regeneration, respectively. In another study, it was observed that granular activated carbon (GAC) spent during carbon-in-pulp process, could be regenerated to virgin carbon activity levels (Bradshaw et al., 1998). Shariaty et al. (2013) used constant temperature heating to show increased water regeneration efficiency for adsorbents with lower dielectric properties.

Most of the studies investigating the effect of dielectric properties of adsorbent/adsorbate on microwave regeneration were completed using constant power. Extending the results from constant power scenarios to constant temperature scenarios is industrially relevant because uncontrolled heating can destroy adsorbents and/or adsorbates. In particular, when assessing the effect of the dielectric properties of adsorbates, previous studies did not consider effects of adsorbate boiling point, selecting adsorbates with boiling points between 56 and 111 °C. It is well-established that the difference between adsorbate boiling point and regeneration temperature impacts desorption efficiency (Fayaz et al., 2015), hence results reported in the literature cannot be exclusively attributed to differences in the dielectric properties of adsorbents and/or adsorbates. This research gap should be addressed through systematic studies investigating the impact of dielectric properties on desorption.

The hypothesis of this study is that during constant temperature regeneration, the dielectric properties of adsorbent/adsorbate affect energy consumption and desorption efficiency. The objective of this study, therefore, is to investigate the role of dielectric properties of adsorbent/adsorbate in microwave regeneration. The materials and regeneration

conditions in this study were chosen to highlight the role of dielectric properties in microwave heating and minimize the effect of other parameters. Specifically, this work uses adsorbents with contrasted dielectric properties (an activated carbon and a polymer-based adsorbent) but the same heat capacity. Unlike other reported studies, however, adsorbates (TMB and BE) with different dielectric properties but the same boiling points are selected to provide a controlled scenario that negates desorption differences attributed to boiling point difference. Additionally, the selected adsorbates have a notably higher boiling point than most other compounds studied for microwave regeneration (Coss and Cha, 2000, Hashisho et al., 2008, Polaert et al., 2010, Price and Schmidt, 1997, Reuß et al., 2002), extending the application potential of these systems to include industrial painting operations where high boiling point VOCs are common.

6.2   Experimental

6.2.1   Adsorbent and adsorbate

Adsorbents tested were beaded activated carbon (BAC, Kureha America, Inc.) and a beaded polymeric adsorbent (V493, DOWEX Optipore, DOW Chemical Company). BAC had a high microwave absorption (high dielectric loss factor) (Çalişkan et al., 2012) and V493 had a low microwave absorption (low dielectric loss factor) (Table 6-1).

Table 6-1 Thermal, dielectric, and structural properties of BAC and V493

Adsorbent	Heat capacity (J/(gK))	Thermal conductivity (W/(mK))	Dielectric loss factor at 2.45 GHz	BET surface area (m²/g)	Total pore volume (cm³/g)
BAC	1.2 [a]	1.7 [a]	4 – 34 [c]	1370[1]	0.55[1]
V493	1.2 [b]	0.1 [b]	0.04 [d]	1100[2]	1.16[2]

[a] Reported values from personal communication with Kureha America, Inc.
[b] Reported values from product information catalogue (Aragón Candelaria and Owens, 2009)
[c] Reported dielectric loss factor range (room temperature) for several activated carbon materials (Atwater and Wheeler Jr, 2003, Atwater and Wheeler Jr, 2004, Jou et al., 2009)
[d] Reported dielectric loss factor (room temperature) for DOWEX V502 polymeric adsorbent (Price and Schmidt, 1997)

Selected adsorbates were TMB (Sigma-Aldrich) and BE (Acros Organics). These adsorbates are commonly generated from painting processes (Kim, 2011, Wang et al., 2013). TMB is non-polar and has low dielectric loss factor while BE is polar and has high dielectric loss factor (Table 6-2). Both adsorbates have the same boiling point (171 °C), allowing for highlighting the effect of dielectric properties differences. Dielectric loss factors of TMB and BE (Table 6-2) were measured at 2.45 GHz using a dielectric probe kit (Keysight/Agilent Technologies, 85070E), connected to network analyzer (Agilent Technologies, VNA-E8362) at room temperature. The probe was vertically immersed in a beaker containing 100 ml of pure chemical.

Table 6-2 Thermal and dielectric properties of BE and TMB at 25 and 190 °C

Compound	Boiling Point (°C)	Density (g/ml)	Heat of vaporization (kJ/mol) (Carl, 2014)		Liquid heat capacity (J/(molK)) (Carl, 2014)		Gas heat capacity (J/(molK)) (Carl, 2014)		Dielectric loss factor at 2.45 GHz
			25 °C	190 °C	25 °C	190 °C	25 °C	190 °C	
TMB	171	0.876	46.9	37.7	213.5	255.0	156.8	223.7	2.60
BE	171	0.900	56.5	44.4	270.5	334.5	166.0	235.1	7.31

6.2.2 Experimental setup and methods

6.2.2.1 Adsorption

The experimental setup includes an adsorption tube, an adsorbate vapor generation system and a gas detection system (Figure 6-1). The tube used for microwave regeneration, was made of quartz (2.2 cm inner diameter, 35.6 cm length) with a coarse fritted glass disc for holding the sample. For conductive regeneration, a stainless steel tube (2.1 cm inner diameter, 15 cm length) was used. Glass-wool at the top and bottom of the fixed beds prevented adsorbent blowout. Both tubes were filled with 4.0 – 4.1 g of dry, virgin adsorbent.

The adsorbate vapor generation system consisted of a syringe pump (New Era Pump System Inc., NE-300) which injected liquid adsorbate into a dry, 10 standard liters per minute (SLPM, measured at 25 °C and 1 atm) air stream. The air flow rate was maintained using a mass flow controller (Alicat Scientific). The gas detection system consisted of a photoionization detector (PID, Rae System, Minirae 2000) that was calibrated before each test using the adsorbate stream generated with the vapor generation system. All adsorption tests were completed at room temperature for 30 min using an inlet VOC concentration of 500 ppm$_v$, allowing for partial loading of the adsorbent. Since adsorbents have different pore

volume, continuing adsorption until saturation would have led to different loadings on each adsorbent. Thus, both adsorbents were loaded to 15.4 ± 0.8 wt%.

6.2.2.2 *Microwave regeneration*

After adsorption, the quartz tube was transferred to the microwave applicator for regeneration (Figure 6-1). The microwave regeneration setup was similar to the one described by Fayaz et al. (2015) and Chowdhury et al. (2012), and included a 2-kW switch-mode power supply (Alter, SM745G.1), a 2-kW microwave source (National Electronics, MH2.0W-S) supplied with a 2.45 GHz magnetron, an isolator (National Electronics), a three stub tuner (National Electronics), and a waveguide applicator connected to a sliding short (Chowdhury et al., 2012). Power was measured and monitored using a dual-directional coupler with 60 db attenuation (Mega Industries), two power sensors (Agilent Technologies, 8481 A), and a dual channel microwave power meter (Agilent Technologies, E44119B). Forward (applied) power was measured throughout all experiment. The power supply and meter were interfaced to a data acquisition and control (DAC) system (National Instrument, Compact DAQ), and a LabVIEW program (National Instrument) was used to record data and control heating. Temperature was measured at the center (height) and middle (width) of the bed using a fiber optic temperature sensor and a signal conditioner (Neoptix, Reflex Signal Conditioner). During regeneration, the DAC system controlled temperature by adjusting the applied power using a proportional-integral-derivative control algorithm. The outlet VOC concentration was continuously measured (10 s sampling interval) using a flame ionization detector (FID, Baseline-Mocon, series 9000). Regeneration was completed at 190 °C for 1 h in 1 SLPM dry N_2 flowing in the same direction as the adsorption flow.

The desorption efficiency was calculated based on gravimetric measurements:

$$\text{Desorption efficiecny (\%)} = \left(1 - \frac{\text{Adsorbent weight after regeneration} - \text{Adsorbent weight before adsorption}}{\text{Adsorbent weight after adsorption} - \text{Adsorbent weight before adsorption}}\right) X100$$
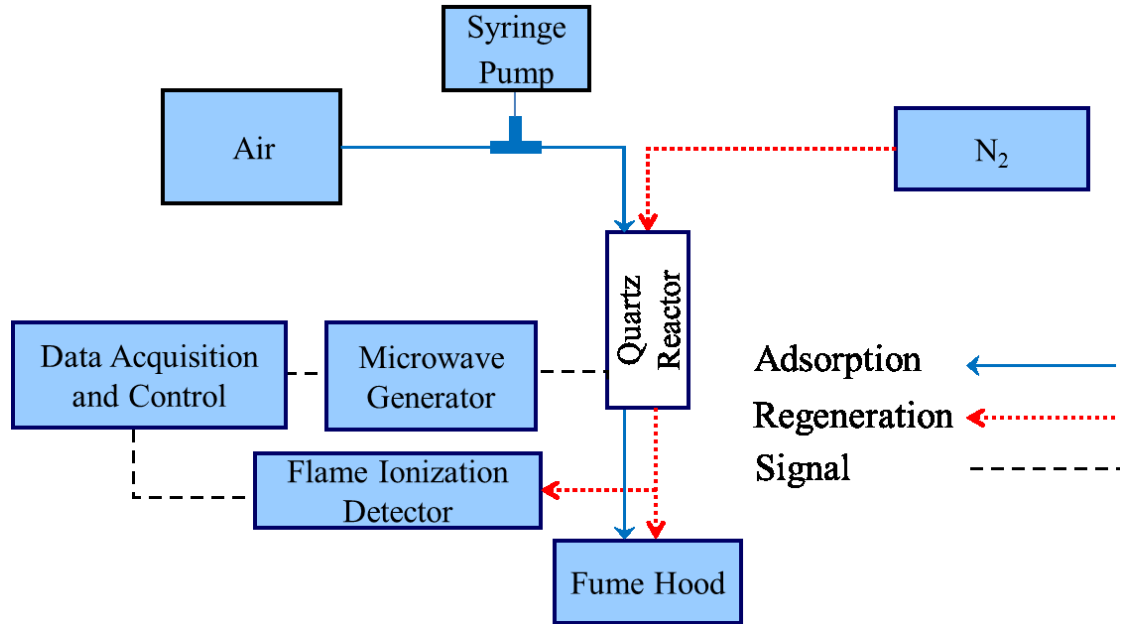
Figure 6-1 Block diagram of the adsorption and microwave regeneration setups

6.2.2.3   *Conductive heating regeneration*

For comparison, conductive heating regeneration was completed with similar conditions as microwave regeneration (190 °C for 1 h in 1 SLPM dry N_2). The experimental setup used for conductive heating regeneration is described in details in previous studies (Fayaz et al., 2015). The setup consisted of a heating module and a DAC system. The heating module included heating tape, insulation tape and a type K thermocouple. During regeneration, the heating tape and insulation tape were wrapped around the adsorption tube and temperature was controlled and recorded by the DAC system. A proportional-integral-derivative algorithm was used to control temperature by controlling the power applied to achieve the set-point temperature. The energy consumed throughout regeneration was calculated by integrating the applied power profile over time.

Each experiment was completed for one cycle of adsorption/regeneration. Blank tests for both regeneration methods were also conducted by heating virgin adsorbents under the same regeneration conditions mentioned above. All the tests were duplicated, and the average results with standard deviations are presented throughout results and discussions section.

6.3   Results and Discussion

Figure 6-2a (V493) and Figure 6-2b (BAC) describe The amount of applied energy (microwave or conductive) required for the different adsorbent/adsorbate systems to reach the desired 190 °C temperature set-point. Adsorbate impacts on microwave regeneration are most significant at the beginning of desorption, before significant adsorbate mass is removed from the adsorbent (Shariaty et al., 2013). The corresponding temperature profiles are provided in Figure 6-3a (V493) and Figure 6-3b (BAC). Moreover, applied power profiles for all regeneration tests are provided in supporting information document.
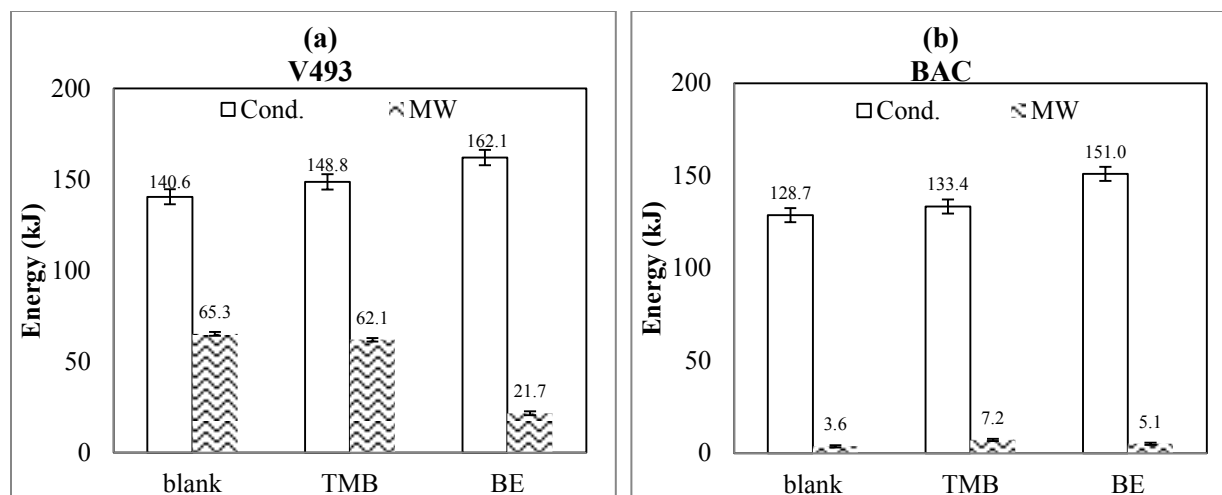
Figure 6-2 Applied energy during conductive (Cond.) and microwave (MW) heating required to reach 190 °C for (a) V493 and (b) BAC samples

For V493 partially loaded with TMB or BE, the applied microwave energy required to reach 190 °C was lower by 5% or 67%, respectively compared to blank V493. Price and Schmidt (1997) showed that polar and non-polar adsorbates increased the dielectric loss factor of a loaded polymeric adsorbent by 6 and 1.75 times compared to the blank adsorbent, respectively. Both TMB and BE have higher loss factors than V493 (Table 6-1 and Table 6-2), hence, after adding adsorbate to the microwave transparent adsorbent, it is expected that loss factor for both loaded samples increased. Therefore the applied power could be more efficiently absorbed and dissipated by the loaded samples, especially the one loaded with polar adsorbate. In fact, the applied microwave energy required to reach 190 °C for V493-TMB was 2.9 times that for V493-BE since BE (polar) has higher dielectric loss factor than TMB (non-polar) (Table 6-2). The difference in applied energy for samples loaded with polar and non-polar adsorbates highlights the importance of the adsorbate's dielectric properties for adsorbents with low loss factor.

117

For temperatures considered here, the heat capacity of BE is higher than that of TMB (Table 6-2). Based solely on these values, it is expected that *less* energy is required for an adsorbent loaded with TMB to reach the set-point temperature than for the adsorbent loaded with BE. The opposite trend, however, was observed for microwave heating of V493 (Figure 6-2a). It can be concluded that the effect of improved dielectric properties of BE outweigh its greater heat capacity. To validate this conclusion, conductive heating regeneration of the same samples was completed. Conductive heating is independent of the dielectric properties of adsorbent or adsorbates, so the role of heat capacity is isolated. As anticipated, the applied energy required to achieve 190 °C for V493-TMB and V493-BE was within 9%. For the blank V493, the applied energy, required to achieve the target temperature is 6 and 13% lower than V493-TMB and V493-BE, respectively, because there is less total mass to heat. The results justify the prior conclusion that for the microwave transparent adsorbent, impacts of adsorbate dielectric properties are more relevant than impacts associated with heat capacities. It should be noted that energy requirements for conductive heating are notably higher than those for microwave heating. This difference is attributed to less efficient heating during conductive heating, with energy losses attributed to heating the sweep gas and adsorption tube or convection and radiation to the surrounding environment (Di and Chang, 1996). For the blank V493, and V493 loaded with TMB and BE, the applied energy with conductive heating is, respectively, 1.2, 1.4, and 6.5 times the applied energy values for microwave heating. The higher value for the case of BE shows the effectiveness of microwave heating for regeneration of a microwave transparent adsorbent loaded with a polar adsorbate.

Activated carbon is microwave absorbing and has a notably larger dielectric loss factor than the polymeric adsorbent (Atwater and Wheeler Jr, 2003, Price and Schmidt, 1997). A wide range of dielectric loss factors have been reported for activated carbons (Table 6-1), and all are at least two orders of magnitude larger than the polymeric adsorbent (Atwater and Wheeler Jr, 2003, Atwater and Wheeler Jr, 2004, Jou et al., 2009). The presence of delocalized π electrons on the surface of activated carbon allows for high microwave dissipation compared to the polymeric material (Çalişkan et al., 2012). As such, with microwave heating, blank BAC requires 94% less energy to reach 190 °C (and does so 72% faster) than blank V493 (Figure 6-2a and Figure 6-2, and Figure 6-3a and Figure 6-3b). For BAC samples, microwave energy is more effectively absorbed resulting in shorter heating time and lower heat losses hence allowing for lower energy consumption. Unlike V493, however, adsorbate addition results in increased applied energy requirements to reach the set-point temperature. The applied energy in systems with adsorbed TMB and BE is 100% and 42% higher than the blank BAC, respectively, implying that the tested adsorbates decreases the overall loss factor of the loaded adsorbent. While an accurate measurement of BAC's loss factor was not available, it can be concluded that the value is larger than the loss factor of BE (7.31), which is consistent with the reported range of dielectric loss factors for other activated carbon materials (Atwater and Wheeler Jr, 2003, Atwater and Wheeler Jr, 2004, Jou et al., 2009). The 41% higher applied energy for BAC-TMB compared to BAC-BE is then attributed to the lower dielectric loss factor of the non-polar adsorbate, causing a more drastic decrease in the net loss factor of the system. Because BAC and V493 have similar heat capacities, differences in applied energies for the blank adsorbents are mainly attributed to differences in the dielectric properties of the adsorbents. For the blank samples, the ratio of applied energy

119

for V493 over that for BAC was more than 18.1 but it decreased to 8.6 and 4.2 when the samples were loaded with TMB and BE, respectively. Decreases in the applied energy ratios for the two loaded adsorbents compared to the blank adsorbents are attributed to adsorbates increasing the net system loss factors for V493 and decreasing the net system loss factors for BAC.

Similar to V493, the use of conductive heating for regenerating BAC negates any impact of adsorbate dielectric properties. For conductive heating, the applied energy required to achieve 190 °C for the BAC-BE and BAC-TMB systems was within 13%. For all BAC systems, the relative difference between applied energy during conductive heating and applied energy during microwave heating is larger than for V493 samples. This suggests that energy improvements from switching from conductive to microwave heating are more significant for microwave absorbing adsorbents.

With V493 (microwave transparent adsorbent), the impact of adsorbate dielectric properties is also evident when observing the rate of temperature increase during the experiments (Figure 6-3a). Temperature reached 190 °C after 7.2 min for blank V493, 6.7 min for V493-TMB, and 2.8 min for V493-BE. When V493 was loaded with BE and TMB, the required time to reach 190 °C decreased by 7% and 61%, respectively. These reductions are consistent with decreases in applied energy required to achieve the set-point temperature (5% and 67% for V493-BE and V493-TMB, respectively). The temperature profile of V493-BE rapidly increased as the concentration of desorbed BE increased in the purge stream. The temperature increase was so fast that the DAC was not fast enough in stabilizing the system's temperature by appropriately adjusting the power level.
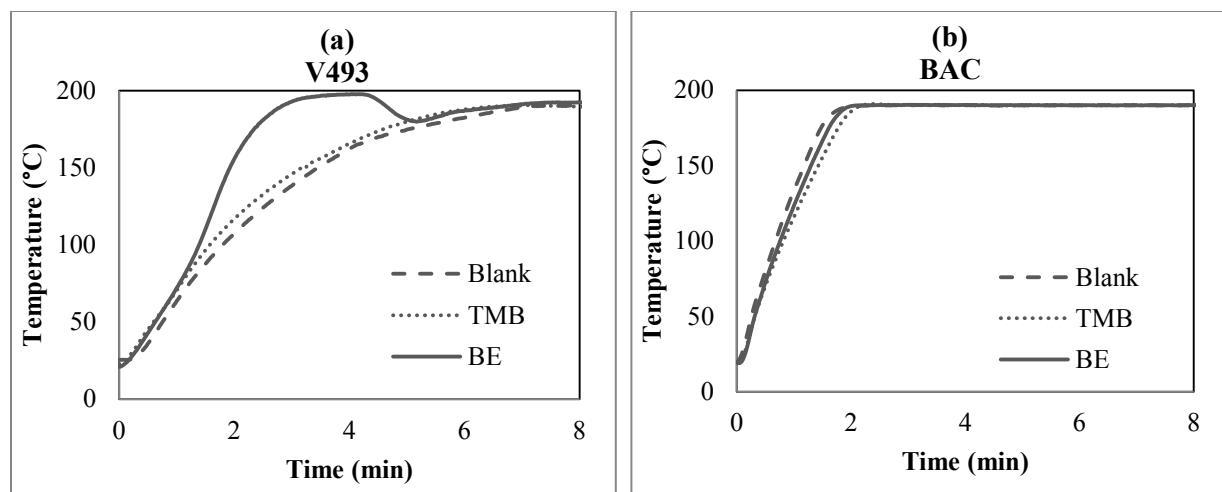
Figure 6-3 Temperature profiles during microwave heating of (a) V493 and (b) BAC samples

In contrast to V493, for all BAC samples, temperature increased to the target value with a similar rate. The similarity of the temperature profiles indicates the dominant role of the BAC when heating the sample to the target temperature with microwaves. For conductive heating, the set-point temperature was achieved between 26 and 28 min for all systems. This slower heating rate is attributed to the heat transfer mechanism and heat losses (Cherbański et al., 2011).

For BAC samples, time to reach 190 °C was 71% (blank), 66% (TMB), and 28% (BE) shorter than the V493 samples. The same reasons presented above for energy requirements can be used to explain the differences in heating rates. Loss factor differences between V493 and BAC systems are most significant for the blank scenarios, followed by the TMB and BE scenarios. In particular, the lower difference in heating times for the BE systems relative to the blank and TMB systems highlights the significant loss factor improvement for V493-BE compared to blank V493.

During desorption, the instantaneous desorbed VOC (i.e., desorption rate) profile could be obtained by monitoring the outlet concentration. Derivative of desorption rate (DDR) represents how fast and intense desorption occurs (Figure 4-4). The maximum DDR and corresponding times during microwave regeneration as well as total applied energy during the 60 min experiments are shown in Table 6-3. Maximum DDR for V493-TMB occurred 4 times later than for V493-BE. Although V493-TMB required 36% more applied energy than V493-BE (Table 6-3), the maximum DDR for BE was 5 times higher than for TMB. Because V493 has a low loss factor and low thermal conductivity, desorption occurs through direct heating of adsorbate molecules in V493 pores. The significantly higher maximum DDR for BE compared to that for TMB, is mainly due to the difference in the dielectric properties of adsorbates. In this scenario (microwave transparent adsorbent), the adsorbate loss factor controls desorption – a higher loss factor for BE compared to TMB leads to faster and more significant desorption with lower energy demand. The interaction between BE and microwave was so high that the maximum desorption rate occurred before the set-point temperature was reached (2.8 min). The difference in molecular size of adsorbates might also contribute to this trend; however, the molecular size difference is overshadowed by difference in dielectric properties of the adsorbate. Similar to heat capacity discussion, impacts of adsorbate dielectric properties outweigh impacts of heats of vaporization when direct energy absorption by the adsorbate occurs.
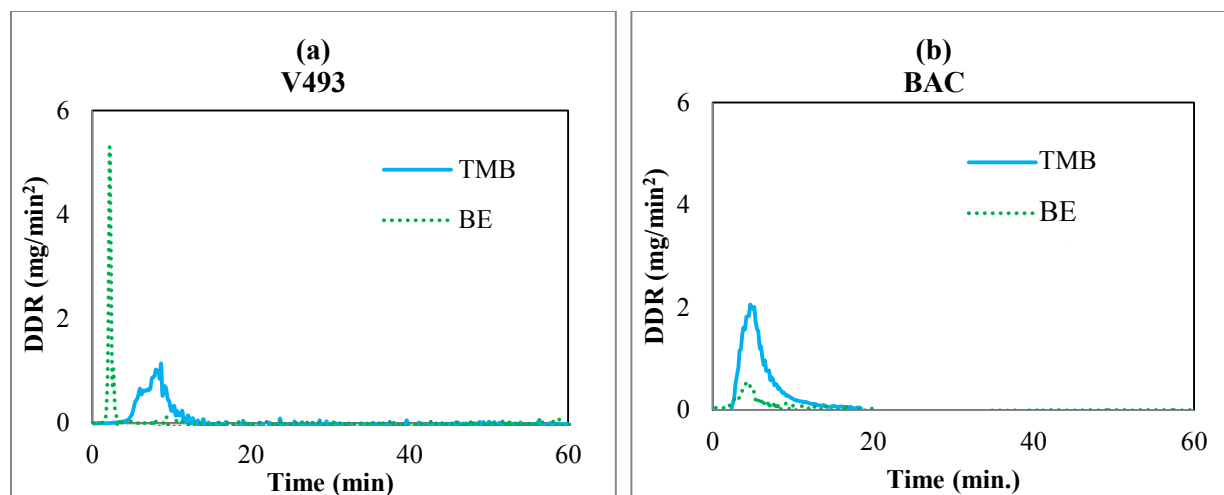
Figure 6-4 DDR during desorption of adsorbents loaded with VOCs

Table 6-3 Microwave desorption performance of tested adsorbent-adsorbate systems

Adsorbent	Adsorbate	Maximum DDR (mg/min^2)	Time of Maximum DDR (min)	Energy Applied (kJ)	Desorption Efficiency (%)	Mass Desorbed per Applied Energy (mg/kJ)
V493	TMB	1.1±0.1	8.8±0.2	552.9±6.8	43.7±2.0	0.5±0.0
	BE	5.3±0.2	2.2±0.1	406.7±5.4	81.3±1.3	1.2±0.1
BAC	TMB	2.1±0.1	4.2±0.0	76.8±3.0	59.8±0.5	5.1±0.0
	BE	0.6±0.1	4.0±0.1	47.2±1.5	42.1±1.0	5.7±0.1

For BAC, maximum DDR for both adsorbates occurred at the same time, about 4 min after starting regeneration (Table 6-3). This is likely because the BAC adsorbent, with high dielectric loss factor, controls the heating rate when loaded with either adsorbates. While the effects of adsorbate dielectric properties are expected to be less significant than with V493, it was unexpected that the maximum DDR for BAC-TMB was higher than that of BAC-BE. For BAC-TMB, the applied energy throughout the entire experiment was 63% higher than that of BAC-BE (Table 6-3). Also, as shown in Table 6-2, the heat of vaporization of BE is

123

consistently higher than that of TMB, respectively. Therefore, for BAC-TMB, higher energy absorption combined with a lower heat of vaporization contributed to a faster desorption and higher regeneration efficiency.

The non-polar adsorbate (TMB) percent desorbed increased by 37% when using a microwave absorbing adsorbent (BAC) instead of a microwave transparent one (V493) (Table 6-3). Because direct energy absorption with TMB is low, adsorbent heating is required to desorb the adsorbate. Since BAC has a higher dielectric loss factor and thermal conductivity than V493, it is the preferred adsorbent, at least in terms of desorption efficiency, for non-polar adsorbates (Reuß et al., 2002).

For V493 loaded with a polar adsorbate, the direct heating of the adsorbate mainly contributed to desorption. However, for BAC loaded with the polar adsorbate, the adsorbate is mainly heated through the BAC. Results, therefore, show that, in terms of desorption efficiency, the preferred scenario for a polar adsorbate is one where direct adsorbate heating can occur.

Desorption efficiencies are not consistent with energy requirements, so results were standardized to assess each system's performance using the mass desorbed per unit energy applied (Table 6-3). For V493-BE compared to V493-TMB, 140% more mass is desorbed per unit of applied energy; for BAC, the difference was only 12%. Once again, adsorbate dielectric property differences are more significant for the microwave transparent adsorbent.

From a practical perspective, selecting an adsorbent for a given adsorbate depends on process objectives (e.g., saving energy or achieving to the highest possible adsorbent/adsorbate recovery). For TMB, the applied energy for desorption from V493 is about 6 times of that for desorption from BAC and desorption efficiency for V493 is 27%

lower than for BAC. Therefore, using a microwave absorbing adsorbent is more favorable for desorption of a non-polar adsorbate. For desorption of BE, applied energy for desorption from V493 was 7.5 times that for desorption from BAC but its desorption efficiency was 93% higher. There is a distinct trade-off between energy requirements and desorption performance. For expensive, recoverable adsorbates, where higher desorption efficiency is favorable, a microwave transparent adsorbent is more suitable. This will also result in less frequent adsorbent replacement, which would provide additional cost-savings. Conversely, for low cost adsorbates, energy savings associated with the use of a microwave absorbing adsorbent may be more relevant for the given process.

6.4 Conclusions

This study investigated the effect of the dielectric properties of adsorbents and adsorbates on constant temperature microwave regeneration. Two adsorbents with different dielectric properties (BAC, DOWEX V493) but the same heat capacity and two VOCs (TMB, BE) with the same boiling point but different dielectric properties were investigated. The dielectric loss factor of V493 (microwave transparent adsorbent) increased after loading with polar or non-polar adsorbates. For BAC (microwave absorbing adsorbent), however, added adsorbate decreased the overall loss factor of the system, resulting in slower heating and increased energy requirements compared to blank BAC. For regeneration at constant temperature, high loss factor adsorbents showed improved energy usage but did not show improved regeneration efficiency. The highest mass desorbed per unit of applied energy was for the adsorbent/adsorbate pair with the highest dielectric loss factor (BAC-BE), and the lowest value was for the system with the lowest dielectric loss factor (V493-TMB). These results indicate improved performance for microwave transparent adsorbents with polar

adsorbates and microwave absorbing adsorbents with non-polar adsorbates. These results confirmed the hypothesis proposed in this study that during microwave heating regeneration at constant temperature, dielectric properties of adsorbent and adsorbate affect energy consumption and desorption efficiency.

6.5   References

ADU, B. & OTTEN, L. 1993. Simultaneous microwave heat and mass transfer characteristics of porous hygroscopic solids. *Journal of Microwave Power and Electromagnetic Energy,* 28**,** 41.

ANIA, C. O., PARRA, J. B., MENÉNDEZ, J. A. & PIS, J. J. 2007. Microwave-assisted regeneration of activated carbons loaded with pharmaceuticals. *Water Research,* 41**,** 3299-3306.

ARAGÓN CANDELARIA, P. R. & OWENS, A. J. 2009. Prediction of architectural coating performance using titanium dioxide characterization applying artificial neural networks. *Journal of Coatings Technology and Research,* 7**,** 431-440.

ATWATER, J. E. & WHEELER JR, R. R. 2003. Complex permittivities and dielectric relaxation of granular activated carbons at microwave frequencies between 0.2 and 26 GHz. *Carbon,* 41**,** 1801-1807.

ATWATER, J. E. & WHEELER JR, R. R. 2004. Microwave permittivity and dielectric relaxation of a high surface area activated carbon. *Applied Physics A: Materials Science and Processing,* 79**,** 125-129.

BANSODE, R. R., LOSSO, J. N., MARSHALL, W. E., RAO, R. M. & PORTIER, R. J. 2003. Adsorption of volatile organic compounds by pecan shell- and almond shell-based granular activated carbons. *Bioresource Technology,* 90**,** 175-184.

BRADSHAW, S. M., VAN WYK, E. J. & DE SWARDT, J. B. 1998. Microwave heating principles and the application to the regeneration of granular activated carbon. *Journal of The South African Institute of Mining and Metallurgy,* 98**,** 201-210.

BURKHOLDER, H. R., FANSLOW, G. E. & BLUHM, D. D. 1986. Recovery of ethanol from a molecular sieve by using dielectric heating. *Industrial and Engineering Chemistry Fundamentals,* 25**,** 414-416.

ÇALIŞKAN, E., BERMÚDEZ, J. M., PARRA, J. B., MENÉNDEZ, J. A., MAHRAMANLIOĜLU, M. & ANIA, C. O. 2012. Low temperature regeneration of activated carbons using microwaves: Revising conventional wisdom. *Journal of Environmental Management,* 102**,** 134-140.

CARL, Y. 2014. Yaws' Handbook of Thermodynamic and Physical Properties of Chemical Compounds.

CHERBAŃSKI, R., KOMOROWSKA-DURKA, M., STEFANIDIS, G. D. & STANKIEWICZ, A. I. 2011. Microwave Swing Regeneration vs Temperature Swing Regeneration—Comparison of Desorption Kinetics. *Industrial and Engineering Chemistry Research,* 50**,** 8632-8644.

CHERBAŃSKI, R. & MOLGA, E. 2009. Intensification of desorption processes by use of microwaves-An overview of possible applications and industrial perspectives. *Chemical Engineering and Processing: Process Intensification,* 48**,** 48-58.

CHOWDHURY, T., SHI, M., HASHISHO, Z., SAWADA, J. A. & KUZNICKI, S. M. 2012. Regeneration of Na-ETS-10 using microwave and conductive heating. *Chemical Engineering Science,* 75**,** 282-288.

COSS, P. M. & CHA, C. Y. 2000. Microwave regeneration of activated carbon used for removal of solvents from vented air. *Journal of the Air and Waste Management Association,* 50**,** 529-535.

DI, P. & CHANG, D. P. Microwave regeneration of volatile organic compounds (VOC) adsorbents. Presented in 89th Annual Conference & Exhibition of A&WMA, Nashville, TN, 1996.

FAYAZ, M., SHARIATY, P., ATKINSON, J. D., HASHISHO, Z., PHILLIPS, J. H., ANDERSON, J. E. & NICHOLS, M. 2015. Using microwave heating to improve the desorption efficiency of high molecular weight VOC from beaded activated carbon. *Environmental Science and Technology,* 49**,** 4536-4542.

HASHISHO, Z., EMAMIPOUR, H., ROOD, M. J., HAY, K. J., KIM, B. J. & THURSTON, D. 2008. Concomitant adsorption and desorption of organic vapor in dry and humid air streams using microwave and direct electrothermal swing adsorption. *Environmental Science and Technology,* 42**,** 9317-9322.

JOU, C. J. G., WU, C. R. & LEE, C. L. 2009. Application of microwave energy to treat granular activated carbon contaminated with chlorobenzene. *Environmental Progress and Sustainable Energy,* 29**,** 272-277.

KHAN, F. I. & KR. GHOSHAL, A. 2000. Removal of Volatile Organic Compounds from polluted air. *Journal of Loss Prevention in the Process Industries,* 13**,** 527-545.

KIM, B. R. 2011. VOC emissions from automotive painting and their control: A review. *Environmental Engineering Research,* 16**,** 1-9.

KUO, C. Y. 2008. Desorption and re-adsorption of carbon nanotubes: Comparisons of sodium hydroxide and microwave irradiation processes. *Journal of Hazardous Materials,* 152**,** 949-954.

LASHAKI, M. J., FAYAZ, M., WANG, H., HASHISHO, Z., PHILLIPS, J. H., ANDERSON, J. E. & NICHOLS, M. 2012. Effect of adsorption and regeneration temperature on irreversible adsorption of organic vapors on beaded activated carbon. *Environmental Science and Technology,* 46**,** 4083-4090.

POLAERT, I., ESTEL, L., HUYGHE, R. & THOMAS, M. 2010. Adsorbents regeneration under microwave irradiation for dehydration and volatile organic compounds gas treatment. *Chemical Engineering Journal,* 162**,** 941-948.

PRICE, D. W. & SCHMIDT, P. S. 1997. Microwave regeneration of adsorbents at low pressure: Experimental kinetics studies. *Journal of Microwave Power and Electromagnetic Energy,* 32**,** 145-154.

REUß, J., BATHEN, D. & SCHMIDT-TRAUB, H. 2002. Desorption by microwaves: Mechanisms of multicomponent mixtures. *Chemical Engineering and Technology,* 25**,** 381-384.

SHARIATY, P., LASHAKI, M. J., HASHISHO, Z., SAWADA, J., KUZNICKI, S. & HUTCHEON, R. Effect of ETS-10 Modification On Its Dielectric Properties and Microwave Regeneration. AIChE, 2013 San Francisco, CA.

WANG, H., NIE, L., LI, J., WANG, Y., WANG, G., WANG, J. & HAO, Z. 2013. Characterization and assessment of volatile organic compounds (VOCs) emissions from typical industries. *Chinese Science Bulletin,* 58**,** 724-730.

WEISSENBERGER, A. P. & SCHMIDT, P. S. 1994. Microwave Enhanced Regeneration of Adsorbents. *MRS Proceedings,* 347**,** 383-387.

CHAPTER 7. A NOVEL TECHNIQUE TO DETERMINE THE ADSORPTION CAPACITY AND BREAKTHROUGH TIME OF ADSORBENTS USING A NON-CONTACT HIGH RESOLUTION MICROWAVE RESONATOR SENSOR

7.1 Introduction

Adsorption is a useful technique for controlling emissions of volatile organic compounds (VOCs) since it allows their recovery and reuse (Hashisho et al., 2008, Kim et al., 2007, Dimotakis et al., 1995). Following adsorption, the loaded adsorbent should be regenerated to restore its adsorption capacity and recover the adsorbed VOCs (Shah et al., 2014). Breakthrough time, which is the time required for the outlet concentration to reach 1%-5% of the inlet concentration, has been recognized as a criterion for ending the adsorption process and switching to the regeneration (Jain et al., 1997). Direct measurement of the effluent concentration during adsorption is typically used to determine breakthrough time (Fayaz et al., 2015, Lashaki et al., 2012, Wang et al., 2012). To perform the breakthrough-time measurement, the monitoring instruments should be directly in contact with the effluent stream, which might be hazardous for the user or might contaminate and damage the detectors in the presence of high boiling point and toxic or corrosive compounds (Lashaki et al., 2012). Therefore, introducing a technique for non-contact determination of breakthrough time could be industrially relevant.

The performance of an adsorption system depends on the adsorption capacity of the adsorbent. Adsorption capacity for different concentrations of a VOC can be expressed in the form of an adsorption isotherm (Pei and Zhang, 2012). Adsorption isotherms for some VOCs

on different adsorbents (e.g., activated carbon or zeolite) could be obtained using several techniques such as dynamic column method (Seo et al., 2009), static volumetric method (Yun et al., 1998), gravimetric method (Cal et al., 1997), and sometimes a combination of these methods (Yun et al., 1999). All the aforementioned techniques used in the studies on determination of adsorption isotherms used adsorbates with low to moderate boiling points such as acetaldehyde, methyl ethyl ketone, benzene, toluene, xylene and cumene (Benkhedda et al., 2000a, Benkhedda et al., 2000b, Cal et al., 1997, Jahandar Lashaki et al., 2012, Kim et al., 2007, Ryu et al., 2002, Yun et al., 1999). Obtaining adsorption isotherms for high boiling point adsorbates or corrosive/toxic compounds can be challenging as these compounds can contaminate/damage instruments and/or pose health risk.

Microwaves signals are electromagnetic waves in the frequency range of 0.3-300 GHz. Microwave techniques have demonstrated a significant potential in areas related to environmental engineering, such as microwave heating for adsorbent regeneration and microwave sensing (Fayaz et al., 2015, Rubel et al., 2009, Abou-Khousa et al., 2015, Al-Dasoqi et al., 2011, Yunus et al., 2011, Yunus and Mukhopadhyay, 2011). Dielectric properties of materials play important roles when microwave techniques are used. Dielectric properties of materials consist of dielectric constant (ε') and loss factor (ε"). The dielectric constant describes a material's ability to be polarized by an electromagnetic field, and loss factor describes a material's ability to convert absorbed energy into heat (Cherbański and Molga, 2009). Microwave sensing uses a non-contact method to monitor the variation of the dielectric properties of materials in the vicinity of the sensor, which makes the sensor attractive for use in harsh environments (e.g., corrosive or toxic gases). Recent studies demonstrated that the residual lifetime of an activated carbon, used in adsorption of water

vapor, can be estimated by monitoring the variations in its dielectric properties (Mason et al., 2014, Rubel et al., 2009).

Mason et al. (2014) developed a microwave cavity resonator to determine the residual lifetime of activated carbon exposed to water vapor. For this purpose the variation in the permittivity of carbon was correlated to its exposure time to water vapor. However, the cavity-based resonator sensor used in that study had moderate quality factor and was in direct contact with the carbon and adsorbate, which can restrict its applications in some harsh and noisy environments. Rebel et al. (2009) developed an in-situ sensing device based on impedance measurement to measure water vapor adsorption capacity of granular activated carbon (GAC) by monitoring capacitance variation in an electronics circuit. Staudt et al. (1999) used a combination of gravimetric and impedance analysis to measure dielectric properties of gas molecules in adsorbed phase, and correlate them to the adsorbed amount. The reported sensors in the previous studies have simple structure and are low cost; however, they are more vulnerable to noise (Varadan et al., 2006) than the resonant-based counterparts since they are operating based on capacitive sensing method. Recently microwave planar resonators have been widely used due to their various range of applications, complementary metal oxide semiconductor (CMOS) compatibility for on-board chip process, easy design and fabrication, and low cost. Study of planar microwave resonators utilizing split ring resonators has been widely popular in sensing applications due to their moderately high quality factors and small size (Korostynska et al., 2014, Lee et al., 2010). Their high performance in non-contact sensing also made planar resonators more useful for gas sensing applications (Potyrailo and Morris, 2007, Potyrailo et al., 2012, Zarifi et al., 2015b, Zarifi et al., 2015c). Microwave planar sensors can be coated with an adsorbent to estimate the concentration of

VOCs. de Fonsecaa et al. (2015) used planar sensor coated with different zeolites as sensitive material to detect different concentrations of toluene in measurement atmosphere. These resonators are sensitive to variation in dielectric properties of the surrounding medium. Specifically, during adsorption, any change in the loading state of the adsorbents can be translated into a change in their electrical properties that result in shift in resonant frequency (f_r) as well as the quality factor (Q) of the resonator's frequency response, where f_r is the frequency at which maximum power transmission occurs, and Q is the ratio of f_r to the -3db frequency bandwidth, the frequency span at which more than half of maximum is transferred through the sensor (Lowell, 1991, Mason et al., 2014, Zarifi et al., 2015a). The significantly high electromagnetic loss in planar microwave resonators leads to a low to moderate quality factor and consequently low resolution in sensing applications. In order to resolve such an issue, a newly developed active sensor is used where the loss of system is compensated using an active feedback (Zarifi et al., 2015a, Zarifi et al., 2015d). This constructive regeneration of power cancels out the effect of high loss and improves the quality factor for orders of magnitude.

The objective of this study is to investigate the application of a microwave resonator sensor for measuring breakthrough time and adsorption capacity of adsorbents loaded with high boiling point VOCs. This sensor utilizes a very high quality factor microwave resonator for contactless sensing of the permittivity change in the adsorbent (Zarifi et al., 2015b). During adsorption, the variations in the sensor's resonant frequency and quality factor are measured and monitored using a vector network analyzer (VNA). These changes are used to determine the breakthrough time and adsorption capacity of a carbonaceous (microwave absorbing or lossy) and a polymeric (microwave transparent) adsorbents loaded with VOCs.

Two high boiling point VOCs with different polarities are used as adsorbates. Adsorbents and adsorbates with contrasted dielectric properties are selected to demonstrate the effectiveness of the proposed technique and device for determining the breakthrough time in non-contact way.

7.2 Experimental

7.2.1 Adsorbents and adsorbates

Beaded activated carbon (BAC, Kureha Corporation) and beaded polymeric adsorbent (V503, DOWEX Optipore, DOW Chemical Company) are two adsorbents used in this work. BAC is a microwave absorbing (lossy) adsorbent, and V503 is a microwave transparent (low loss) adsorbent. Both adsorbents are in the form of spherical beads, and widely used for capturing VOCs from industrial streams (Lashaki et al., 2012). For BAC, Brunauer Emmett Teller (BET) surface area and total pore volume are 1339 m^2/g and 0.56 cm^3/g, respectively (Zarifi et al., 2015a). For V503, BET surface area and total pore volume are 963 m^2/g and 0.79 cm^3/g, respectively (Zarifi et al., 2015a). 1,2,4-trimethylbenzene (TMB, 98%, Sigma-Aldrich) and 2-butoxyethanol (BE, 99%, Acros Organics) were used as adsorbates. These two compounds are common VOCs emitted during painting and surface coating operations (Kim, 2011, Wang et al., 2013). Both compounds have the same boiling point (171 °C); however, BE is polar while TMB is non-polar. Therefore, the dielectric constant and loss factor of BE are higher than of TMB (Reuß et al., 2002). The contrasted dielectric properties of the select adsorbents and adsorbates allow testing the performance of the sensor for an adsorbent/adsorbate system with low permittivity (i.e., V503/TMB) and a system with high permittivity (i.e., BAC/BE).

7.2.2   Experimental setup and methods

7.2.2.1   *Adsorption*

The experimental setup is presented in Figure 7-1a. The setup consisted of an adsorption tube, adsorbate vapor generation system, gas detection system and data acquisition and control (DAC) system. The tube was made of quartz with 2.2 cm inner diameter and 35.6 cm length. Prior to each adsorption experiment, it was filled with 4.1±0.1g of the adsorbent. A fritted glass disk held the adsorbent bed in place. The vapor generation system consisted of a syringe pump (KD Scientific, KDS-220) that injected liquid adsorbate into a dry air stream to achieve the target concentration. The air flow rate was initially set to 10 standard liters per minute (SLPM, 25 °C and 1 atm) using a mass flow controller (Alicat Scientific). The gas detection system consisted of a photoionization detector (PID, Minirae 2000, Rae Systems) that monitored concentration of the adsorbate at the tube's outlet. The measured concentration was linearly correlated to a voltage signal, sent to DAC, and recorded by LabVIEW program. The PID was calibrated before each experiment using the adsorbate stream, generated with the vapor generation system. When the outlet concentration reached the inlet concentration, the adsorbent was considered to be saturated. For each adsorbate, the inlet concentrations in the inlet stream were selected according to the adsorbate relative pressure, of 0.03, 0.1, 0.2, 0.4 and 0.6. Using the ideal gas low, the liquid injection rate of the syringe pump was calculated so that the inlet concentration of the adsorbate in the air stream was equal to the corresponding relative pressure. Before starting each adsorption test, the inlet concentration was measure by PID to make sure that it is equal to the desired value. The DAC system consisted of a LabVIEW program (National Instruments) and a data logger (National

Instruments, Compact DAQ) equipped with analog input and output modules to record outlet VOC concentration.

After saturation, adsorption capacity was determined using Equation (1):

$$\text{Adsorption capacity (g/g)} = \frac{W_{AA} - W_{BA}}{W_{BA}} \qquad (1)$$

where W_{AA} is the adsorbent weight after adsorption and W_{BA} is the adsorbent weight before adsorption.

All gravimetric measurements were conducted while the reactor was capped to avoid any adsorbate loss.

(a)   (b)
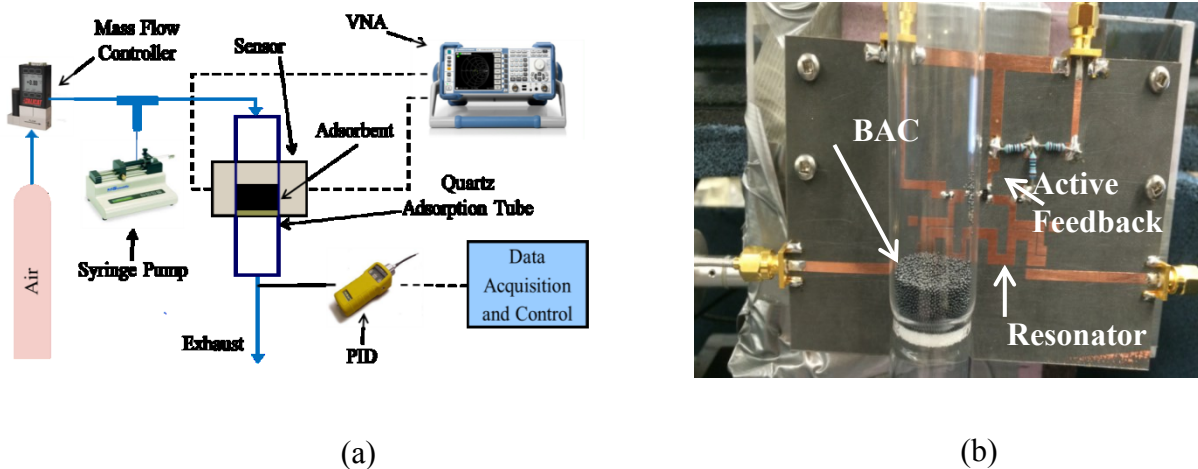
Figure 7-1 (a) Schematic diagram of the adsorption setup and, (b) Picture of the microwave resonator sensor used for non-contact testing of BAC

7.2.2.2 *Dielectric properties measurements*

During adsorption, the dielectric properties of virgin adsorbents and adsorbates affect the slope and direction of the resonant frequency (i.e., up or down frequency shift). Therefore,

the dielectric properties of adsorbents and adsorbates should be measured to qualitatively verify the experimental results from the proposed sensor.

The apparatus used to acquire complex permittivity (dielectric properties) of materials under test consists of a VNA (supplied by Rohde and Schwarz), equipped with an open-ended coaxial probe (Keycom), and data acquisition software. Measurements of the solvents were performed at 25 °C and 1 atmosphere. After placing the sample in a quartz tube (2 cm inner diameter, 2 cm length), dielectric property measurements were conducted from 500MHz to 2GHz. Reflection coefficients of the electromagnetic waves from materials under test at each frequency were measured. The material affects the phase and magnitude of the reflected power observed by the VNA, from which the complex permittivity is calculated.

7.2.2.3 *Sensor analysis*

A microwave planar open-ended resonator sensor is used to monitor the changes in the dielectric properties of BAC and V503 during adsorption of VOCs. The resonant profile of the sensor (S_{21}-parameter) is observed and recorded during adsorption process and the main parameters such as resonant frequency (f_r) and quality factor (Q) are extracted from the resonant profile. As noted earlier, the resonant frequency is defined as the frequency where the maximum power transmission occurs. Moreover, the quality factor is a ratio of the resonant frequency to the -3 dB bandwidth of the resonant profile as $Q = f_r/\Delta f_{3dB}$. In the developed sensor, the resonant frequency is initially designed at 1.42 GHz with a controllable quality factor. The quality factor can be controlled and adjusted in a range of 200 to 200000 (Zarifi et al., 2015c).

The sensor used in this study is a half wavelength resonator, illustrated in Figure 7-1b. The resonant frequency is related to the effective permittivity of the wave-propagation environment according to Equation 2 (Zarifi et al., 2015a).

$$f_r = \frac{c}{2\lambda_g\sqrt{\varepsilon_{\text{eff}}}} \tag{2}$$

where $c = 3\times10^8$ (m/s) is the speed of light, f_r (Hz) the resonant frequency, ε_{eff}_the effective permittivity of the wave-propagation environment, and λ_g (m) represents the guided wavelength.

During adsorption the changes in the dielectric properties of adsorbent are detected by the sensor through measuring the changes in quality factor and resonant frequency. The environmental conditions around the sensor were kept stable during all experiments (e.g., no temperature change nor mechanical shock around the setup). For each test, steady state results before starting and after finishing adsorption confirmed the stable environmental conditions around the sensor. The passive resonator coupled with transmission line was turned into an active resonator by introducing a positive feedback loop. The loop acts as a negative resistor to the device and returns the lost energy due to radiation or lossy substrate back into the system, resulting in a high quality factor resonator (Jones et al., 2014). The utilized microwave sensor was fabricated on a RO5880 (Roger Corporation) substrate with permittivity of 2.2, loss tangent of 0.0009 and thickness of 0.787 mm. Also, the thickness of the copper trace on the sensor was 35 microns.

The effective distance that the sensor is sensitive to the changes in the dielectric properties is 8 cm. During adsorption, the sensor was placed at a fixed distance of 1 cm away from the tube and the sensing area was 1 cm from the bottom of the adsorbent bed

(Figure 7-2b). The position of the sensor with respect to the tube was selected so that the measurements were conducted with the highest possible accuracy. The resonator along with the adsorbent could then be described using a simple circuit model, expressed as a parallel capacitor and a resistor, where the changes in the capacitance and resistance could be described by variations in the resonant frequency and quality factor provided by the sensor, respectively. During adsorption, the dielectric properties of an adsorbent/adsorbate system, exposed to microwaves, change according to Cole and Cole equation (Staudt et al., 1999). The equivalent complex permittivity in the medium is described as $\varepsilon = \varepsilon' - j\varepsilon''$ where ε' is the dielectric constant which is related to the equivalent capacitor, and ε'' is the dielectric loss factor which is related to the equivalent resistor. Thus, the changes in the quality factor and resonant frequency of the sensor could be obtained from the changes in the dielectric properties of the loaded adsorbent. According to Equation 2, as the effective permittivity of the medium increases, the resonant frequency shifts downward. Such an ultrahigh quality factor reduces the minimum detectable permittivity variation of materials according to Equation 3 and increases the resolution of the device in permittivity sensing. This enables the non-contact high precision operation of the sensor (Zarifi et al., 2015a):

$$|\Delta\varepsilon_{min}| = \frac{9\varepsilon\sqrt{3}}{2V_{omax}Q} \times \sqrt{4kTBR} \tag{3}$$

where Q is the quality factor (-), k is the Boltzmann constant (1.38×10^{-23} m^{2}kg s^{-2}K^{-1}), T is the room temperature (K), B is the measured bandwidth (Hz), R is the resistance (Ω), ε is the complex permittivity (-), and V_{omax} is the maximum amplitude of the resonance profile (V).

All the tests were completed in duplicates, and the average results with standard deviations are presented. However, the standard deviation values were so small that they might not be clearly observed in the figures (i.e., ≤6 kHz and ≤0.011 g adsorbate/g adsorbent for frequency and adsorption capacity, respectively).

7.3   Results and Discussion

A comparison between the simulated resonant profiles in passive and active states of the resonator sensor is demonstrated in Figure 7-2a. The simulation is performed in high frequency software simulator (HFSS) based on finite element method and the electric filed distribution around the sensor is shown in Figure 7-2b. Electric field distribution around the sensor is an important factor in determining the performance of the sensor in non-contact operations. Changes in the dielectric properties of materials in the near vicinity of the sensor can alter the electric field and changes in the electric field can be translated to changes in the frequency and quality factor in the response profile of the sensor. Electric field simulation illustrates strong hot-spots on the microstrip resonator at the resonant frequency. These hot spots are the most suitable positions for placing the tested materials and allow the sensor to achieve the maximum sensitivity.
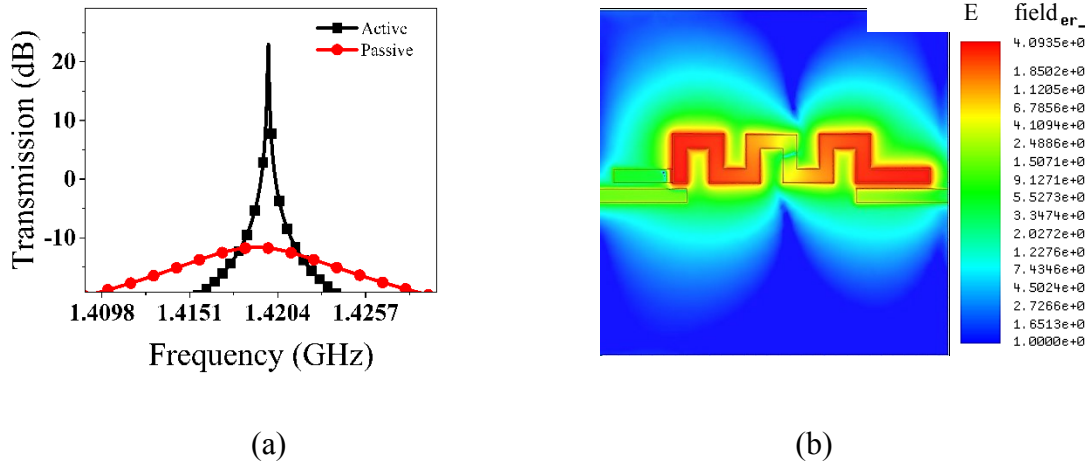
Figure 7-2 (a) Comparison between active and passive response profile in Full Wave Simulation, (b) Electric Field distribution in surface of sensor at 1.42 GHz

7.3.1 Breakthrough time

Figure 7-3a shows the location of the adsorbent bed with respect to the sensor. During adsorption, the accumulation of the adsorbed molecules in liquid-like phase in the adsorbent as well as gas concentration between the adsorbent beads change the dielectric properties of the loaded adsorbent. The changes in the dielectric properties of the adsorbent are detected in terms of quality factor and resonant frequency shift (i.e., ΔQ and Δf_r, respectively). The downward direction of gas flow during adsorption resulted in saturation of the adsorbent bed from top to bottom. The extension of the saturation zone through the bed (from point a to b in Figure 7-3a) alters the electric field of the sensor and creates more shift in the quality factor and resonant frequency. Figure 7-3b shows variations in the relative quality factor and outlet concentration during adsorption of BE on V503 for different relative pressures. For different relative pressures, when the saturation zone approaches the end of the bed, the quality factor stops changing (i.e., $\Delta Q = \Delta Q_{final}$). Meanwhile, the adsorbent gets saturated and the outlet

141

concentration starts increasing. Therefore, the time that the quality factor stops changing is similar to the breakthrough time.
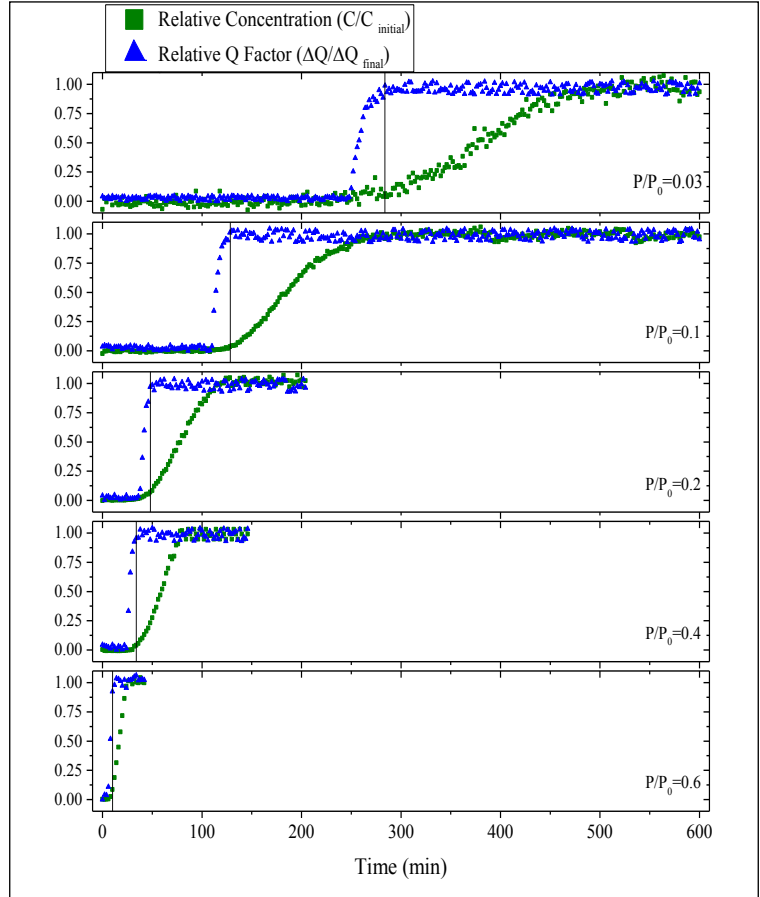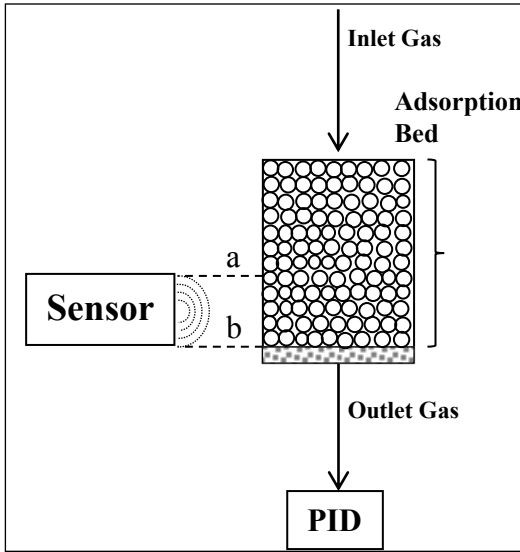
(a)   (b)

Figure 7-3 Changes to the effluent concentration (expressed as $C/C_{initial}$) and quality factor (expressed as $\Delta Q/\Delta Q_{final}$) during adsorption of BE on V503

t_Q is defined as the time that ΔQ reaches 95% of ΔQ_{final}, and breakthrough time (t_b) is defined as the time that the outlet concentration reaches 5% of the inlet concentration (i.e. when $C/C_{initial} = 0.05$). Figure 7-4 indicates that for all experiments in this study, regardless of the adsorbent and adsorbate type, the difference between t_b and t_Q is less than 5%. Therefore, breakthrough time can be estimated by monitoring the changes in the quality factor.
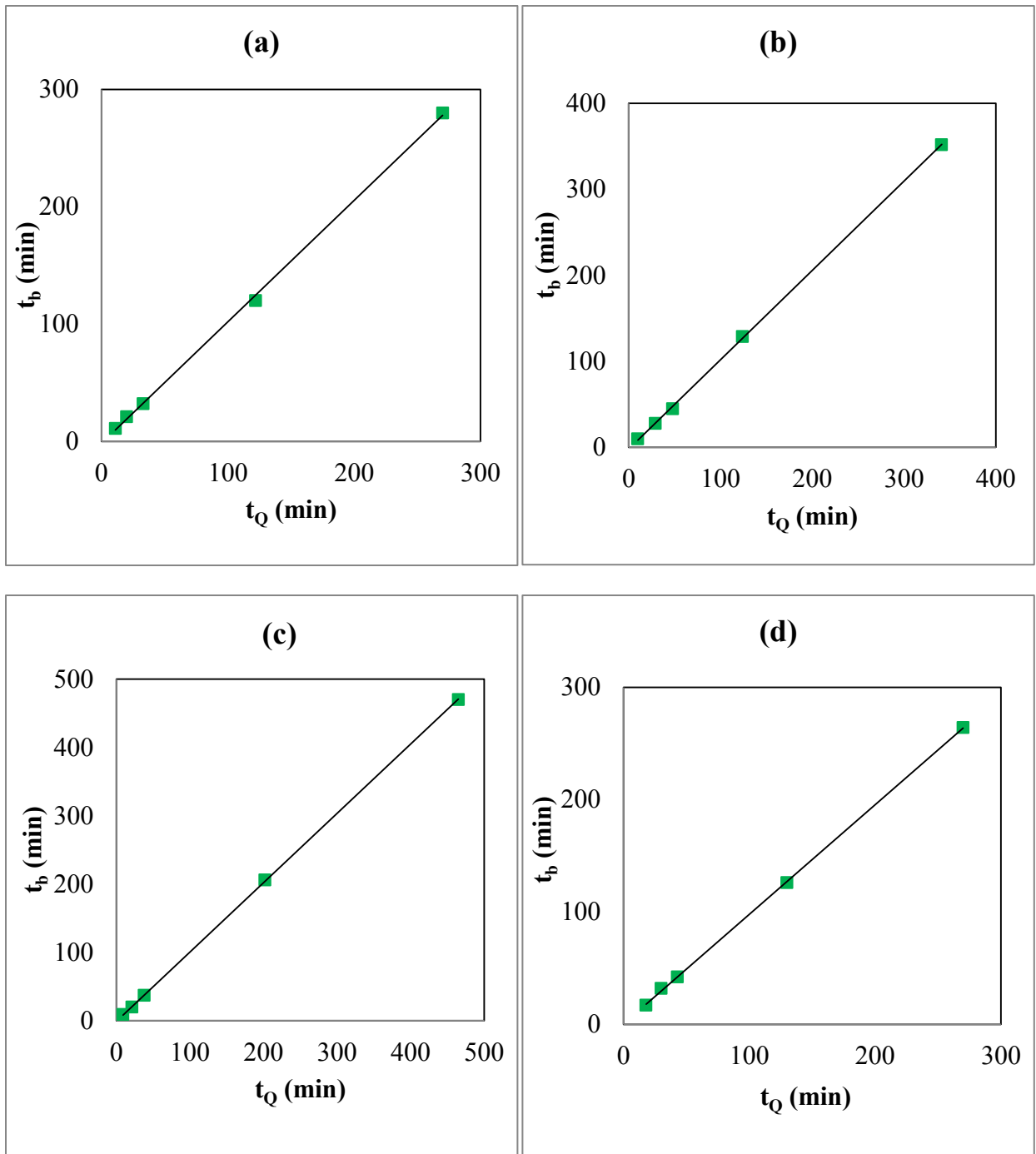
Figure 7-4 t_b versus t_Q for adsorption of (a) TMB on BAC (b) TMB on V503 (c) BE on BAC and (d) BE on V503

7.4 Adsorption capacity

The high quality factor of the resonator enables it to detect very small changes in the dielectric properties of the sensitive area in front of the sensor based on the shift of the resonant frequency. Therefore, in addition to adsorbed VOC, the VOC concentration in the space between the beads affects permittivity in the environment and consequently, the resonant frequency. Adsorption, however, results in more significant shift in resonant frequency; because after adsorption VOC state changed from gas phase to liquid-like phase in the adsorbent pores (Zarifi et al., 2015a). When the saturation zone reaches the sensitive area, the resonant frequency gradually increases until the adsorbent reaches complete saturation (Figure 7-5).
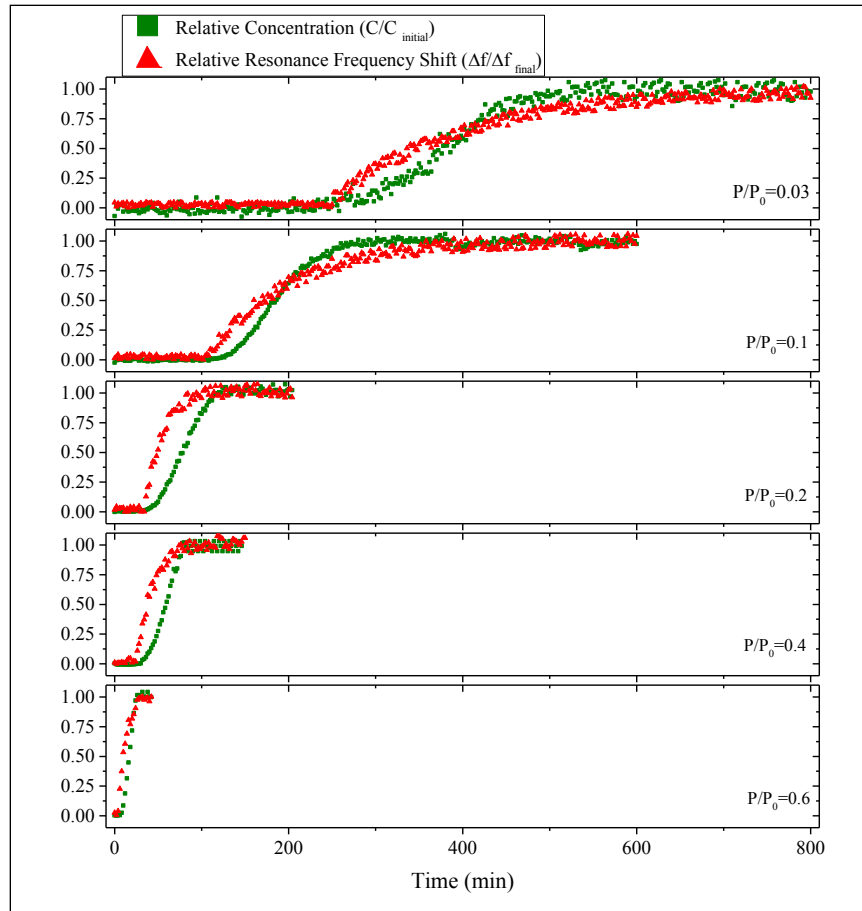
Figure 7-5 Change to the concentration and relative frequency shift during adsorption of BE on V503

Figure 7-6 illustrates the equilibrium adsorption capacities and resonant frequency shifts at different relative pressures of TMB and BE adsorbing on BAC and V503. The higher adsorption capacities for V503 at higher relative pressures could be attributed to 44% higher total pore volume of V503 compared to that for BAC.
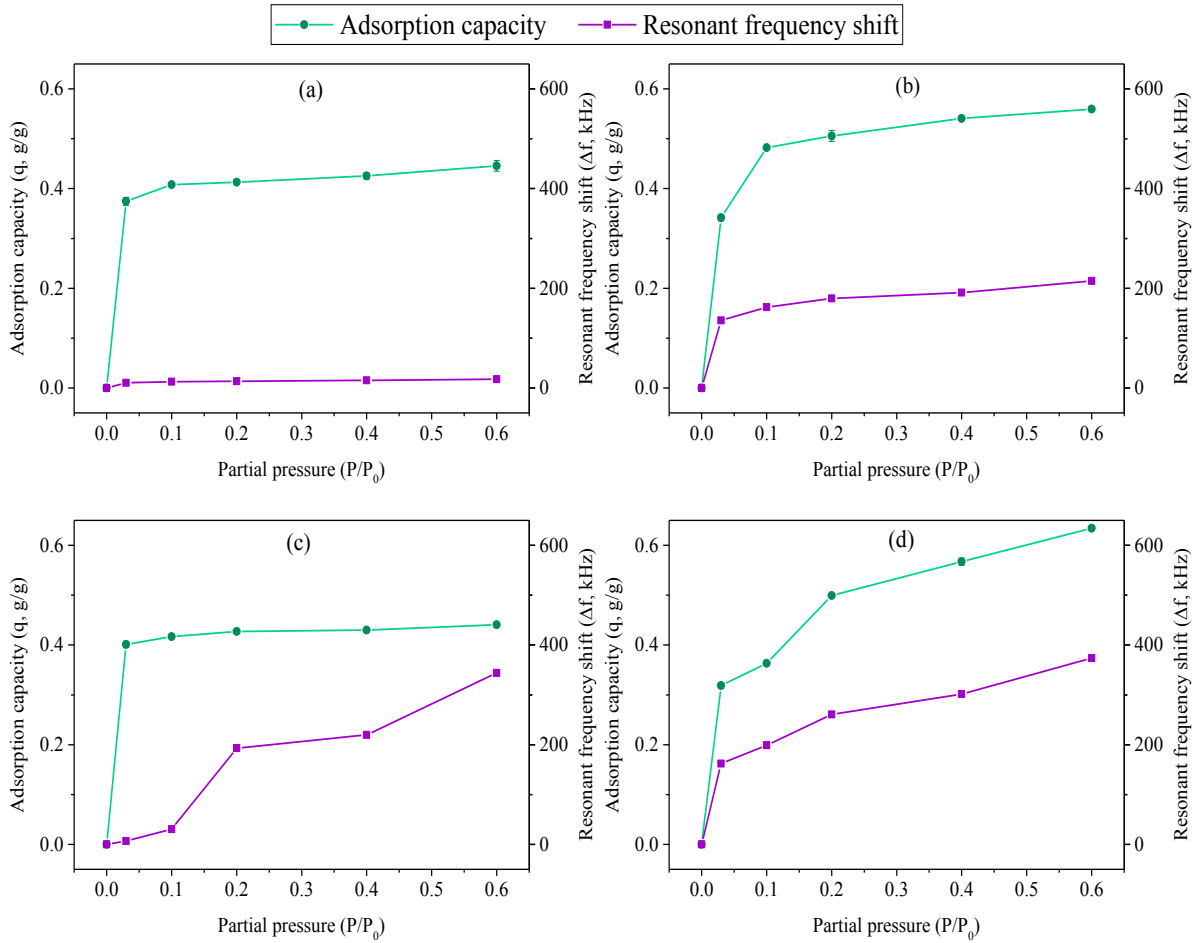
Figure 7-6 Adsorption capacity and resonant frequency shift versus partial pressure for (a) TMB on BAC (b) TMB on V503 (c) BE on BAC and (d) BE on V503

During the adsorption process, the variation in the permittivity of the adsorbent depends on the number of adsorbate molecules (i.e., dipoles) in the adsorbent bed because the interactions between microwaves and the adsorbate molecules in the system are responsible for polarizing the molecules, consequently changing the dielectric properties of the adsorbent and shifting the resonant frequency of the sensor (Staudt et al., 1999, Channen and McIntosh, 1955). The changes in dielectric properties, however, are more considerable for polar molecules with permanent dipole moments. Figure 7-7 shows that BE with a polar molecular

structure has higher permittivity than TMB with a non-polar molecular structure. Nevertheless, non-polar compounds are also affected by microwaves through inducing dipole moments in the molecules; therefore, during adsorption of non-polar adsorbate onto the adsorbent, the resonant frequency also changes (Staudt et al., 1999).

For BAC/TMB system, the resonant frequency shift does not significantly change with relative pressure due to the lower permittivity of TMB compared to that of BAC (Figure 7-7). The low dielectric properties of TMB could be attributed to its non-polar molecular structure while the high dielectric properties of BAC is due to the presence of delocalized π electrons, resulting in enhanced polarization interactions with microwaves (Çalişkan et al., 2012). Since BE and BAC have comparable effective permittivities, at low inlet concentrations resonant frequency shift only changes due to adsorbed BE (i.e. low gas concentration did not have significant contribution to the resonant frequency change). For higher concentrations of BE, however, the resonant frequency changed more noticeably because more BE is present in the adsorbed phase as well as in the gas phase.

The effective permittivity of V503 is lower than that of TMB and BE; therefore, when V503 was loaded with either adsorbates, the resonant frequency notably changed. Because BE has higher effective permittivity than TMB, the change in the resonant frequency for V503 loaded with BE is more notable than for V503 loaded with TMB.
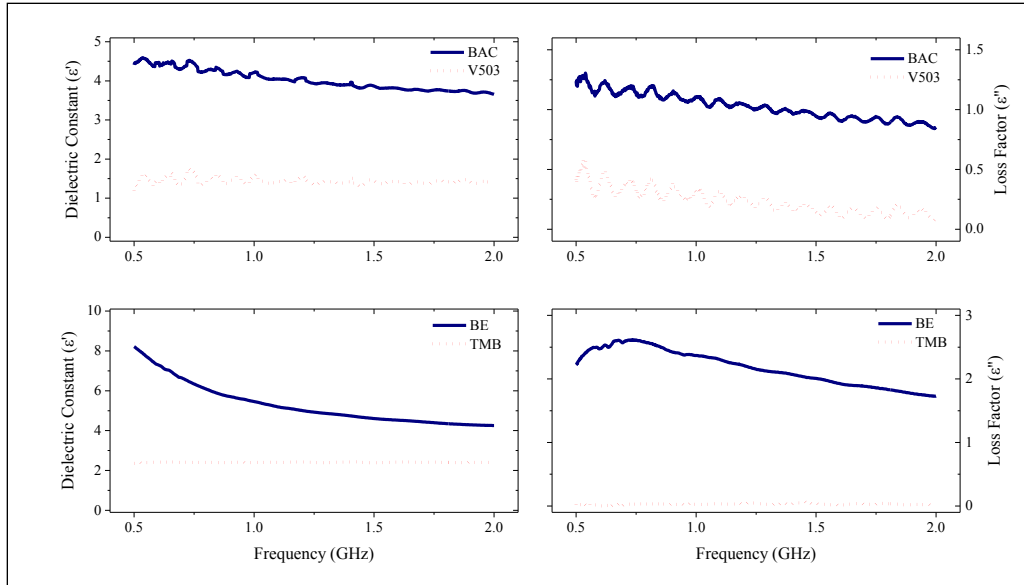
Figure 7-7 Dielectric properties of BAC, V503, BE, and TMB for the frequencies
between 0.5 to 2.0 GHz

For all experiments, increasing the relative pressure increases the adsorption capacity
and resonant frequency shift; therefore, for each test a linear correlation between adsorption
capacity and final resonant frequency can be developed (Figure 7-8). BAC has higher
permittivity in comparison to TMB; therefore, a change in adsorption capacity has resulted in
a small change in the sensor's resonant frequency shift. For the other adsorbent/adsorbate
scenarios, the adsorbate has comparable or higher dielectric properties than the corresponding
adsorbent; consequently, the changes in the resonant frequency are more noticeable. As a
result, changes in adsorption capacity could be monitored more distinctly for low permittivity
adsorbents, loaded with adsorbates with comparable or higher permittivities.
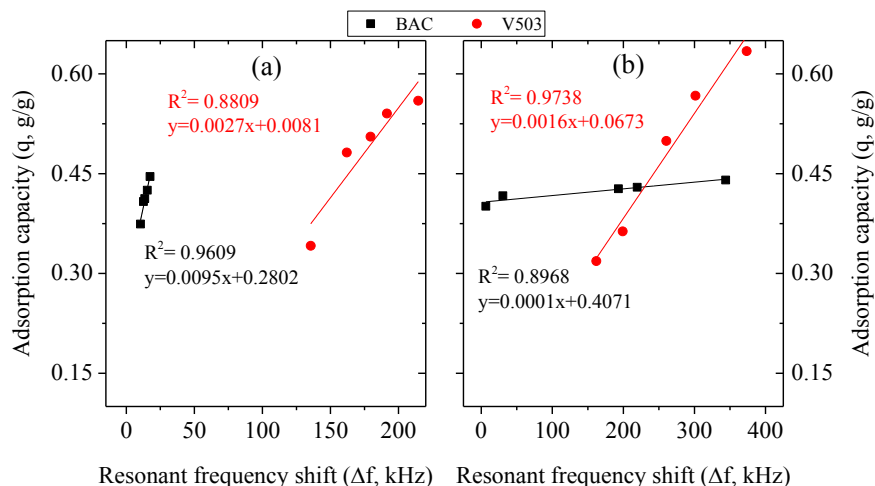
Figure 7-8 Final shift in resonant frequency versus adsorption capacity of TMB and BE on BAC and V503

The results obtained in this study are encouraging as they show the potential of the sensor for monitoring breakthrough time and adsorption capacity during adsorption. However, additional research is still needed to better understand and characterize the performance of the sensor. For instance, additional research is needed to verify the performance of the sensor under different operating parameters such as temperature, flowrate, composition. Increasing the adsorption temperature is expected to reduce the adsorption capacity and consequently decrease the permittivity change in the adsorbent bed, which results in small changes in the sensor's characteristics (quality factor and resonant frequency). On the other hand, the high accuracy measurement results for the adsorbates with contrasted dielectric properties suggest the applicability of the sensor for monitoring multicomponent adsorption.

The reported sensor and the sensing method can potentially be used in conjunction with portable and mobile devices. As such, VNA can be replaced by a low cost voltage controlled oscillator and a frequency to voltage converter can potentially be used as the readout circuitry. This device can be integrated with smart-phones for wireless data gathering

149

purposes, which demonstrates the reliability, low-cost, and real-time operation of the device with long lifetime.

7.5 Conclusion

In this study a newly developed non-contact high resolution real-time microwave sensor was used to determine the breakthrough time and adsorption capacity for adsorbents/adsorbates with different dielectric properties. The sensor was used to monitor the changes in the dielectric properties of the adsorbents during adsorption of TMB on BAC or V503 using the sensor quality factor and resonant frequency. Those parameters were related to breakthrough time and adsorption capacity. Adsorption tests were completed at select relative pressures (0.03, 0.1, 0.2, 0.4, and 0.6) of adsorbates in the influent stream. For all experiments, the difference between the breakthrough time ($t_{5\%}$) and the settling time of the quality factor variation (time that the quality factor was 0.95 of its final value), was less than 5%. Additionally, a strong linear correlation (R^2=0.88-0.97) between adsorption capacity and the final value of the resonant frequency shift was observed. These results are in agreement with the hypothesis proposed in this study that is the possible application of the sensor in determining breakthrough time and adsorption capacity of adsorbents in non-contact way.

7.6　References

DOWEX OPTIPORE V503 [Online]. Available: www.dow.com [Accessed April 20th, 2015].

PIDs for continuous monitoring of VOCs [Online]. Available: http://www.jmtestsystems.com/ [Accessed June 17th, 2016].

Rogers Corporation [Online]. Available: www.rogerscorp.com/index.aspx [Accessed Nov. 10th, 2015].

ABOU-KHOUSA, M., AL-DURRA, A. & AL-WAHEDI, K. 2015. Microwave Sensing System for Real-Time Monitoring of Solid Contaminants in Gas Flows. *IEEE Sensors Journal,* 15**,** 5296-5302.

AL-DASOQI, N., MASON, A., ALKHADDAR, R. & AL-SHAMMA'A, A. Use of sensors in wastewater quality monitoring - A review of available technologies. World Environmental and Water Resources Congress 2011: Bearing Knowledge for Sustainability - Proceedings of the 2011 World Environmental and Water Resources Congress, 2011. 3379-3388.

BENKHEDDA, J., JAUBERT, J. N., BARTH, D. & PERRIN, L. 2000a. Experimental and modeled results describing the adsorption of toluene onto activated carbon. *Journal of Chemical and Engineering Data,* 45**,** 650-653.

BENKHEDDA, J., JAUBERT, J. N., BARTH, D., PERRIN, L. & BAILLY, M. 2000b. Adsorption isotherms of m-xylene on activated carbon: Measurements and correlation with different models. *Journal of Chemical Thermodynamics,* 32**,** 401-411.

CAL, M. P., ROOD, M. J. & LARSON, S. M. 1997. Gas phase adsorption of volatile organic compounds and water vapor on activated carbon cloth. *Energy and Fuels,* 11**,** 311-315.

ÇALIŞKAN, E., BERMÚDEZ, J. M., PARRA, J. B., MENÉNDEZ, J. A., MAHRAMANLIOĜLU, M. & ANIA, C. O. 2012. Low temperature regeneration of activated carbons using microwaves: Revising conventional wisdom. *Journal of Environmental Management,* 102**,** 134-140.

CHANNEN, E. W. & MCINTOSH, R. 1955. INVESTIGATION OF THE PHYSICALLY ADSORBED STATE BY MEANS OF DIELECTRIC MEASUREMENTS. *Canadian Journal of Chemistry,* 33**,** 172-183.

CHERBAŃSKI, R. & MOLGA, E. 2009. Intensification of desorption processes by use of microwaves-An overview of possible applications and industrial perspectives. *Chemical Engineering and Processing: Process Intensification,* 48**,** 48-58.

DE FONSECA, B., ROSSIGNOL, J., BEZVERKHYY, I., BELLAT, J. P., STUERGA, D. & PRIBETICH, P. 2015. Detection of VOCs by microwave transduction using dealuminated faujasite DAY zeolites as gas sensitive materials. *Sensors and Actuators B: Chemical,* 213**,** 558-565.

DIMOTAKIS, E. D., CAL, M. P., ECONOMY, J., ROOD, M. J. & LARSON, S. M. 1995. Chemically treated activated carbon cloths for removal of volatile organic carbons from gas streams: evidence for enhanced physical adsorption. *Environmental Science & Technology,* 29**,** 1876-1880.

FAYAZ, M., SHARIATY, P., ATKINSON, J. D., HASHISHO, Z., PHILLIPS, J. H., ANDERSON, J. E. & NICHOLS, M. 2015. Using Microwave Heating To Improve the Desorption Efficiency of High Molecular Weight VOC from Beaded Activated Carbon. *Environmental Science & Technology,* 49**,** 4536–4542.

HASHISHO, Z., EMAMIPOUR, H., ROOD, M. J., HAY, K. J., KIM, B. J. & THURSTON, D. 2008. Concomitant adsorption and desorption of organic vapor in dry and humid air streams using microwave and direct electrothermal swing adsorption. *Environmental Science and Technology,* 42**,** 9317-9322.

JAHANDAR LASHAKI, M., FAYAZ, M., NIKNADDAF, S. & HASHISHO, Z. 2012. Effect of the adsorbate kinetic diameter on the accuracy of the Dubinin-Radushkevich equation for modeling adsorption of organic vapors on activated carbon. *Journal of Hazardous Materials,* 241-242**,** 154-163.

JAIN, R. K., AURELLE, Y., CABASSUD, C., ROIUSTAN, M. & SHELTON, S. B. 1997. *Environmental Technologies and Trends: International and Policy Perspectives*, Springer.

JONES, A. M., KELLY, J. F., TEDESCHI, J. & MCCLOY, J. S. 2014. Design considerations for high-Q bandpass microwave oscillator sensors based upon resonant amplification. *Applied Physics Letters,* 104**,** 253507.

KIM, B. R. 2011. VOC emissions from automotive painting and their control: A review. *Environmental Engineering Research,* 16**,** 1-9.

KIM, J. H., LEE, S. J., KIM, M. B., LEE, J. J. & LEE, C. H. 2007. Sorption equilibrium and thermal regeneration of acetone and toluene vapors on an activated carbon. *Industrial and Engineering Chemistry Research,* 46**,** 4584-4594.

KOROSTYNSKA, O., MASON, A. & AL-SHAMMA'A, A. 2014. Microwave sensors for the non-invasive monitoring of industrial and medical applications. *Sensor Review,* 34**,** 182-191.

LASHAKI, M. J., FAYAZ, M., WANG, H., HASHISHO, Z., PHILIPS, J. H., ANDERSON, J. E. & NICHOLS, M. 2012. Effect of Adsorption and Regeneration Temperature on Irreversible Adsorption of Organic Vapors on Beaded Activated Carbon. *Environmental Science and Technology,* 46**,** 4083-4090.

LEE, H. J., LEE, H. S., YOO, K. H. & YOOK, J. G. 2010. DNA sensing using split-ring resonator alone at microwave regime. *Journal of Applied Physics,* 108.

LOWELL, S. & SHIELDS, J. E. 1991. *Powder surface area and porosity,* London ; New York, Chapman & Hall.

MASON, A., KOROSTYNSKA, O., WYLIE, S. & AL-SHAMMA'A, A. I. 2014. Non-destructive evaluation of an activated carbon using microwaves to determine residual life. *Carbon,* 67**,** 1-9.

PEI, J. & ZHANG, J. S. 2012. Determination of adsorption isotherm and diffusion coefficient of toluene on activated carbon at low concentrations. *Building and Environment,* 48**,** 66-76.

POTYRAILO, R. A. & MORRIS, W. G. 2007. Multianalyte chemical identification and quantitation using a single radio frequency identification sensor. *Analytical Chemistry,* 79**,** 45-51.

POTYRAILO, R. A., NAGRAJ, N., SURMAN, C., BOUDRIES, H., LAI, H., SLOCIK, J. M., KELLEY-LOUGHNANE, N. & NAIK, R. R. 2012. Wireless sensors and sensor networks for homeland security applications. *Trends in Analytical Chemistry,* 40**,** 133-145.

REUß, J., BATHEN, D. & SCHMIDT-TRAUB, H. 2002. Desorption by microwaves: Mechanisms of multicomponent mixtures. *Chemical Engineering and Technology,* 25**,** 381-384.

RUBEL, G. O., PETERSON, G. W. & FLETCHER, N. K. 2009. In situ sensing of adsorbed water in activated carbon using impedance measurements. *Carbon,* 47**,** 2442-2447.

RYU, Y. K., LEE, H. J., YOO, H. K. & LEE, C. H. 2002. Adsorption equilibria of toluene and gasoline vapors on activated carbon. *Journal of Chemical and Engineering Data,* 47**,** 1222-1225.

SEO, J., KATO, S., ATAKA, Y. & CHINO, S. 2009. Performance test for evaluating the reduction of VOCs in rooms and evaluating the lifetime of sorptive building materials. *Building and Environment,* 44**,** 207-215.

SHAH, I. K., PRE, P. & ALAPPAT, B. J. 2014. Effect of thermal regeneration of spent activated carbon on volatile organic compound adsorption performances. *Journal of the Taiwan Institute of Chemical Engineers,* 45**,** 1733-1738.

STAUDT, R., RAVE, H. & KELLER, J. U. 1999. Impedance spectroscopic measurements of pure gas adsorption equilibria on zeolites. *Adsorption,* 5**,** 159-167.

VARADAN, V. K., VINOY, K. J. & GOPALAKRISHNAN, S. 2006. *Smart Material Systems and MEMS*, John Wiley & Sons, Ltd.

WANG, H., JAHANDAR LASHAKI, M., FAYAZ, M., HASHISHO, Z., PHILIPS, J. H., ANDERSON, J. E. & NICHOLS, M. 2012. Adsorption and Desorption of Mixtures of Organic Vapors on Beaded Activated Carbon. *Environmental Science and Technology,* 46**,** 8341-8350.

WANG, H., NIE, L., LI, J., WANG, Y., WANG, G., WANG, J. & HAO, Z. 2013. Characterization and assessment of volatile organic compounds (VOCs) emissions from typical industries. *Chinese Science Bulletin,* 58**,** 724-730.

YUN, J. H., CHOI, D. K. & KIM, S. H. 1999. Equilibria and dynamics for mixed vapors of BTX in an activated carbon bed. *AIChE Journal,* 45**,** 751-760.

YUN, J. H., HWANG, K. Y. & CHOI, D. K. 1998. Adsorption of benzene and toluene vapors on activated carbon fiber at 298, 323, and 348 K. *Journal of Chemical and Engineering Data,* 43**,** 843-845.

YUNUS, M. A. M., MUKHOPADHYAY, S. & PUNCHIHEWA, A. Application of independent component analysis for estimating nitrate contamination in natural water sources using planar electromagnetic sensor. Proceedings of the International Conference on Sensing Technology, ICST, 2011. 538-543.

YUNUS, M. A. M. & MUKHOPADHYAY, S. C. 2011. Novel planar electromagnetic sensors for detection of nitrates and contamination in natural water sources. *IEEE Sensors Journal,* 11**,** 1440-1447.

ZARIFI, M. H., FAYAZ, M., GOLDTHORP, J., ABDOLRAZZAGHI, M., HASHISHO, Z. & DANESHMAND, M. 2015a. Microbead-assisted high resolution microwave planar ring resonator for organic-vapor sensing. *Applied Physics Letters,* 106**,** 062903.

ZARIFI, M. H., MOHAMMADPOUR, A., FARSINEZHAD, S., WILTSHIRE, B. D., NOSRATI, M., ASKAR, A. M., DANESHMAND, M. & SHANKAR, K. 2015b. Time-Resolved Microwave Photoconductivity (TRMC) Using Planar Microwave Resonators: Application to the Study of Long-Lived Charge Pairs in Photoexcited Titania Nanotube Arrays. *The Journal of Physical Chemistry C,* 119**,** 14358-14365.

ZARIFI, M. H., SOHRABI, A., SHAIBANI, P. M., DANESHMAND, M. & THUNDAT, T. 2015c. Detection of volatile organic compounds using microwave sensors. *IEEE Sensors Journal,* 15**,** 248-254.

ZARIFI, M. H., THUNDAT, T. & DANESHMAND, M. 2015d. High resolution microwave microstrip resonator for sensing applications. *Sensors and Actuators A: Physical,* 233**,** 224-230.

CHAPTER 8. MONITORING THE RESIDUAL CAPACITY OF ACTIVATED CARBON IN A VOC ABATEMENT SYSTEM USING A PLANAR MICROWAVE RESONATOR SENSOR

8.1 Introduction

In 2013, a total of 2.1 megatonnes of volatile organic compounds (VOCs) were emitted in Canada, with large contributions from the oil and gas sector and industries handling paints and solvents (31% and 15%, respectively) (Anderson et al., 2012). Adsorption on activated carbon is a widely used technique for controlling VOC emissions (Bansode et al., 2003, Khan and Kr. Ghoshal, 2000, Lashaki et al., 2012, Weissenberger and Schmidt, 1994). Adsorption is typically followed by regeneration to recover the adsorbent for reuse. During successive adsorption/regeneration cycles, heel buildup reduces the working capacity and lifetime of the adsorbent (Jahandar Lashaki et al., 2012). Heel buildup is defined as non-desorbed adsorbate remained in adsorbent pores after regeneration, and it could be due to non-desorbable physisorption, oligomerization, chemical adsorption, and adsorbate decomposition (Ania et al., 2004, Ania et al., 2005, Çalişkan et al., 2012, Ha and Vinitnantharat, 2000, Thakkar and Manes, 1987).

During numerous adsorption/regeneration cycles, the exposure of accumulated heel to high regeneration temperatures progressively changes the heel nature from physisorbed into irreversibly adsorbed species (e.g., coke) (Ferro-Garcia et al., 1996, Niknaddaf et al., 2015). As heel accumulation continues and the adsorbent is progressively more spent (exhausted), it becomes less effective in capturing VOCs. Therefore, it needs to be reactivated or replaced

with virgin adsorbent. Hence, monitoring the adsorption capacity of the adsorbent is helpful for understanding its residual lifetime and maintaining effective performance of the abatement process.

The residual capacity of the adsorbent could be estimated using conventional characterization methods such as apparent density (AD) measurements, adsorption isotherm measurements, and micropore surface analysis (Lashaki et al., 2012, Rivera-Utrilla et al., 2003). Lashaki et al. (2012) reported that heel buildup linearly reduced pore volume as well as Brunauer Emmett Teller (BET) surface area of a microporous activated carbon adsorbent. Similar trends were also reported during irreversible adsorption of chlorophenol on activated carbon (Rivera-Utrilla et al., 2003). The measurement of an adsorbent's AD through standard methods can also be used for determining the degree of exhaustion of the adsorbent (ASTM, 2014). However, these techniques have drawbacks of long analysis times, up to a few days in some cases, involve delicate and/or expensive instruments, or they cannot be done in-situ, and hence are not ideal for real-time, automated monitoring of full-scale systems. Therefore, the development of a fast, low-cost, and reliable technique for real-time monitoring of the degree of exhaustion of adsorbents is desirable.

Recent studies have demonstrated the potential of impedance measurement methods and microwave devices for adsorption capacity estimation and monitoring of the residual lifetime of activated carbon. Rubel et al. (2009a) reported an in-situ sensing device based on impedance measurement to relate the capacitance of granular activated carbon (GAC) to water loading. They employed a resistor–capacitor circuit equipped with a dielectric cavity to measure the capacitance of GAC by monitoring the voltage response across a charging–discharging capacitor. The sensor was inexpensive and easy to use; however, contrary to

resonant-based sensors, it could be negatively affected by electrical low frequency noises and the natural hysteresis of capacitive sensors. In another study, Rubel et. al. (2009b), demonstrated the impedance change of impregnated activated carbon exposed to SO_2 at ambient temperature. The impedance measurement was performed using a dual parallel plate mesh electrode configuration that measured the electrical conductivity of the carbon bed using an impedance analyzer operating at 10 Hz. During exposure of the impregnated activated carbon to SO_2, the impedance proportionally increased with increasing SO_2 partial pressure and then dropped. It was found that SO_2 was initially physisorbed onto activated carbon, and was then oxidized to SO_3 and H_2SO_4. Mason et. al. (2014) developed a microwave-based technique for estimating the residual life of a GAC using a cavity resonator. In the reported technique, an activated carbon sample was placed in a resonant cylindrical cavity waveguide and the material properties were measured in real-time. The transmitted signal attenuation was correlated with the exposure time of carbon to water vapor.

Planar microwave resonator sensors have recently demonstrated a significant potential in sensing applications (Zarifi et al., 2016a, Zarifi et al., 2015a, Zarifi et al., 2016b, Zarifi et al., 2015c) including VOC gas sensing (Korostynska et al., 2014, Lee et al., 2010). These resonator sensors can be used in many non-contact gas sensing scenarios due to their low cost, robustness, simplicity, and compatibility with complementary metal oxide semiconductor (CMOS) technology for miniaturization (Potyrailo and Morris, 2007, Potyrailo et al., 2012, Zarifi et al., 2015b).

The resonant frequency and amplitude of the microwave planar resonator sensor respond to changes in the dielectric properties of the medium surrounding the sensor. Dielectric properties of materials consist of dielectric constant (ε') and loss factor (ε''). The

dielectric constant describes a material's ability to be polarized by an electromagnetic field, and loss factor describes a material's ability to convert absorbed energy into heat (Cherbański and Molga, 2009). The sensor is able to monitor the changes in the dielectric properties of its vicinity by measuring the changes in different parameters such as resonant frequency (f_r), which is the frequency at which maximum power transmission occurs. Since the operation principle of the sensor is based on electric field alteration, they can operate in a non-contact mode, which makes them attractive for harsh (e.g., corrosive or toxic gases) and electrically noisy environments.

In this paper, the application of a non-contact, high resolution microwave resonator sensor for estimating the degree of exhaustion (i.e., residual life) of adsorbents is investigated. Activated carbon samples previously used in a real-world VOC capture system and with different degrees of exhaustion are studied. The results are correlated with pore volume, BET surface area, and apparent density measurements. Since the composition of heel can potentially affect the changes in the dielectric properties of spent BAC relative to the virgin BAC, the heel composition is characterized using thermogravimetric analysis (TGA) and X-ray photoelectron spectroscopy (XPS).

8.2 Experimental

8.2.1 Adsorbents

Five partially and fully spent BAC samples (with ADs ranging from 0.675 to 0.807 g/cm^3) were studied. These samples were collected from two paint booth emissions control systems in light duty vehicle assembly plants at a point immediately after the desorption step in the cyclic adsorption/regeneration system. The samples were from two different adsorption/desorption systems run with different adsorbate streams, one starting with virgin

159

BAC (AD of 0.606 g/cm^3) and one with reactivated BAC (AD of 0.623 g/cm^3), which were also analyzed for comparison. Virgin BAC was the starting material for the samples with AD of 0.707, 0.746 and 0.807 g/cm^3. Reactivated BAC was the starting material for the samples with AD of 0.675 and 0.760 g/cm^3.

8.2.2 Experimental setup and methods

The experimental setup (Figure 8-1a) consisted of a quartz tube (2.2 cm inner diameter, 35.6 cm length) containing 5 cm^3 of the BAC in front of the microwave planar sensor, which was connected to a vector network analyzer (VNA, Rohde and Schwarz ZVL 135) to measure the transmitted and received power. A fritted glass disc was placed in the middle of the tube to support the BAC samples.

The core of the active microwave planar sensor is a half-wavelength, meander shaped, open-ended resonator that is electrically and magnetically coupled to input/output microstrip transmission lines (Figure 8-1b). The VNA provides the sensor with a constant power over the desired bandwidth. Because of the sensor's band-pass filtering behavior, the output power has a Gaussian type profile, the maximum of which is the resonant frequency. Within this transmission, the points exhibiting maximum electrical field concentration (end points of the open-loop meandered resonator) are called "hot-spots" as they offer the largest sensitivity. Hence, the sample inside the holder was placed in front of one of the hot-spots (Figure 8-1b). The resonant frequency of the resonator depends on the effective permittivity in its near environment according to the following equation (Rubel et al., 2009a):

$$f_r = \frac{c}{\lambda_g \sqrt{\varepsilon_{eff}}}$$

(4)

where $c = 3 \times 10^8$ (m/s) is the speed of light, f_r (Hz) is the resonant frequency, ε_{eff} is the effective permittivity of the wave-propagation environment, and λ_g (m) represents the guided wavelength.

Activated carbon with a porous structure can be considered an inhomogeneous medium; therefore, its effective dielectric properties should be calculated using effective medium methods, such as Maxwell-Garnett or Bruggeman equations (Karkkainen et al., 2001). During consecutive adsorption/regeneration cycles, heel builds up in the pores of the BAC, which results in a change of the effective permittivity of the BAC. Therefore, for BAC samples, the effective permittivity changes with the level of heel buildup.

(a)   (b)
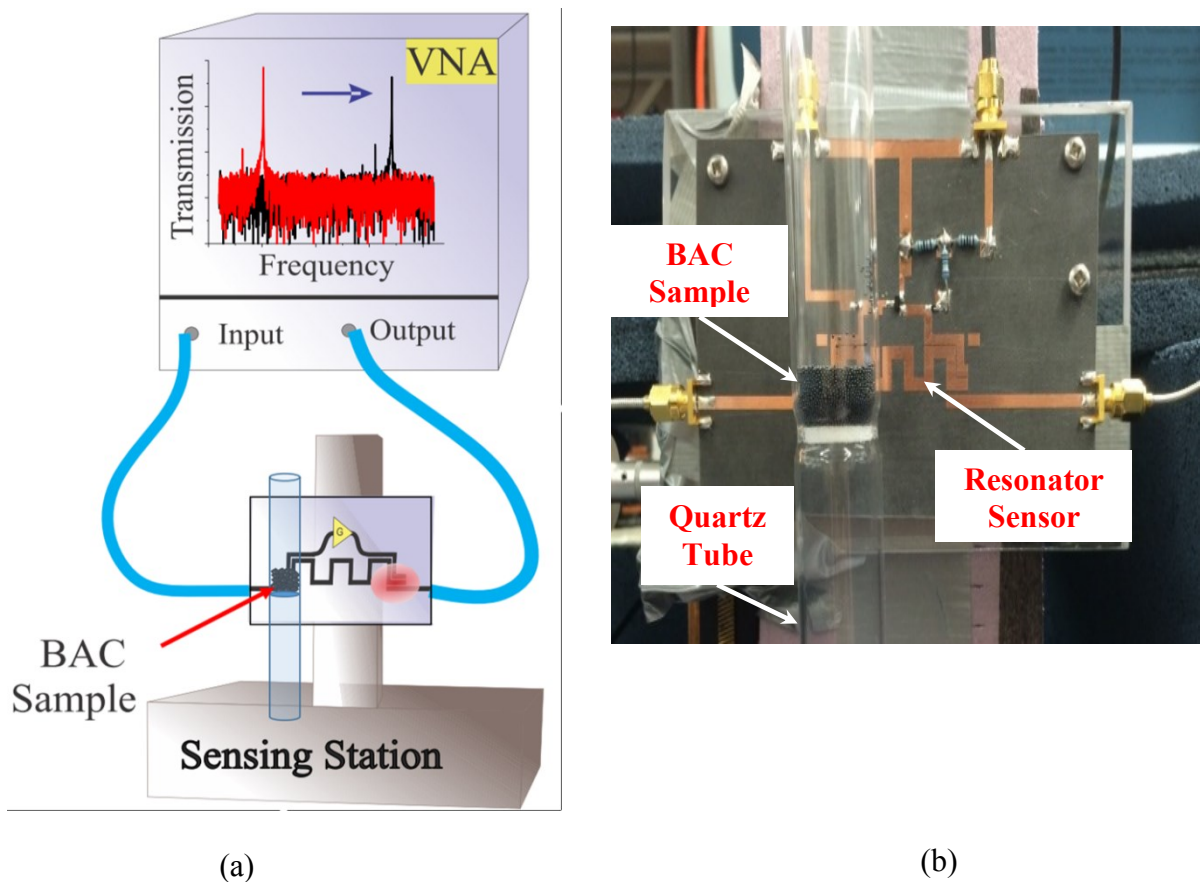
Figure 8-1 (a) Schematic diagram of the experimental setup (b) Sample's location in front of the sensor

The sensor can detect the variation in dielectric properties of materials in its vicinity up to 8 cm away from the sensor surface. For all measurements, the sensor was positioned using a lab stand at a fixed distance of 1 cm away from the quartz tube. For each sample, the measurements were conducted in triplicate and average values were reported.

8.2.3   Sensor analysis

The open-ended microstrip resonator sensor was carried on a low-loss microwave substrate and coupled to two input and output transmission lines. The microwave substrate (RO5880, Roger Corporation) has a permittivity of 2.2, loss tangent of 0.0009 and thickness of 0.787 mm. The copper trace on the sensor has a thickness of 37 microns with electrical conductivity of 5.8×10^7 S/m.

The effective permittivity variation in the sensor vicinity can be monitored through the variation in the resonant frequency of the resonant profile (S_{21}). As noted earlier, the resonant frequency (f_r) is defined as the frequency at which maximum power transmission occurs, and corresponds to the frequency of the maximum amplitude of the resonant profile (Lee et al., 2010). A VNA was used to extract the electrical response and the resonant profile of the implemented sensor. The bandwidth (Δf_{-3dB}) is defined as the frequency span, where more than half of maximum power is transferred through the sensor. The quality factor (Q) which represents the profile's sharpness, is defined as the ratio of the resonant frequency to the -3dB bandwidth (i.e., $Q = f_r/\Delta f_{-3dB}$). After setting the empty reactor in the vicinity of the sensing area, the resonant frequency was approximately 1.42 GHz with a quality factor of $Q \cong 200$ in passive mode. This moderately high Q for passive state is not sufficient to be used in highly sensitive measurements. In order to increase the quality factor, the passive resonator with microstrip transmission line design was reinforced by a positive feedback loop. The loop

functioned as a negative resistor to the sensor and retrieved the lost radiation and/or conductor energy to the system, resulting in an ultra-high quality factor (Jones et al., 2014). According to Equation (2), having such an ultra-high quality factor decreases the minimum detectable range of permittivity, $|\Delta\varepsilon_{min}|$, which is defined as follows (Zarifi et al., 2015d):

$$|\Delta\varepsilon_{min}| = \frac{9\varepsilon\sqrt{3}}{2V_{omax}Q} \times \sqrt{4kTBR} \tag{5}$$

where k (1.38×10^{-23} m^2kg $s^{-2}K^{-1}$) is the Boltzmann constant, T (K) is the temperature, B (Hz) is the measured bandwidth, R (Ω) is the resistance, ε is the permittivity, and V_{omax} (V) is the maximum amplitude of the resonant profile. The sensor measurements were conducted at room temperature (23 °C) and relative humidity of 14%. More details on the sensor structure design and operation are provided by Zarifi et. al. (2015b).

8.2.4 BAC characterization

To measure the apparent density of each sample, a 250 cm^3 separatory funnel was filled with 125 cm^3 of BAC. The BAC was allowed to flow from the funnel into a 100 cm^3 graduated cylinder at an approximate rate of 1 cm^3/s. The graduated cylinder was filled with BAC up to 100 cm^3 and the mass of BAC was recorded using a balance within an accuracy of 0.1 g. The apparent density is the ratio of the BAC mass to the BAC volume in the graduated cylinder (ASTM, 2014).

Micropore surface analysis for each sample was completed using a micropore surface analyzer (iQ2MP, Quantachrome). Nitrogen adsorption was measured at -196 °C. Before starting the analysis, samples were degassed for 5 h at 120 °C. To calculate specific surface area, the BET method was used (Brunauer et al., 1938) at relative pressures ranging from 0.01 to 0.07, which allowed for high coefficient of determination (R^2) values and positive BET constants (C). Total pore volume was recorded at P/P_0 = 0.975. To provide pore size

distribution (PSD) and micropore volume, the quench solid density functional theory (QSDFT) method and the V-t method were used, respectively (Chiang et al., 2006).

Surface elemental composition (C, O, and N) of all BACs was determined with XPS using an AXIS 165 spectrometer (Kratos Analytical) as described elsewhere (Jahandar Lashaki et al., 2016). Survey scans (with signal to noise ratio of >10) were collected for binding energy spanning from 1100 eV to 0 with analyzer pass energy of 160 eV and a step of 0.4 eV. CasaXPS software was used to process the scans and the results were reported in terms of atomic concentration.

To estimate the composition of the heel, derivative thermogravimetric analysis (DTG) was completed on each sample (TGA/DSC 1, Mettler Toledo). Samples were heated from 25 °C to 800 °C using a heating rate of 2 °C/min in 50 standard cm^3/min of N_2. The fraction of heel removed at 800 °C during TGA analysis (Heel desorption %) was calculated by dividing the cumulative weight loss at 800 °C (corrected based on the weight loss of virgin BAC) by the cumulative heel increase from AD measurements (relative to virgin BAC) (Jahandar Lashaki et al., 2016).

8.3 Results and Discussion

Figure 8-2 shows that with an increase in AD, the nitrogen adsorption isotherms gradually shifted downward. The AD increase is due to heel buildup in the BAC pores following consecutive VOC adsorption/regeneration cycles, which decreased the available adsorption sites. Additional cycles would result in fully spent BAC and thus necessitates BAC replacement. Data for virgin BAC without heel are indicated by the samples with AD of 0.606 g/cm^3. While heel formation reduced nitrogen uptake, the adsorption isotherm type for all

BACs remained type I, characterized by a steep increase at low relative pressures ($P/P_0 < 0.2$) (Sing et al., 2008).
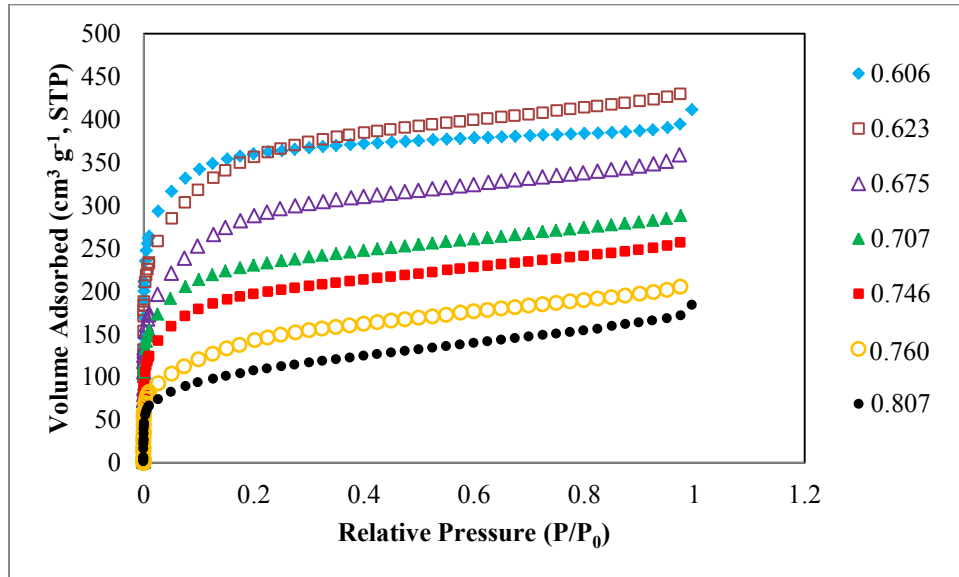
Figure 8-2 Nitrogen adsorption isotherms for BAC samples with different degrees of exhaustion, as characterized by ADs ranging from 0.606 g/cm^3 (virgin BAC) to 0.807 g/cm^3. Filled markers correspond to samples with virgin BAC as starting material while empty markers correspond to samples with reactivated BAC as starting material.

With the increase in heel buildup, BET surface area, micropore and total pore volume linearly decreased (Figure 8-3). This is consistent with previous observations (Lashaki et al., 2012, Rivera-Utrilla et al., 2003). The strong correlation (R^2 from 0.95 to 0.99) between AD and the BET surface area, micropore, and total pore volumes indicates that AD is a good surrogate for these parameters. Mesopore volumes (not shown in Figure 8-3) for all spent samples were very similar (0.15±0.01 cm^3/g), indicating no change with the increase in heel formation; therefore, heel formation mainly reduced micropore volume.
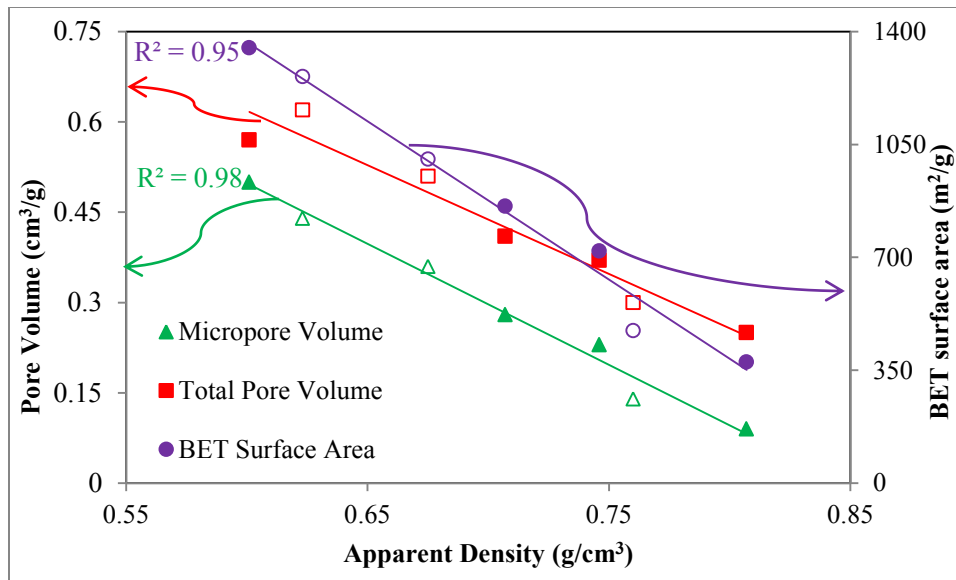
Figure 8-3 BET surface area, micropore volume, and total pore volume for virgin, reactivated and spent BAC samples with various degrees of exhaustion as characterized by apparent density. Filled markers correspond to samples with virgin BAC as starting material while empty markers correspond to samples with reactivated BAC as starting material.

The PSD profiles for virgin, reactivated and spent BAC samples are shown in Figure 8-4. Heel formation markedly reduced micropore volume, particularly for pores < 16 Å, as the two peaks for virgin BAC were not observed for the spent samples. For the samples with the highest AD (0.760 and 0.807 g/cm^3), the available micropore volume was significantly reduced, particularly for narrow micropores (< 7 Å). Compared to the other samples, the reactivated sample and the samples with reactivated BAC as their precursor (samples with AD of 0.675 and 0.760) had a higher fraction of large micropore volume (pore width > 16 Å) as a result of carbon burn-off and pore enlargement during the reactivation process.
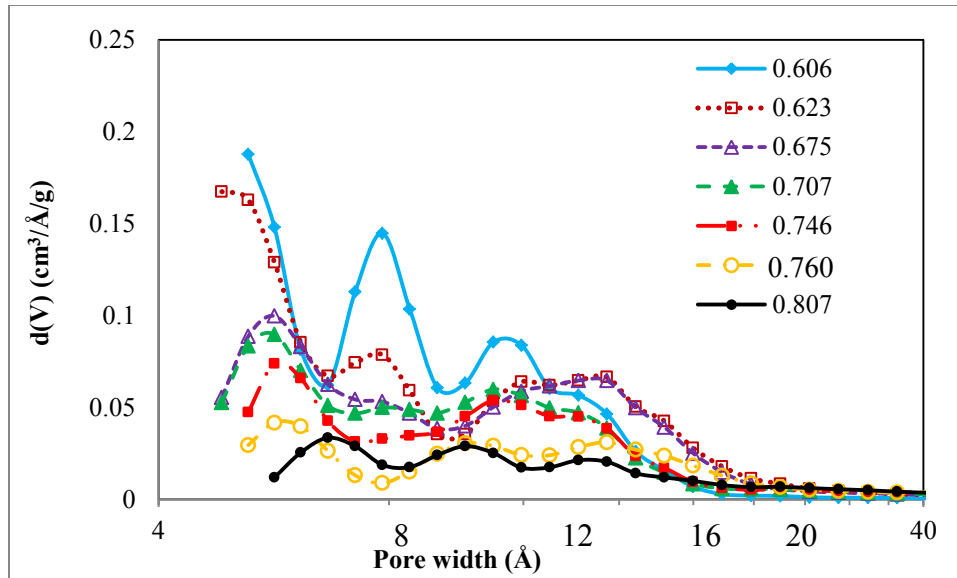
Figure 8-4 PSDs of virgin, reactivated and spent BAC samples having AD as shown in legend. Filled markers correspond to samples with virgin BAC as starting material while empty markers correspond to samples with reactivated BAC as starting material.

As previously mentioned, the planar microwave resonator sensor is sensitive to the change in the dielectric properties in its immediate environment. These changes are reflected in the sensor's resonant frequency shift, in a non-contact method. Samples with differing degrees of exhaustion (different AD) were placed 1 cm from the sensor. Permittivity differences among the samples resulted in different measured resonant frequency responses, with a strong linear correlation ($R^2=0.94$) between the AD and resonant frequency shift of the sensor (Figure 8-5). The accumulation of VOC in the pores and resulting change in AD leads to changes in dielectric properties and effective permittivity of the BAC, resulting in a change of the resonant frequency. The linear correlation between the AD and resonant frequency shift is in accordance with previous research on wood samples that showed the effective permittivity of a porous material (a mixture of pores (air) and wood substance) linearly depends on the bulk density (ρ_0) (Tanaka et al., 2014). The sensor-based measurement

167

method shows very good correlation to AD, but requires no sample pretreatment (e.g. degassing) and provides the results in a real-time, non-contact manner. The duration of resonant frequency measurement was much faster than micropore surface analysis; less than 1 min for resonant frequency versus 1 to 3 days for BET surface area, pore volume and PSD measurements for each sample.
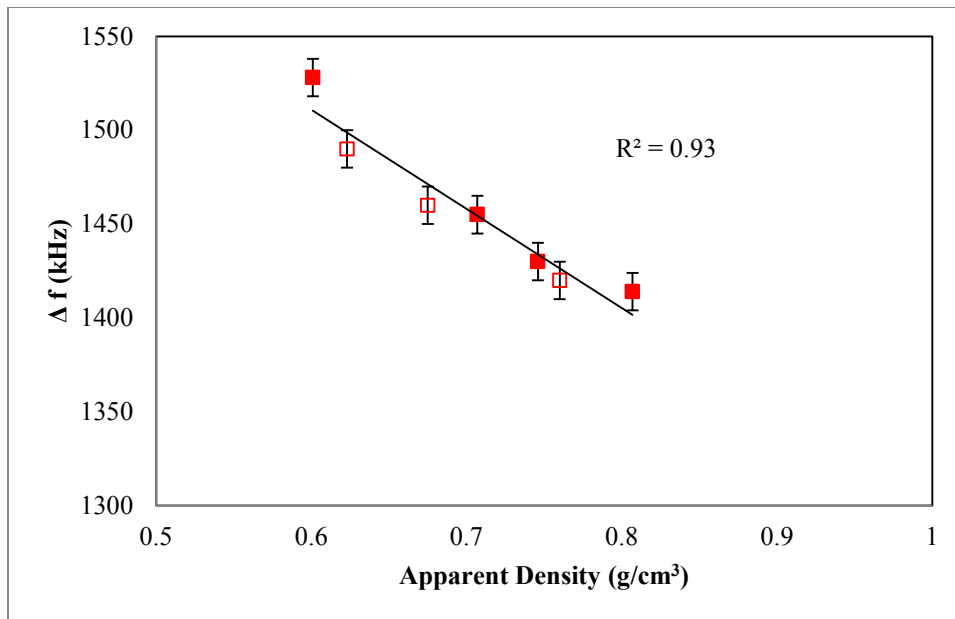
Figure 8-5 Variation in resonant frequency with apparent density of virgin, reactivated and spent BAC samples. Filled markers correspond to samples with virgin BAC as starting material while empty markers correspond to samples with reactivated BAC as starting material.

The AD was linearly correlated to BET surface area, micropore and total pore volume (Figure 8-3). Therefore, the linear correlation between resonant frequency and AD leads to linear correlations between resonant frequency and BET surface area (R^2=0.81), micropore volume (R^2=0.93) and total pore volume (R^2=0.92) of the samples. As such, once calibrated for an adsorbent, the sensor could be used to estimate the AD as well as the surface area and pore volume of an adsorbent.

In addition to the change in porosity of the BAC samples, the heel composition can potentially affect the effective permittivity of the BAC samples. Therefore, an analysis of the heel composition of the samples is warranted. Figure 8-6 shows heel desorption percentage for the spent samples, defined as the fraction of total heel removed during TGA analysis as the temperature ramped up to 800 °C. For virgin and reactivated BAC, this percentage is undefined because these samples have no heel to be desorbed. For the spent samples, in general, the thermal stability of the heel on the BAC increased with the increase in heel formation. This could be due to the exposure of the heel to repeated high regeneration temperatures during regeneration cycles, which resulted in conversion of heel to non-desorbable species (e.g., coke) with high stability (Ferro-Garcia et al., 1996, Niknaddaf et al., 2015). As mentioned earlier, the samples are from different adsorption/desorption systems where different adsorbates were tested for different number of cycles. Therefore, for each sample, the heel amount, desorbability, and composition depend on the sample history.
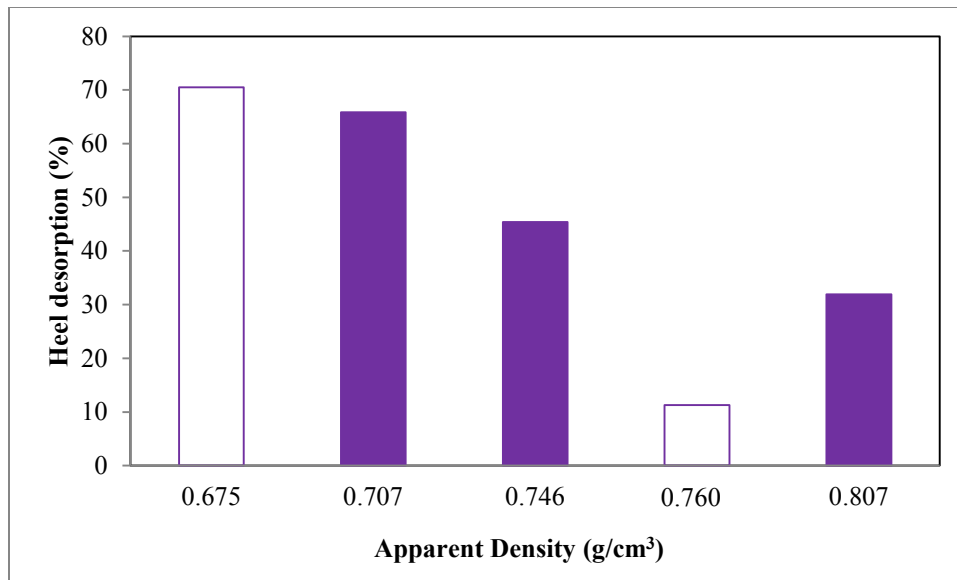
Figure 8-6 Heel desorption percentage for spent BAC samples. Filled bars correspond to samples with virgin BAC as starting material while empty bars correspond to samples with reactivated BAC as starting material.

The DTG analysis profiles for virgin, reactivated and spent BACs are shown in Figure 8-7. These profiles are determined from the TGA analysis, showing the rate of mass loss from the sample as the TGA temperature was steadily increased from 25 °C to 800 °C. Typically, heavy VOCs are responsible for the non-desorbed physisorbed portion of the heel, which appeared as a DTG peak at a lower temperature range (200 to 400 °C). Adsorbate molecules may also be chemisorbed on activated carbon, which result in the second DTG peak in the moderate temperature range (400 to 600 °C). During regeneration, some adsorbate molecules may also be subject to pyrolysis reactions on the surface of carbon, which would result in non-desorbable coke formation (Ania et al., 2005, Niknaddaf et al., 2015). In summary, DTG analysis showed that the thermal stability of the heel on different BAC samples were different, possibly due to different composition, type/age of heel, which may potentially affect the effective permittivity. A linear correlation between the AD and resonant

170

frequency shift (Figure 8-5), however, indicated that available pore volume appears to be a more significant parameter determining the effective permittivity and resonant frequency shift.
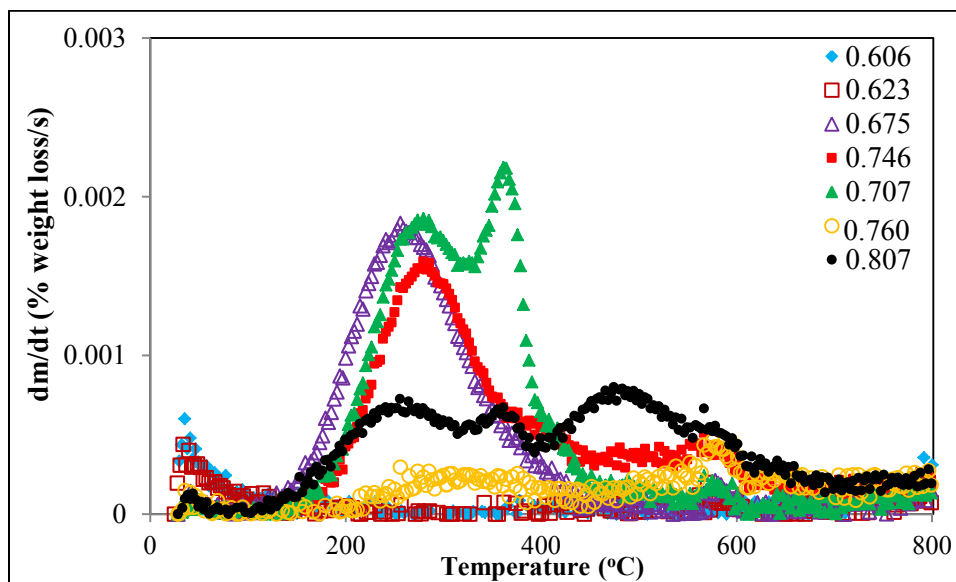
Figure 8-7 DTG profiles for virgin, reactivated and spent BAC samples. Filled markers correspond to samples with virgin BAC as starting material while empty markers correspond to samples with reactivated BAC as starting material.

The linear correlation between the resonant frequency and AD shows that the effect of heel composition on resonant frequency is not significant. This unexpected result could be due to the higher dielectric constant and loss factor of the heel and of BAC compared to those for empty pores and/or to the similarity in heel composition (mainly carbonaceous) of the spent samples. To confirm this hypothesis, surface elemental composition of BAC samples was measured using XPS (Figure 8-8). A comparison of the surface elemental composition of virgin, reactivated, and spent BAC samples showed that heel formation increased the non-carbon elements (O and N). However, carbon remained the dominant element in the heel (between 86.4 and 96.2 %). The change in the elemental composition of BAC samples did not

171

affect the resonant frequency shift measured by the sensor, since the carbon contents of the samples are within 10%. Therefore, the change in the resonant frequency appears to be proportional to the volume of heel.
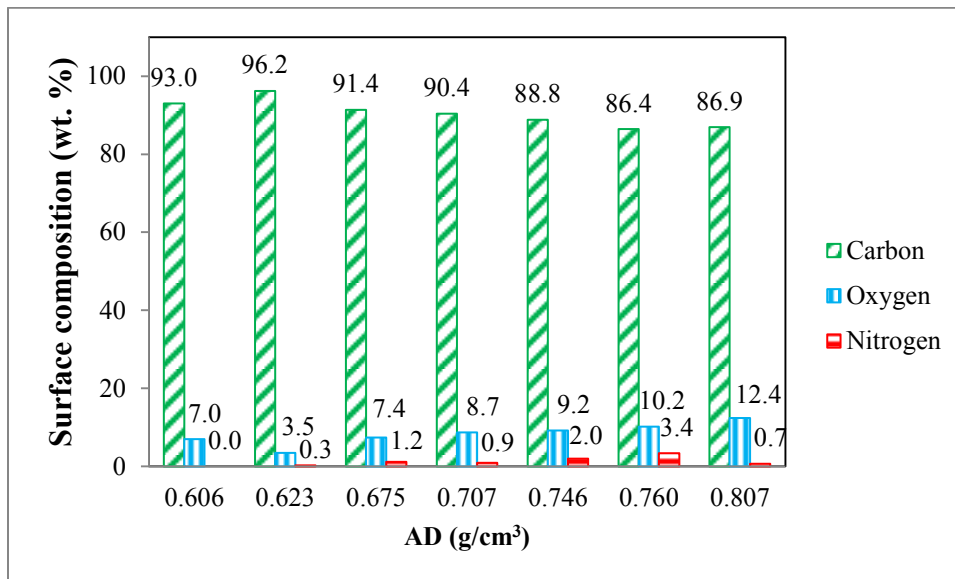
Figure 8-8 Surface elemental composition of virgin, reactivated and spent BAC samples via XPS.

8.4 Conclusions

This study presents a non-contact, high resolution microwave resonator sensor for determining the exhaustion degree (residual lifetime) of BAC samples used in a VOC abatement system. In this work, five industrial samples that had been partially or fully spent through many adsorption/regeneration cycles were used. The resonant frequency shift was linearly correlated ($R^2 = 0.81 - 0.93$) with the adsorbent apparent density, BET surface area and pore volume. Moreover, the effect of adsorbent porosity on dielectric property variation appeared to be more important than the heel composition. Finally, the ability of the sensor for fast, non-contact measurement (unlike AD measurements), and without sample pretreatment,

potentially allows for in-situ measurement and real-time monitoring of continuously operating systems.

8.5 References

Rogers Corporation [Online]. Available: www.rogerscorp.com/index.aspx [Accessed Nov. 10th, 2015].

ANDERSON, J. E., LEONE, T. G., SHELBY, M. H., WALLINGTON, T. J., BIZUB, J. J., FOSTER, M., LYNSKEY, M. G. & POLOVINA, D. 2012. Octane Numbers of Ethanol-Gasoline Blends: Measurements and Novel Estimation Method from Molar Composition. *SAE Technical Paper.* Copyright © 2012 SAE International.

ANIA, C. O., MENÉNDEZ, J. A., PARRA, J. B. & PIS, J. J. 2004. Microwave-induced regeneration of activated carbons polluted with phenol. A comparison with conventional thermal regeneration. *Carbon,* 42**,** 1377-1381.

ANIA, C. O., PARRA, J. B., MENÉNDEZ, J. A. & PIS, J. J. 2005. Effect of microwave and conventional regeneration on the microporous and mesoporous network and on the adsorptive capacity of activated carbons. *Microporous and Mesoporous Materials,* 85**,** 7-15.

ASTM 2014. Standard Test Method for Apparent Density of Activated Carbon, Designation: D2854 − 09.

BANSODE, R. R., LOSSO, J. N., MARSHALL, W. E., RAO, R. M. & PORTIER, R. J. 2003. Adsorption of volatile organic compounds by pecan shell- and almond shell-based granular activated carbons. *Bioresource Technology,* 90**,** 175-184.

BRUNAUER, S., EMMETT, P. H. & TELLER, E. 1938. Adsorption of gases in multimolecular layers. *Journal of the American Chemical Society,* 60**,** 309-319.

ÇALIŞKAN, E., BERMÚDEZ, J. M., PARRA, J. B., MENÉNDEZ, J. A., MAHRAMANLIOĜLU, M. & ANIA, C. O. 2012. Low temperature regeneration of activated carbons using microwaves: Revising conventional wisdom. *Journal of Environmental Management,* 102**,** 134-140.

CHIANG, Y. C., LEE, C. C. & SU, W. P. 2006. Adsorption behaviors of activated carbons for the exhaust from spray painting booths in vehicle surface coating. *Toxicological and Environmental Chemistry,* 88**,** 453-467.

CHERBAŃSKI, R. & MOLGA, E. 2009. Intensification of desorption processes by use of microwaves-An overview of possible applications and industrial perspectives. *Chemical Engineering and Processing: Process Intensification,* 48**,** 48-58.

FERRO-GARCIA, M. A., RIVERA-UTRILLA, J., BAUTISTA-TOLEDO, I. & MORENO-CASTILLA, C. 1996. Chemical and thermal regeneration of an activated carbon saturated with chlorophenols. *Journal of Chemical Technology and Biotechnology,* 67**,** 183-189.

HA, S. R. & VINITNANTHARAT, S. 2000. Competitive removal of phenol and 2,4-dichlorophenol in biological activated carbon system. *Environmental Technology,* 21**,** 387-396.

JAHANDAR LASHAKI, M., ATKINSON, J. D., HASHISHO, Z., PHILLIPS, J. H., ANDERSON, J. E., NICHOLS, M. & MISOVSKI, T. 2016. Effect of desorption purge gas oxygen impurity on irreversible adsorption of organic vapors. *Carbon,* 99**,** 310-317.

JAHANDAR LASHAKI, M., FAYAZ, M., NIKNADDAF, S. & HASHISHO, Z. 2012. Effect of the adsorbate kinetic diameter on the accuracy of the Dubinin-Radushkevich equation for modeling adsorption of organic vapors on activated carbon. *Journal of Hazardous Materials,* 241-242**,** 154-163.

JONES, A. M., KELLY, J. F., TEDESCHI, J. & MCCLOY, J. S. 2014. Design considerations for high-Q bandpass microwave oscillator sensors based upon resonant amplification. *Applied Physics Letters,* 104**,** 253507.

KARKKAINEN, K., SIHVOLA, A. & NIKOSKINEN, K. 2001. Analysis of a three-dimensional dielectric mixture with finite difference method. *IEEE Transactions on Geoscience and Remote Sensing,* 39**,** 1013-1018.

KHAN, F. I. & KR. GHOSHAL, A. 2000. Removal of Volatile Organic Compounds from polluted air. *Journal of Loss Prevention in the Process Industries,* 13**,** 527-545.

KOROSTYNSKA, O., MASON, A. & AL-SHAMMA'A, A. 2014. Microwave sensors for the non-invasive monitoring of industrial and medical applications. *Sensor Review,* 34**,** 182-191.

LASHAKI, M. J., FAYAZ, M., WANG, H., HASHISHO, Z., PHILIPS, J. H., ANDERSON, J. E. & NICHOLS, M. 2012. Effect of adsorption and regeneration temperature on irreversible adsorption of organic vapors on beaded activated carbon. *Environmental Science and Technology,* 46**,** 4083-4090.

LEE, H. J., LEE, H. S., YOO, K. H. & YOOK, J. G. 2010. DNA sensing using split-ring resonator alone at microwave regime. *Journal of Applied Physics,* 108.

MASON, A., KOROSTYNSKA, O., WYLIE, S. & AL-SHAMMA'A, A. I. 2014. Non-destructive evaluation of an activated carbon using microwaves to determine residual life. *Carbon,* 67**,** 1-9.

NIKNADDAF, S., ATKINSON, J. D., SHARIATY, P., LASHAKI, M. J., HASHISHO, Z., PHILIPS, J. H., ANDERSON, J. E. & NICHOLS, M. 2015. Heel Formation during Volatile Organic Compound Desorption from Activated Carbon Fiber Cloth. *Carbon*.

POTYRAILO, R. A. & MORRIS, W. G. 2007. Multianalyte chemical identification and quantitation using a single radio frequency identification sensor. *Analytical Chemistry,* 79**,** 45-51.

POTYRAILO, R. A., NAGRAJ, N., SURMAN, C., BOUDRIES, H., LAI, H., SLOCIK, J. M., KELLEY-LOUGHNANE, N. & NAIK, R. R. 2012. Wireless sensors and sensor networks for homeland security applications. *Trends in Analytical Chemistry,* 40**,** 133-145.

RIVERA-UTRILLA, J., FERRO-GARCíA, M. A., BAUTISTA-TOLEDO, I., SÁNCHEZ-JIMÉNEZ, C., SALVADOR, F. & MERCHÁN, M. D. 2003. Regeneration of ortho-chlorophenol-exhausted activated carbons with liquid water at high pressure and temperature. *Water Research,* 37**,** 1905-1911.

RUBEL, G. O., PETERSON, G. W. & FLETCHER, N. K. 2009a. In situ sensing of adsorbed water in activated carbon using impedance measurements. *Carbon,* 47**,** 2442-2447.

RUBEL, G. O., PETERSON, G. W., FLETCHER, N. K., PARKER III, J. E. & JEFFERS, R. B. 2009b. Measurement of the impedance change of impregnated activated carbon during exposure to SO2 vapors at ambient temperatures. *Carbon,* 47**,** 3566-3573.

SING, K. S. W., EVERETT, D. H., HAUL, R. A. W., MOSCOU, L., PIEROTTI, R. A., ROUQUEROL, J. & SIEMIENIEWSKA, T. 2008. Reporting Physisorption Data for Gas/Solid Systems. *Handbook of Heterogeneous Catalysis.* Wiley-VCH Verlag GmbH & Co. KGaA.

TANAKA, S., SHIRAGA, K., OGAWA, Y., FUJII, Y. & OKUMURA, S. 2014. Applicability of effective medium theory to wood density measurements using terahertz time-domain spectroscopy. *Journal of Wood Science,* 60**,** 111-116.

THAKKAR, S. & MANES, M. 1987. Adsorptive displacement analysis of many-component priority pollutants on activated carbon. *Environmental science and technology,* 21**,** 546-549.

WEISSENBERGER, A. P. & SCHMIDT, P. S. 1994. Microwave Enhanced Regeneration of Adsorbents. *MRS Proceedings,* 347**,** 383-387.

ZARIFI, M. H., FARSINEZHAD, S., ABDOLRAZZAGHI, M., DANESHMAND, M. & SHANKAR, K. 2016a. Selective microwave sensors exploiting the interaction of analytes with trap states in TiO2 nanotube arrays. *Nanoscale,* 8**,** 7466-7473.

ZARIFI, M. H., MOHAMMADPOUR, A., FARSINEZHAD, S., WILTSHIRE, B. D., NOSRATI, M., ASKAR, A. M., DANESHMAND, M. & SHANKAR, K. 2015a. Time-Resolved Microwave Photoconductivity (TRMC) Using Planar Microwave Resonators: Application to the Study of Long-Lived Charge Pairs in Photoexcited Titania Nanotube Arrays. *The Journal of Physical Chemistry C,* 119**,** 14358-14365.

ZARIFI, M. H., RAHIMI, M., DANESHMAND, M. & THUNDAT, T. 2016b. Microwave ring resonator-based non-contact interface sensor for oil sands applications. *Sensors and Actuators B: Chemical,* 224**,** 632-639.

ZARIFI, M. H., SOHRABI, A., SHAIBANI, P. M., DANESHMAND, M. & THUNDAT, T. 2015b. Detection of volatile organic compounds using microwave sensors. *IEEE Sensors Journal,* 15**,** 248-254.

ZARIFI, M. H., THUNDAT, T. & DANESHMAND, M. 2015c. High resolution microwave microstrip resonator for sensing applications. *Sensors and Actuators A: Physical,* 233**,** 224-230.

ZARIFI, M. H., FAYAZ, M., GOLDTHORP, J., ABDOLRAZZAGHI, M., HASHISHO, Z. & DANESHMAND, M. 2015d. Microbead-assisted high resolution microwave planar ring resonator for organic-vapor sensing. *Applied Physics Letters,* 106**,** 062903.

CHAPTER 9. CONCLUSIONS AND RECOMMENDATIONS

The main goal of this study is to investigate the factors affecting heel buildup and possible ways to reduce it. At the beginning of this study, conductive heating regeneration was used to identify the volatile organic compounds (VOCs) that irreversibly adsorb onto a microporous beaded activated carbon and reduce the adsorption capacity (Chapter 3). Then, the performance of microwave and conductive heating techniques for regeneration of beaded activated carbon (BAC) loaded with a high boiling point VOC (n-dodecane) was compared and assessed based on the regeneration efficiency and energy consumption (Chapter 4). In the next step, the combined effect of adsorbent porosity, regeneration temperature and heating rate on heel buildup was investigated through microwave regeneration of BAC loaded with 1,2,4-trimethylbenzene (TMB) (Chapter 5). The effect of dielectric properties of adsorbent and adsorbate on microwave regeneration was investigated in Chapter 6. In the next two chapters (Chapter 7 and 8), the application of a non-contact microwave sensor for determining breakthrough time and adsorption capacity, and for estimating residual life-time of spent BACs were studied.

9.1 Conclusions

1) During 5 consecutive adsorption/conductive regeneration of BAC, loaded with different VOCs, it was found that the level of heel buildup for compounds with higher boiling points is considerably high. Other than TXIB, the rest of the tested oxygenated compounds have low molecular weights and boiling points and provided small heel. It was found that high molecular weight alkanes (e.g., n-dodecane) and Amines (e.g., diethanolamine and methyl diethanolamine), which have high boiling points and low vapor pressures, have also considerable contribution to heel buildup.

2) During regeneration of BAC loaded with n-dodecane, the minimum energy required to completely regenerate the adsorbent (100% desorption efficiency) using microwave regeneration was 6% of that needed with conductive heating regeneration, owing to more rapid heating rates and lower heat loss. Analyses of adsorbent PSD and surface chemistry confirmed that neither heating method altered the physical/chemical properties of BAC. Additionally, gas chromatography (with flame ionization detector) confirmed that neither regeneration method detectably altered the adsorbate composition during desorption. Improvements in energy consumption and desorption efficiency and stable adsorbate and adsorbent properties make microwave heating an attractive method for activated carbon regeneration particularly when high-affinity VOC adsorbates are present.

3) To systematically investigate the effect of adsorbent porosity, regeneration temperature and heating rate on heel formation, two adsorbents with the same micropore volumes and different mesopore volumes were subject to five successive adsorption/ regeneration cycles. The regenerations were completed at a moderate temperature (288 °C) and an elevated temperature (400 °C) using different heating rates (25, 50, 100, and 150 °C/min). It was observed that exposure of desorbate to a sufficiently high regeneration temperature resulted in coke formation on the surface of carbon, particularly at higher heating rates. For regeneration at moderate lower temperature, both incomplete regeneration (physisorption) and coke formation have contribution to heel formation. For regeneration at high temperature, however, heel formation was solely due to coke formation. In both regeneration temperatures, increasing heating rate increased coke formation on BACs. Both large micropores (8-

179

20 Å) and mesopores contribute to heel formation, however, their contributions were significantly less than that of narrow micropores.

4) To highlight the effect of dielectric properties of adsorbents and adsorbates on microwave regeneration, two adsorbents (BAC, DOWEX V493) with different dielectric properties but same heat capacity, and two VOCs (TMB, BE) with the same boiling points but different dielectric properties were selected to complete adsorption/microwave regeneration tests. The dielectric loss factor of V493 (microwave transparent adsorbent) increased after loading with polar or non-polar adsorbates, as evidenced by lower energy requirements to heat to 190 °C and faster heating rates. For BAC (microwave absorbing adsorbent), however, added adsorbate decreased the overall loss factor of the system, resulting in slower heating and increased energy requirements compared to blank BAC. The maximum DDR for V493-BE occurred sooner and was 5 times higher than of V493-TMB, highlighting the importance of adsorbate dielectric properties during regeneration of a microwave transparent adsorbent. For regeneration at constant temperature high loss factor adsorbents improve energy usage but do not necessarily improve regeneration efficiency. The highest mass desorbed per unit of absorbed applied energy was for the adsorbent/adsorbate pair with the highest dielectric loss factor (BAC-BE), and the lowest value was for the system with the lowest dielectric loss factor (V493-TMB).

5) During adsorption of TMB on BAC or V503, the changes in the dielectric properties of the adsorbents were monitored using a non-contact microwave sensor using two electromagnetic parameters: quality factor and resonant frequency. It was observed that the breakthrough time could be determined with less than 5% relative error, using

180

the time that the quality factor reached 0.95 of its final value. For different adsorbent-adsorbate pairs, adsorption isotherms were developed and related to the shift in the resonant frequency. For all tests, with increase of relative pressure, adsorption capacity and resonant frequency increased; therefore a strong linear correlation (R^2=0.88-0.97) between adsorption capacity and final resonant frequency could be found.

9.2   Recommendations

1. During this study, conductive and microwave regenerations of BAC loaded with n-dodecane were completed using constant power. To highlight the effect of heating method on regeneration performance, the regeneration tests can be completed at constant temperature using the same heating rate. The preliminary experiments showed that using the same regeneration temperature, microwave heating was more effective in regeneration of n-dodecane, relative to conductive heating.

2. During microwave regeneration of BACs loaded with TMB, the effect of flow rate was not investigated. The variation in flow rate can potentially change heel formation. Moreover, changing adsorbate from TMB to a polar adsorbate with higher dielectric properties or changing adsorbate to a mixture of VOCs with different dielectric properties, can affect microwave regeneration performance. Thus, it is suggested that the similar experiments be conducted using different adsorbates; particularly for mixtures, the outlet concentrations can be monitored and analyzed using a GC-MS.

CHAPTER 10. BIBLIOGRAPHY

ABOU-KHOUSA, M., AL-DURRA, A. & AL-WAHEDI, K. 2015. Microwave Sensing System for Real-Time Monitoring of Solid Contaminants in Gas Flows. *IEEE Sensors Journal,* 15**,** 5296-5302.

ADU, B. & OTTEN, L. 1993. Simultaneous microwave heat and mass transfer characteristics of porous hygroscopic solids. *Journal of Microwave Power and Electromagnetic Energy,* 28**,** 41.

ÁGUEDA, V. I., CRITTENDEN, B. D., DELGADO, J. A. & TENNISON, S. R. 2011. Effect of channel geometry, degree of activation, relative humidity and temperature on the performance of binderless activated carbon monoliths in the removal of dichloromethane from air. *Separation and Purification Technology,* 78**,** 154-163.

AL-DASOQI, N., MASON, A., ALKHADDAR, R. & AL-SHAMMA'A, A. Use of sensors in wastewater quality monitoring - A review of available technologies. World Environmental and Water Resources Congress 2011: Bearing Knowledge for Sustainability - Proceedings of the 2011 World Environmental and Water Resources Congress, 2011. 3379-3388.

AL-HAJERI, S., WYLIE, S. R., SHAW, A. & AL-SHAMMA'A, A. I. 2009. Real time EM waves monitoring system for oil industry three phase flow measurement. *Journal of Physics: Conference Series,* 178.

AL-KIZWINI, M. A., WYLIE, S. R., AL-KHAFAJI, D. A. & AL-SHAMMA'A, A. I. 2013. The monitoring of the two phase flow-annular flow type regime using microwave sensor technique. *Measurement: Journal of the International Measurement Confederation,* 46**,** 45-51.

ÁLVAREZ, P. M., BELTRÁN, F. J., GÓMEZ-SERRANO, V., JARAMILLO, J. & RODRIGUEZ, E. M. 2004. Comparison between thermal and ozone regenerations of spent activated carbon exhausted with phenol. *Water Research,* 38**,** 2155-2165.

ANCHEYTA, J. 2013. *Modeling of Processes and Reactors for Upgrading of Heavy Petroleum*, CRC Press.

ANDERSON, J. E., LEONE, T. G., SHELBY, M. H., WALLINGTON, T. J., BIZUB, J. J., FOSTER, M., LYNSKEY, M. G. & POLOVINA, D. 2012. Octane Numbers of

Ethanol-Gasoline Blends: Measurements and Novel Estimation Method from Molar Composition. *SAE Technical Paper.* Copyright © 2012 SAE International.

ANIA, C. O., MENÉNDEZ, J. A., PARRA, J. B. & PIS, J. J. 2004. Microwave-induced regeneration of activated carbons polluted with phenol. A comparison with conventional thermal regeneration. *Carbon,* 42**,** 1377-1381.

ANIA, C. O., PARRA, J. B., MENÉNDEZ, J. A. & PIS, J. J. 2005. Effect of microwave and conventional regeneration on the microporous and mesoporous network and on the adsorptive capacity of activated carbons. *Microporous and Mesoporous Materials,* 85**,** 7-15.

ANIA, C. O., PARRA, J. B., MENÉNDEZ, J. A. & PIS, J. J. 2007. Microwave-assisted regeneration of activated carbons loaded with pharmaceuticals. *Water Research,* 41**,** 3299-3306.

ARAGÓN CANDELARIA, P. R. & OWENS, A. J. 2009. Prediction of architectural coating performance using titanium dioxide characterization applying artificial neural networks. *Journal of Coatings Technology and Research,* 7**,** 431-440.

ASHTON, S. L., CUTMORE, N. G., ROACH, G. J., WATT, J. S., ZASTAWNY, H. W. & MCEWAN, A. J. Development and trial of microwave techniques for measurement of multiphase flow of oil, water and gas. SPE - Asia Pacific Oil & Gas Conference, 1994. 681-689.

ASTM 2014. Standard Test Method for Apparent Density of Activated Carbon, Designation: D2854 − 09.

ATWATER, J. E. & WHEELER JR, R. R. 2003. Complex permittivities and dielectric relaxation of granular activated carbons at microwave frequencies between 0.2 and 26 GHz. *Carbon,* 41**,** 1801-1807.

ATWATER, J. E. & WHEELER JR, R. R. 2004. Microwave permittivity and dielectric relaxation of a high surface area activated carbon. *Applied Physics A: Materials Science and Processing,* 79**,** 125-129.

BANSAL, R. C. & GOYAL, M. 2005. *Activated carbon adsorption,* Boca Raton, Taylor & Francis.

BANSODE, R. R., LOSSO, J. N., MARSHALL, W. E., RAO, R. M. & PORTIER, R. J. 2003. Adsorption of volatile organic compounds by pecan shell- and almond shell-based granular activated carbons. *Bioresource Technology,* 90**,** 175-184.

BAROCHI, G., ROSSIGNOL, J. & BOUVET, M. 2011. Development of microwave gas sensors. *Sensors and Actuators, B: Chemical,* 157**,** 374-379.

BASU, P. 2013. *Biomass Gasification, Pyrolysis and Torrefaction: Practical Design and Theory*, Elsevier Science.

BERNOU, C., REBIÈRE, D. & PISTRÉ, J. 2000. Microwave sensors: a new sensing principle. Application to humidity detection. *Sensors and Actuators, B: Chemical,* 68**,** 88-93.

BENKHEDDA, J., JAUBERT, J. N., BARTH, D. & PERRIN, L. 2000a. Experimental and modeled results describing the adsorption of toluene onto activated carbon. *Journal of Chemical and Engineering Data,* 45**,** 650-653.

BENKHEDDA, J., JAUBERT, J. N., BARTH, D., PERRIN, L. & BAILLY, M. 2000b. Adsorption isotherms of m-xylene on activated carbon: Measurements and correlation with different models. *Journal of Chemical Thermodynamics,* 32**,** 401-411.

BOURAOUI, M. M. 1991. *Microwave and convective drying of potato slices.* M.Sc. Dissertation, The University of British Columbia.

BOURGEOIS, W., ROMAIN, A. C., NICOLAS, J. & STUETZ, R. M. 2003. The use of sensor arrays for environmental monitoring: Interests and limitations. *Journal of Environmental Monitoring,* 5**,** 852-860.

BRADSHAW, S. M., VAN WYK, E. J. & DE SWARDT, J. B. 1997. Preliminary economic assessment of microwave regeneration of activated carbon for the carbon in pulp process. *Journal of Microwave Power and Electromagnetic Energy,* 32**,** 131-144.

BRADSHAW, S. M., VAN WYK, E. J. & DE SWARDT, J. B. 1998. Microwave heating principles and the application to the regeneration of granular activated carbon. *Journal of The South African Institute of Mining and Metallurgy,* 98**,** 201-210.

BRIGGS, D. & SEAH, M. P. 1983. *Practical surface analysis: By auger and x-ray photoelectron spectroscopy,* New York, USA, Wiley: Chichester.

BRUNAUER, S., EMMETT, P. H. & TELLER, E. 1938. Adsorption of gases in multimolecular layers. *Journal of the American Chemical Society,* 60**,** 309-319.

BURKHOLDER, H. R., FANSLOW, G. E. & BLUHM, D. D. 1986. Recovery of ethanol from a molecular sieve by using dielectric heating. *Industrial and Engineering Chemistry Fundamentals,* 25**,** 414-416.

CAL, M. P., ROOD, M. J. & LARSON, S. M. 1997. Gas phase adsorption of volatile organic compounds and water vapor on activated carbon cloth. *Energy and Fuels,* 11**,** 311-315.

ÇALIŞKAN, E., BERMÚDEZ, J. M., PARRA, J. B., MENÉNDEZ, J. A., MAHRAMANLIOĜLU, M. & ANIA, C. O. 2012. Low temperature regeneration of activated carbons using microwaves: Revising conventional wisdom. *Journal of Environmental Management,* 102**,** 134-140.

CARL, Y. 2014. Yaws' Handbook of Thermodynamic and Physical Properties of Chemical Compounds.

CHA, C. Y., WALLACE, S., GEORGE, A. H. & ROGERS, S. 2004. Microwave technology for treatment of fume hood exhaust. *Journal of Environmental Engineering,* 130**,** 338-348.

CHANG, S. H., WANG, K. S., LIANG, H. H., CHEN, H. Y., LI, H. C., PENG, T. H., SU, Y. C. & CHANG, C. Y. 2010. Treatment of Reactive Black 5 by combined electrocoagulation-granular activated carbon adsorption-microwave regeneration process. *Journal of Hazardous Materials,* 175**,** 850-857.

CHANNEN, E. W. & MCINTOSH, R. 1955. INVESTIGATION OF THE PHYSICALLY ADSORBED STATE BY MEANS OF DIELECTRIC MEASUREMENTS. *Canadian Journal of Chemistry,* 33**,** 172-183.

CHATZOPOULOS, D., VARMA, A. & IRVINE, R. L. 1993. Activated carbon adsorption and desorption of toluene in the aqueous phase. *AIChE Journal,* 39**,** 2027-2041.

CHANG YUL, C. & CARLISLE, C. T. 2001. Microwave process for volatile organic compound abatement. *Journal of the Air and Waste Management Association,* 51**,** 1628-1641.

CHERBAŃSKI, R. & MOLGA, E. 2009. Intensification of desorption processes by use of microwaves-An overview of possible applications and industrial perspectives. *Chemical Engineering and Processing: Process Intensification,* 48**,** 48-58.

CHERBAŃSKI, R., KOMOROWSKA-DURKA, M., STEFANIDIS, G. D. & STANKIEWICZ, A. I. 2011. Microwave swing regeneration Vs temperature swing

regeneration - Comparison of desorption kinetics. *Industrial and Engineering Chemistry Research,* 50**,** 8632-8644.

CHIANG, C. Y., LIU, Y. Y., CHEN, Y. S. & LIU, H. S. 2012. Absorption of hydrophobic volatile organic compounds by a rotating packed bed. *Industrial and Engineering Chemistry Research,* 51**,** 9441-9445.

CHIANG, Y. C., LEE, C. C. & SU, W. P. 2006. Adsorption behaviors of activated carbons for the exhaust from spray painting booths in vehicle surface coating. *Toxicological and Environmental Chemistry,* 88**,** 453-467.

CHOWDHURY, T., SHI, M., HASHISHO, Z., SAWADA, J. A. & KUZNICKI, S. M. 2012. Regeneration of Na-ETS-10 using microwave and conductive heating. *Chemical Engineering Science,* 75**,** 282-288.

COSS, P. M. & CHA, C. Y. 2000. Microwave regeneration of activated carbon used for removal of solvents from vented air. *Journal of Air & Waste Management Association,* 50**,** 529-535.

CLARK, D. F. & SUTTON, W. H. 1994. *Microwave Processing of Materials*, The National Academies Press.

C.MOLDOVEANU, S. 2009. *Pyrolysis of Organic Molecules Applications to Health and Environmental Issues,* Winston-Salem, NC, USA.

DE FONSECA, B., ROSSIGNOL, J., BEZVERKHYY, I., BELLAT, J. P., STUERGA, D. & PRIBETICH, P. 2014. VOCs Detection by Microwave Transduction Using Zeolites as Sensitive Material. *Procedia Engineering,* 87**,** 1019-1022.

DE JONGE, R. J., BREURE, A. M. & VAN ANDEL, J. G. 1996. Reversibility of adsorption of aromatic compounds onto powdered activated carbon (PAC). *Water Research,* 30**,** 883-892.

DEMIR, S. & SARAL, A. 2013. Identification and apportionment of sources of ozone-forming potential for proper reduction strategies. *Clean - Soil, Air, Water,* 41**,** 107-112.

DI, P. & CHANG, D. P. Microwave regeneration of volatile organic compounds (VOC) adsorbents. Presented at 89th Annual Conference & Exhibition of A&WMA, Nashville, TN, 1996.

DIMOTAKIS, E. D., CAL, M. P., ECONOMY, J., ROOD, M. J. & LARSON, S. M. 1995. Chemically treated activated carbon cloths for removal of volatile organic carbons from gas streams: evidence for enhanced physical adsorption. *Environmental Science and Technology,* 29**,** 1876-1880.

DETCHANAMURTHY, S. & GOSTOMSKI, P. A. 2012. Biofiltration for treating VOCs: an overview. *Reviews in Environmental Science and Biotechnology***,** 1-11.

DOWEX OPTIPORE V503 [Online]. Available: www.dow.com [Accessed April 20th, 2015].

DUNN, R. F. & EL-HALWAGI, M. M. 1994. Selection of optimal VOC-condensation systems. *Waste Management,* 14**,** 103-113.

EPA, U. 1993. Control of Volatile Organic Compound Emissions from Reactor Processes and Distilation Operations Processes in the Synthetic Organic Chemical Manufacturing Industry. *Guideline series*.

FABRIZI, G., FIORETTI, M. & MAINERO ROCCA, L. 2013. Occupational exposure to complex mixtures of volatile organic compounds in ambient air: Desorption from activated charcoal using accelerated solvent extraction can replace carbon disulfide? *Analytical and Bioanalytical Chemistry,* 405**,** 961-976.

FANG, C. S. & LAI, P. M. C. 1996. Microwave regeneration of spent powder activated carbon. *Chemical Engineering Communications,* 147**,** 17-27.

FAYAZ, M., SHARIATY, P., ATKINSON, J. D., HASHISHO, Z., PHILLIPS, J. H., ANDERSON, J. E. & NICHOLS, M. 2015. Using microwave heating to improve the desorption efficiency of high molecular weight VOC from beaded activated carbon. *Environmental Science and Technology,* 49**,** 4536-4542.

FAYAZ, M., WANG, H., JAHANDAR LASHAKI, M., HASHISHO, Z., PHILIPS, J. H. & ANDERSON, J. E. 2011. Accumulation of adsorbed of organic vapors from automobile painting operations on bead activated carbon. *Proceedings of the Air and Waste Management Association's Annual Conference and Exhibition, Orlando, FL.*

FERRO-GARCIA, M. A., JOLY, J. P., RIVERA-UTRILLA, J. & MORENO-CASTILLA, C. 1995. Thermal desorption of chlorophenols from activated carbons with different porosity. *Langmuir,* 11**,** 2648-2651.

FERRO-GARCIA, M. A., RIVERA-UTRILLA, J., BAUTISTA-TOLEDO, I. & MORENO-CASTILLA, C. 1996. Chemical and thermal regeneration of an activated carbon

saturated with chlorophenols. *Journal of Chemical Technology and Biotechnology,* 67**,** 183-189.

FU, Y., WANG, L. & ZHOU, Z. 2012 Microwave regeneration of field-spent granular activated carbon from power plants. *Advanced Materials Research.*

GAUR, V. & SHANKAR, P. A. 2008. Surface modification of activated Carbon for the Removal of water impurities. *Water conditioning & purification*.

GRANT, T. M. & KING, C. J. 1990. Mechanism of irreversible adsorption of phenolic compounds by activated carbons. *Industrial and Engineering Chemistry Research,* 29**,** 264-271.

GRITTI, F. & GUIOCHON, G. 2015. The quantitative impact of the mesopore size on the mass transfer mechanism of the new 1.9 μm fully porous Titan-C18 particles. I: Analysis of small molecules. Journal of Chromatography A, 1384, 76-87.

HA, S. R. & VINITNANTHARAT, S. 2000. Competitive removal of phenol and 2,4-dichlorophenol in biological activated carbon system. *Environmental Technology,* 21**,** 387-396.

HARRIOTT, P. & CHENG, A. T.-Y. 1988. KINETICS OF SPENT ACTIVATED CARBON REGENERATION. *AIChE Journal,* 34**,** 1656-1662.

HASHISHO, Z., EMAMIPOUR, H., CEVALLOS, D., ROOD, M. J., HAY, K. J. & KIM, B. J. 2007. Rapid response concentration-controlled desorption of activated carbon to dampen concentration fluctuations. *Environmental Science and Technology,* 41**,** 1753-1758.

HASHISHO, Z., EMAMIPOUR, H., ROOD, M. J., HAY, K. J., KIM, B. J. & THURSTON, D. 2008. Concomitant adsorption and desorption of organic vapor in dry and humid air streams using microwave and direct electrothermal swing adsorption. *Environmental Science and Technology,* 42**,** 9317-9322.

HASHISHO, Z., ROOD, M. & BOTICH, L. 2005. Microwave-swing adsorption to capture and recover vapors from air streams with activated carbon fiber cloth. *Environmental Science and Technology,* 39**,** 6851-6859.

HASHISHO, Z., ROOD, M. J., BAROT, S. & BERNHARD, J. 2009. Role of functional groups on the microwave attenuation and electric resistivity of activated carbon fiber cloth. *Carbon,* 47**,** 1814-1823.

HENNING, K. D., BONGARTZ, W. & DEGEL, J. Adsorptive Recovery of Problematic Solvents. Paper presented at the Meeting of the Nineteenth Biennial Conference on Carbon 1989 Pennsylvania State University, USA.

HSIEH, L., YANG, H., LIN, Y. & TSAI, C. 2012. Levels and composition of volatile organic compounds from the electric oven during roasting pork activities. *Sustainable environment research,* 22, 7.

HUA-SHAN, T. & CHIH-JU, G. J. 1999. Application of granular activated carbon packed-bed reactor in microwave radiation field to treat phenol. *Chemosphere,* 38**,** 2667-2680.

JAHANDAR LASHAKI, M., ATKINSON, J. D., HASHISHO, Z., PHILLIPS, J. H., ANDERSON, J. E. & NICHOLS, M. 2016. The role of beaded activated carbon's pore size distribution on heel formation during cyclic adsorption/desorption of organic vapors. *Journal of Hazardous Materials,* 315**,** 42-51.

JAHANDAR LASHAKI, M., ATKINSON, J. D., HASHISHO, Z., PHILLIPS, J. H., ANDERSON, J. E., NICHOLS, M. & MISOVSKI, T. 2016. Effect of desorption purge gas oxygen impurity on irreversible adsorption of organic vapors. *Carbon,* 99**,** 310-317.

JAHANDAR LASHAKI, M., FAYAZ, M., NIKNADDAF, S. & HASHISHO, Z. 2012. Effect of the adsorbate kinetic diameter on the accuracy of the Dubinin–Radushkevich equation for modeling adsorption of organic vapors on activated carbon. *Journal of Hazardous Materials,* 241–242**,** 154-163.

JAIN, R. K., AURELLE, Y., CABASSUD, C., ROIUSTAN, M. & SHELTON, S. B. 1997. *Environmental Technologies and Trends: International and Policy Perspectives*, Springer.

JONES, D. A., LELYVELD, T. P., MAVROFIDIS, S. D., KINGMAN, S. W. & MILES, N. J. 2002. Microwave heating applications in environmental engineering - A review. *Resources, Conservation and Recycling,* 34**,** 75-90.

JOU, G. C.-J. 1998. Application of activated carbon in a microwave radiation field to treat trichloroethylene. *Carbon,* 36**,** 1643-1648.

KARKKAINEN, K., SIHVOLA, A. & NIKOSKINEN, K. 2001. Analysis of a three-dimensional dielectric mixture with finite difference method. *IEEE Transactions on Geoscience and Remote Sensing,* 39**,** 1013-1018.

KHAN, F. I. & KR. GHOSHAL, A. 2000. Removal of Volatile Organic Compounds from polluted air. *Journal of Loss Prevention in the Process Industries,* 13**,** 527-545.

KIM, B. R., KALIS, E. M. & ADAMS, J. A. 2001. Integrated emissions management for automotive painting operations. *Pure and Applied Chemistry,* 73**,** 1277-1280.

KIM, J. H., RYU, Y. K., HAAM, S., LEE, C. H. & KIM, W. S. 2001. Adsorption and steam regeneration of n-hexane, MEK, and toluene on activated carbon fiber. *Separation Science and Technology,* 36**,** 263-281.

KIM, J. H., LEE, S. J., KIM, M. B., LEE, J. J. & LEE, C. H. 2007. Sorption equilibrium and thermal regeneration of acetone and toluene vapors on an activated carbon. *Industrial and Engineering Chemistry Research,* 46**,** 4584-4594.

KOROSTYNSKA, O., MASON, A. & AL-SHAMMA'A, A. 2012. Monitoring of nitrates and phosphates in wastewater: Current technologies and further challenges. *International Journal on Smart Sensing and Intelligent Systems,* 5**,** 149-176.

KOROSTYNSKA, O., MASON, A. & AL-SHAMMA'A, A. 2014. Microwave sensors for the non-invasive monitoring of industrial and medical applications. *Sensor Review,* 34**,** 182-191.

KUBOTA, M., HANADA, T., YABE, S., KUCHAR, D. & MATSUDA, H. 2011. Water desorption behavior of desiccant rotor under microwave irradiation. *Applied Thermal Engineering,* 31**,** 1482-1486.

KUO, C. Y. 2008. Desorption and re-adsorption of carbon nanotubes: Comparisons of sodium hydroxide and microwave irradiation processes. *Journal of Hazardous Materials,* 152**,** 949-954.

LASHAKI, M. J., FAYAZ, M., WANG, H., HASHISHO, Z., PHILIPS, J. H., ANDERSON, J. E. & NICHOLS, M. 2012. Effect of adsorption and regeneration temperature on irreversible adsorption of organic vapors on beaded activated carbon. *Environmental Science and Technology,* 46**,** 4083-4090.

LEGRAS, B., POLAERT, I., THOMAS, M. & ESTEL, L. 2013. About using microwave irradiation in competitive adsorption processes. *Applied Thermal Engineering,* 164–171.

LEE, H. J., LEE, H. S., YOO, K. H. & YOOK, J. G. 2010. DNA sensing using split-ring resonator alone at microwave regime. *Journal of Applied Physics,* 108.

LI, C. & MOE, W. M. 2005. Activated carbon load equalization of discontinuously generated acetone and toluene mixtures treated by biofiltration. *Environmental Science and Technology,* 39**,** 2349-2356.

LI, L., LIU, S. & LIU, J. 2011. Surface modification of coconut shell based activated carbon for the improvement of hydrophobic VOC removal. *Journal of Hazardous Materials,* 192**,** 683-690.

LI, W., WANG, X. & PENG, J. 2013. Effects of microwave heating on porous structure of regenerated powdered activated carbon used in xylose. *Environmental Technology (United Kingdom),* 34**,** 2917-2925.

LIU, P. K. T., FELTCH, S. M. & WAGNER, N. J. 1987. Thermal desorption behavior of aliphatic and aromatic hydrocarbons loaded on activated carbon. *Industrial and Engineering Chemistry Research,* 26**,** 1540-1545.

LIU, X., QUAN, X., BO, L., CHEN, S. & ZHAO, Y. 2004. Simultaneous pentachlorophenol decomposition and granular activated carbon regeneration assisted by microwave irradiation. *Carbon,* 42**,** 415-422.

LOWELL, S. & SHIELDS, J. E. 1991. *Powder surface area and porosity,* London ; New York, Chapman & Hall.

LU, Q. & SORIAL, G. A. 2004. Adsorption of phenolics on activated carbon - Impact of pore size and molecular oxygen. *Chemosphere,* 55**,** 671-679.

LU, Q. & SORIAL, G. A. 2007. The effect of functional groups on oligomerization of phenolics on activated carbon. *Journal of Hazardous Materials,* 148**,** 436-445.

LU, Q. & SORIAL, G. A. 2009. A comparative study of multicomponent adsorption of phenolic compounds on GAC and ACFs. *Journal of Hazardous Materials,* 167**,** 89-96.

LU, Q. L. & SORIAL, G. A. 2004. The role of adsorbent pore size distribution in multicomponent adsorption on activated carbon. *Carbon,* 42**,** 3133-3142.

LUKOMSKAYA, A. Y., TARKOVSKAYA, I. A. & STRELKO, V. V. 1986. Chemisorption of o-xylene on activated carbons. *Theoretical and Experimental Chemistry,* 22**,** 357-360.

LUO, L., RAMIREZ, D., ROOD, M. J., GREVILLOT, G., HAY, K. J. & THURSTON, D. L. 2006. Adsorption and electrothermal desorption of organic vapors using activated carbon adsorbents with novel morphologies. *Carbon,* 44**,** 2715-2723.

MAGNE, P. & WALKER JR, P. L. 1986. Phenol adsorption on activated carbons: Application to the regeneration of activated carbons polluted with phenol. *Carbon,* 24**,** 101-107.

MASON, A., KOROSTYNSKA, O., WYLIE, S. & AL-SHAMMA'A, A. I. 2014. Non-destructive evaluation of an activated carbon using microwaves to determine residual life. *Carbon,* 67**,** 1-9.

MATTSON, J. A., MARK JR, H. B., MALBIN, M. D., WEBER JR, W. J. & CRITTENDEN, J. C. 1969. Surface chemistry of active carbon: Specific adsorption of phenols. *Journal of Colloid And Interface Science,* 31**,** 116-130.

MD YUNUS, M. A. & MUKHOPADHYAY, S. C. 2011. Planar electromagnetic sensor for the detection of nitrate and contamination in natural water sources using electrochemical impedance spectroscopy approach. *Lecture Notes in Electrical Engineering.*

MEIER, M., TURNER, M., VALLEE, S., CONNER, W. C., LEE, K. H. & YNGVESSON, K. S. 2009. Microwave regeneration of zeolites in a 1 meter column. *AIChE Journal,* 55**,** 1906-1913.

MENÉNDEZ, J. A., ARENILLAS, A., FIDALGO, B., FERNÁNDEZ, Y., ZUBIZARRETA, L., CALVO, E. G. & BERMÚDEZ, J. M. 2010. Microwave heating processes involving carbon materials. *Fuel Processing Technology,* 91**,** 1-8.

MIURA, M., KAGA, H., SAKURAI, A., KAKUCHI, T. & TAKAHASHI, K. 2004. Rapid pyrolysis of wood block by microwave heating. *Journal of Analytical and Applied Pyrolysis,* 71, 187-199.

MOLDOVEANU, S. C. 2009. *Pyrolysis of Organic Molecules: Applications to Health and Environmental Issues*, Elsevier Science.

NIGAR, H., NAVASCUÉS, N., DE LA IGLESIA, O., MALLADA, R. & SANTAMARÍA, J. 2015. Removal of VOCs at trace concentration levels from humid air by Microwave Swing Adsorption, kinetics and proper sorbent selection. *Separation and Purification Technology,* 151**,** 193-200.

NIKNADDAF, S., ALAM, M., ABEDEH, G., MOHAMMADREZA, F., ATKINSON, J. D., HASHISHO, Z., PHILIPS, J. H., ANDERSON, J. E. & NICHOLS, M. EFFECT OF DESORPTION CONDITIONS AND ADSORBATE PROPERTIES ON HEEL

FORMATION DURING REGENERATION OF ACTIVATED CARBON FIBER CLOTH Conference on Carbon, 2016 Pennsylvania State University, USA.

NIKNADDAF, S., ATKINSON, J. D., SHARIATY, P., LASHAKI, M. J., HASHISHO, Z., PHILIPS, J. H., ANDERSON, J. E. & NICHOLS, M. 2015. Heel Formation during Volatile Organic Compound Desorption from Activated Carbon Fiber Cloth. *Carbon,*196,131-138.

OLIVIER, J. P. 1998. Improving the models used for calculating the size distribution of micropore volume of activated carbons from adsorption data. *Carbon,* 36, 1469-1472.

OSEI-TWUM, E. Y., ABUZAID, N. S. & NAHKLA, G. 1996. Carbon-catalyzed oxidative coupling of phenolic compounds. *Bulletin of Environmental Contamination and Toxicology,* 56**,** 513-519.

PEI, J. & ZHANG, J. S. 2012. Determination of adsorption isotherm and diffusion coefficient of toluene on activated carbon at low concentrations. *Building and Environment,* 48**,** 66-76.

PIDs for continuous monitoring of VOCs [Online]. Available: http://www.jmtestsystems.com/ [Accessed June 17th, 2016].

POLAERT, I., ESTEL, L., HUYGHE, R. & THOMAS, M. 2010. Adsorbents regeneration under microwave irradiation for dehydration and volatile organic compounds gas treatment. *Chemical Engineering Journal,* 162**,** 941-948.

POLAERT, I., LEDOUX, A., ESTEL, L., HUYGHE, R. & THOMAS, M. 2007. Microwave assisted regeneration of zeolite. *International Journal of Chemical Reactor Engineering,* 5.

POTYRAILO, R. A. & MORRIS, W. G. 2007. Multianalyte chemical identification and quantitation using a single radio frequency identification sensor. *Analytical Chemistry,* 79**,** 45-51.

POTYRAILO, R. A., NAGRAJ, N., SURMAN, C., BOUDRIES, H., LAI, H., SLOCIK, J. M., KELLEY-LOUGHNANE, N. & NAIK, R. R. 2012. Wireless sensors and sensor networks for homeland security applications. *Trends in Analytical Chemistry,* 40**,** 133-145.

POPESCU, M., JOLY, J. P., CARRÉ, J. & DANATOIU, C. 2003. Dynamical adsorption and temperature-programmed desorption of VOCs (toluene, butyl acetate and butanol) on activated carbons. *Carbon,* 41**,** 739-748.

PRICE, D. W. & SCHMIDT, P. S. 1997. Microwave regeneration of adsorbents at low pressure: Experimental kinetics studies. *Journal of Microwave Power and Electromagnetic Energy,* 32**,** 145-154.

PRICE, D. W. & SCHMIDT, P. S. 1998. VOC recovery through microwave regeneration of adsorbents: Comparative economic feasibility studies. *Journal of the Air and Waste Management Association,* 48**,** 1146-1155.

PRICE, D. W. & SCHMIDT, P. S. 1998. VOC recovery through microwave regeneration of adsorbents: Process design studies. *Journal of the Air and Waste Management Association,* 48**,** 1135-1145.

QUAN, X., LIU, X., BO, L., CHEN, S., ZHAO, Y. & CUI, X. 2004. Regeneration of acid orange 7-exhausted granular activated carbons with microwave irradiation. *Water Research,* 38**,** 4484-4490.

Quantachrome Autosorb 1 Operating Manual, 2006

REUß, J., BATHEN, D. & SCHMIDT-TRAUB, H. 2002. Desorption by microwaves: Mechanisms of multicomponent mixtures. *Chemical Engineering and Technology,* 25**,** 381-384.

RIVERA-UTRILLA, J., FERRO-GARCíA, M. A., BAUTISTA-TOLEDO, I., SÁNCHEZ-JIMÉNEZ, C., SALVADOR, F. & MERCHÁN, M. D. 2003. Regeneration of ortho-chlorophenol-exhausted activated carbons with liquid water at high pressure and temperature. *Water Research,* 37**,** 1905-1911.

ROBERS, A., FIGURA, M., THIESEN, P. H. & NIEMEYER, B. 2005. Desorption of odor-active compounds by microwaves, ultrasound, and water. *AIChE Journal,* 51**,** 502-510.

RODRı´GUEZ-MIRASOL, J., BEDIA, J. & CORDERO, C. 2005. Influence of water vapor on the adsorption of VOCs on lignin-based activated carbons. *Separation Science and Technology,* 40, 3113–3135.

Rogers Corporation [Online]. Available: www.rogerscorp.com/index.aspx [Accessed Nov. 10th, 2015].

ROUSSY, G., ZOULALIAN, A., CHARREYRE, M. & THIEBAUT, J. M. 1984. How microwaves dehydrate zeolites. *The Journal of Physical Chemistry,* 88**,** 5702-5708.

RUBEL, G. O., PETERSON, G. W. & FLETCHER, N. K. 2009. In situ sensing of adsorbed water in activated carbon using impedance measurements. *Carbon,* 47**,** 2442-2447.

RUBEL, G. O., PETERSON, G. W., FLETCHER, N. K., PARKER III, J. E. & JEFFERS, R. B. 2009. Measurement of the impedance change of impregnated activated carbon during exposure to SO2 vapors at ambient temperatures. *Carbon,* 47**,** 3566-3573.

RUDLING, J. & BJÖRKHOLM, E. 1987. Irreversibility effects in liquid desorption of organic solvents from activated carbon. *Journal of Chromatography A,* 392**,** 239-248.

RYU, Y. K., LEE, H. J., YOO, H. K. & LEE, C. H. 2002. Adsorption equilibria of toluene and gasoline vapors on activated carbon. *Journal of Chemical and Engineering Data,* 47**,** 1222-1225.

SCHNABEL, S., MOULIN, P., NGUYEN, Q. T., ROIZARD, D. & APTEL, P. 1998. Removal of volatile organic components (VOCs) from water by pervaporation: separation improvement by Dean vortices. *Journal of Membrane Science,* 142**,** 129-141.

SCHNELLE, K. B. J. & BROWN, C. A. 2002. Air pollution control technology handbook.

SEO, J., KATO, S., ATAKA, Y. & CHINO, S. 2009. Performance test for evaluating the reduction of VOCs in rooms and evaluating the lifetime of sorptive building materials. *Building and Environment,* 44**,** 207-215.

SHAH, I. K., PRE, P. & ALAPPAT, B. J. 2014. Effect of thermal regeneration of spent activated carbon on volatile organic compound adsorption performances. *Journal of the Taiwan Institute of Chemical Engineers,* 45**,** 1733-1738.

SHARIATY, P., LASHAKI, M. J., HASHISHO, Z., SAWADA, J., KUZNICKI, S. & HUTCHEON, R. Effect of ETS-10 Modification On Its Dielectric Properties and Microwave Regeneration. AIChe, 2013 San Francisco, CA.

SHEN, W., LI, Z. & LIU, Y. 2008. Surface Chemical Functional Groups Modification of Porous Carbon. *Recent patents on Chemical Engineering,* 1**,** 27-40.

SING, K. S. W., EVERETT, D. H., HAUL, R. A. W., MOSCOU, L., PIEROTTI, R. A., ROUQUEROL, J. & SIEMIENIEWSKA, T. 2008. Reporting Physisorption Data for Gas/Solid Systems. *Handbook of Heterogeneous Catalysis.* Wiley-VCH Verlag GmbH & Co. KGaA.

STAUDT, R., RAVE, H. & KELLER, J. U. 1999. Impedance spectroscopic measurements of pure gas adsorption equilibria on zeolites. *Adsorption,* 5**,** 159-167.

STEHLIK, P., DVORAK, R., BEBAR, L. & PARIZEK, T. Up to date technologies for off-gas cleaning. Proceedings of the 2008 Global Symposium on Recycling, Waste Treatment and Clean Technology, REWAS 2008. 1367-1372.

SUZUKI, M., MISIC, D. M., KOYAMA, O. & KAWAZOE, K. 1978. Study of thermal regeneration of spent activated carbons: Thermogravimetric measurement of various single component organics loaded on activated carbons. *Chemical Engineering Science,* 33**,** 271-279.

TAI, H. S. & LEE, C. L. 2007. Desorption of methy-ethyl-ketone from granular activated carbon with microwave radiation. *Environmental Progress,* 26**,** 299-303.

TANAKA, S., SHIRAGA, K., OGAWA, Y., FUJII, Y. & OKUMURA, S. 2014. Applicability of effective medium theory to wood density measurements using terahertz time-domain spectroscopy. *Journal of Wood Science,* 60**,** 111-116.

TANG, F. & YANG, X. 2012. A "deactivation" kinetic model for predicting the performance of photocatalytic degradation of indoor toluene, o-xylene, and benzene. *Building and Environment,* 56**,** 329-334.

TAMON, H. & OKAZAKI, M. 1996. Influence of acidic surface oxides of activated carbon on gas adsorption characteristics. *Carbon,* 34**,** 741-746.

TEFERA, D. T., JAHANDAR LASHAKI, M., FAYAZ, M., HASHISHO, Z., PHILIPS, J. H., ANDERSON, J. E. & NICHOLS, M. 2013. Two-dimensional modeling of volatile organic compounds adsorption onto beaded activated carbon. *Environmental Science and Technology,* 47, 11700-11710.

THAKKAR, S. & MANES, M. 1987. Adsorptive displacement analysis of many-component priority pollutants on activated carbon. *Environmental science and technology,* 21**,** 546-549.

TURNER, M. D., LAURENCE, R. L., CONNER, W. C. & YNGVESSON, K. S. 2000. Microwave radiation's influence on sorption and competitive sorption in zeolites. *AIChE Journal,* 46**,** 758-768.

VARADAN, V. K., VINOY, K. J. & GOPALAKRISHNAN, S. 2006. *Smart Material Systems and MEMS*, John Wiley & Sons, Ltd.

VIDIC, R. D., SUIDAN, M. T. & BRENNER, R. C. 1993. Oxidative coupling of phenols on activated carbon: impact on adsorption equilibrium. *Environmental Science & Technology,* 27**,** 2079-2085.

WANG, H., JAHANDAR LASHAKI, M., FAYAZ, M., HASHISHO, Z., PHILIPS, J. H., ANDERSON, J. E. & NICHOLS, M. 2012. Adsorption and Desorption of Mixtures of Organic Vapors on Beaded Activated Carbon. *Environmental Science & Technology,* 46**,** 8341-8350.

WANG, H., NIE, L., LI, J., WANG, Y., WANG, G., WANG, J. & HAO, Z. 2013. Characterization and assessment of volatile organic compounds (VOCs) emissions from typical industries. *Chinese Science Bulletin,* 58**,** 724-730.

WEISSENBERGER, A. P. & SCHMIDT, P. S. 1994. Microwave Enhanced Regeneration of Adsorbents. *MRS Proceedings,* 347.

XIN-HUI, D., SRINIVASAKANNAN, C., QU, W. W., XIN, W., JIN-HUI, P. & LI-BO, Z. 2012. Regeneration of microwave assisted spent activated carbon: Process optimization, adsorption isotherms and kinetics. *Chemical Engineering and Processing: Process Intensification,* 53**,** 53-62.

YONGE, D. R., KEINATH, T. M., POZNANSKA, K. & JIANG, Z. P. 1985. Single-solute irreversible adsorption on granular activated carbon. *Environmental Science and Technology,* 19**,** 690-694.

YOUNGQUIST, G. R. 1970. Diffusion and flow of gases in porous solids. *Industrial and Engineering Chemistry Research,* 62, 52-63.

YUN, J. H., CHOI, D. K. & KIM, S. H. 1999. Equilibria and dynamics for mixed vapors of BTX in an activated carbon bed. *AIChE Journal,* 45**,** 751-760.

YUN, J. H., HWANG, K. Y. & CHOI, D. K. 1998. Adsorption of benzene and toluene vapors on activated carbon fiber at 298, 323, and 348 K. *Journal of Chemical and Engineering Data,* 43**,** 843-845.

YUNUS, M. A. M., MUKHOPADHYAY, S. & PUNCHIHEWA, A. Application of independent component analysis for estimating nitrate contamination in natural water sources using planar electromagnetic sensor. Proceedings of the International Conference on Sensing Technology, ICST, 2011. 538-543.

YUNUS, M. A. M. & MUKHOPADHYAY, S. C. 2011. Novel planar electromagnetic sensors for detection of nitrates and contamination in natural water sources. *IEEE Sensors Journal,* 11**,** 1440-1447.

ZARIFI, M. H., FARSINEZHAD, S., ABDOLRAZZAGHI, M., DANESHMAND, M. & SHANKAR, K. 2016a. Selective microwave sensors exploiting the interaction of analytes with trap states in TiO2 nanotube arrays. *Nanoscale,* 8**,** 7466-7473.

ZARIFI, M. H., MOHAMMADPOUR, A., FARSINEZHAD, S., WILTSHIRE, B. D., NOSRATI, M., ASKAR, A. M., DANESHMAND, M. & SHANKAR, K. 2015a. Time-Resolved Microwave Photoconductivity (TRMC) Using Planar Microwave Resonators: Application to the Study of Long-Lived Charge Pairs in Photoexcited Titania Nanotube Arrays. *The Journal of Physical Chemistry C,* 119**,** 14358-14365.

ZARIFI, M. H., RAHIMI, M., DANESHMAND, M. & THUNDAT, T. 2016b. Microwave ring resonator-based non-contact interface sensor for oil sands applications. *Sensors and Actuators B: Chemical,* 224**,** 632-639.

ZARIFI, M. H., SOHRABI, A., SHAIBANI, P. M., DANESHMAND, M. & THUNDAT, T. 2015b. Detection of volatile organic compounds using microwave sensors. *IEEE Sensors Journal,* 15**,** 248-254.

ZARIFI, M. H., THUNDAT, T. & DANESHMAND, M. 2015c. High resolution microwave microstrip resonator for sensing applications. *Sensors and Actuators A: Physical,* 233**,** 224-230.

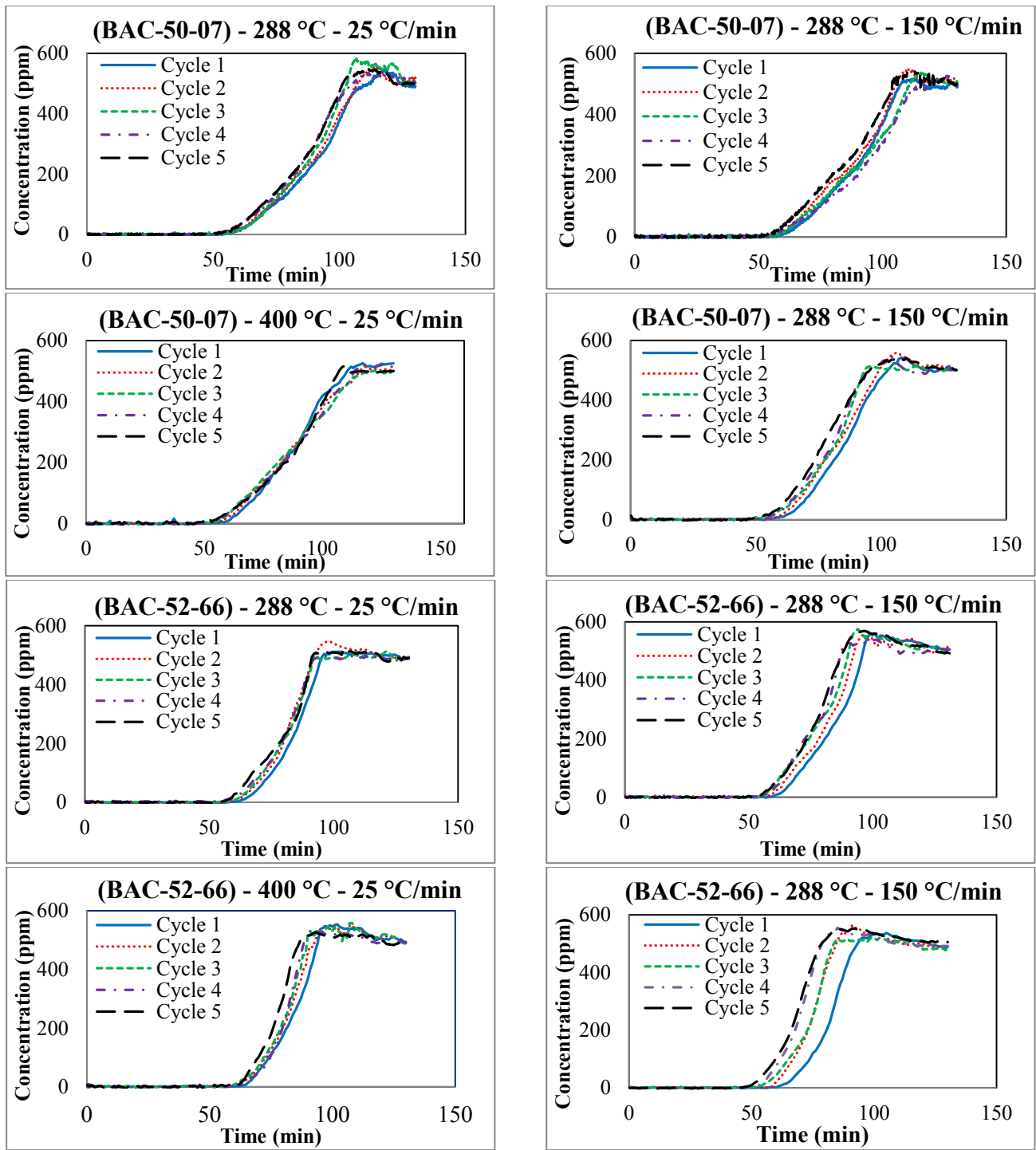# APPENDIX A. SUPPLEMENTARY DATA FOR CHAPTER 5

Figure A-1 Sample adsorption breakthrough curves for BAC-50-07 and BAC-52-66 regenerated at 288 and 400 °C using different heating rates. Titles are labeled as (x)-y-z where x, y, and z correspond to adsorbent type, regeneration temperature, and regeneration heating rate, respectively.
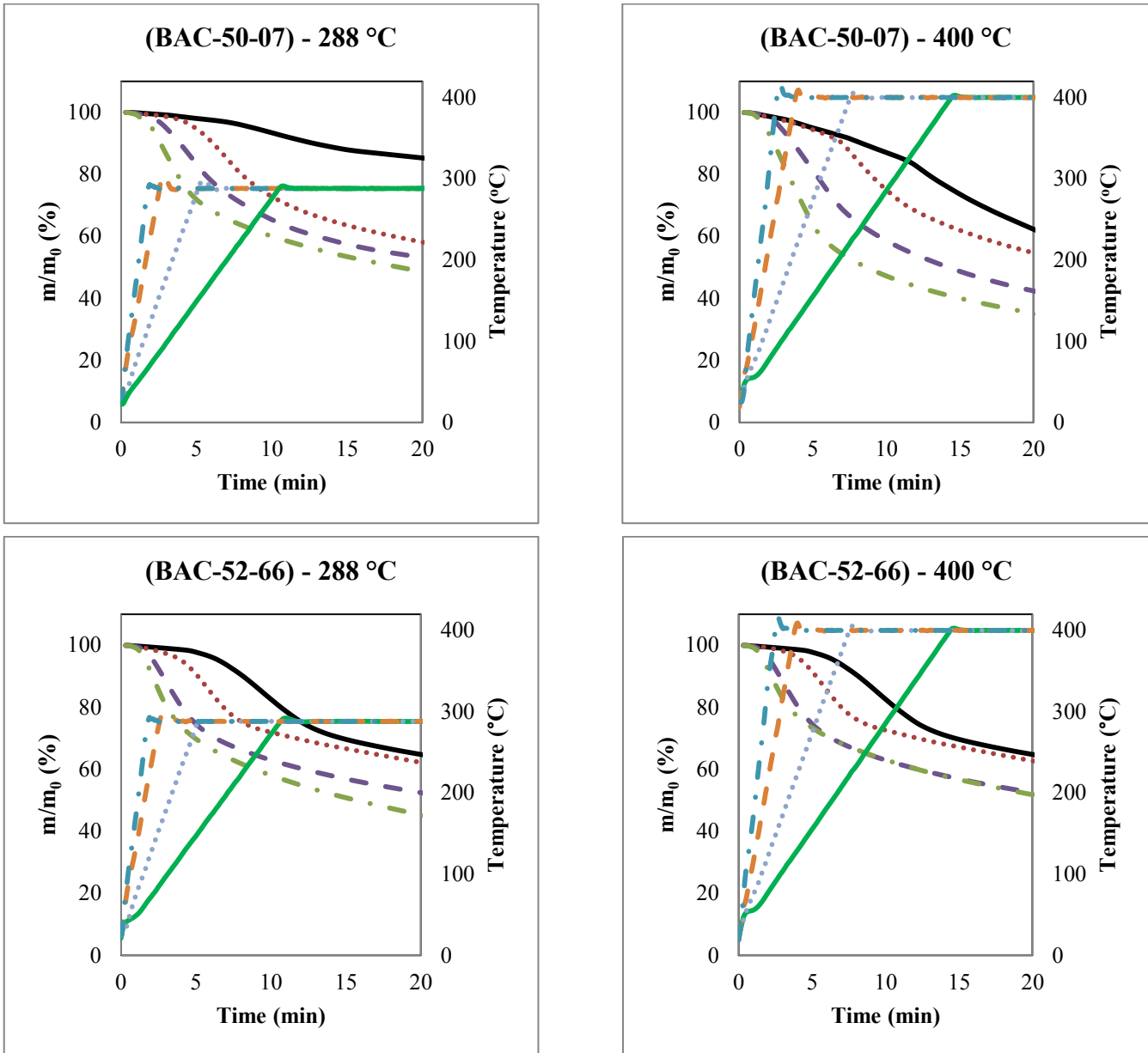
Figure A-2 Adsorbate mass fraction in the pores during regeneration of BACs at two regeneration temperatures using different heating rates. Titles are labeled as (x)-y where x and y correspond to adsorbent type and regeneration temperature, respectively.

APPENDIX B. SUPPLEMENTARY DATA FOR CHAPTER 6
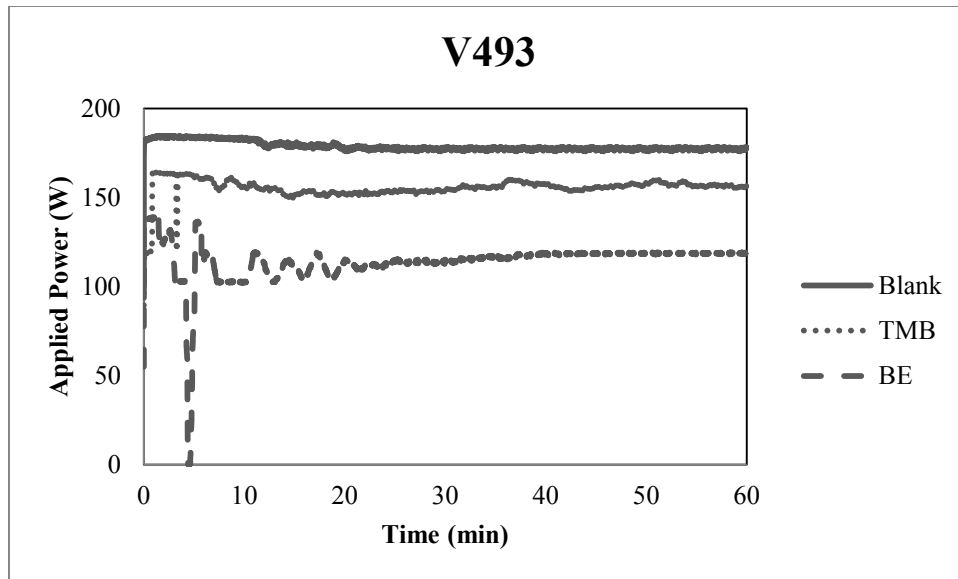
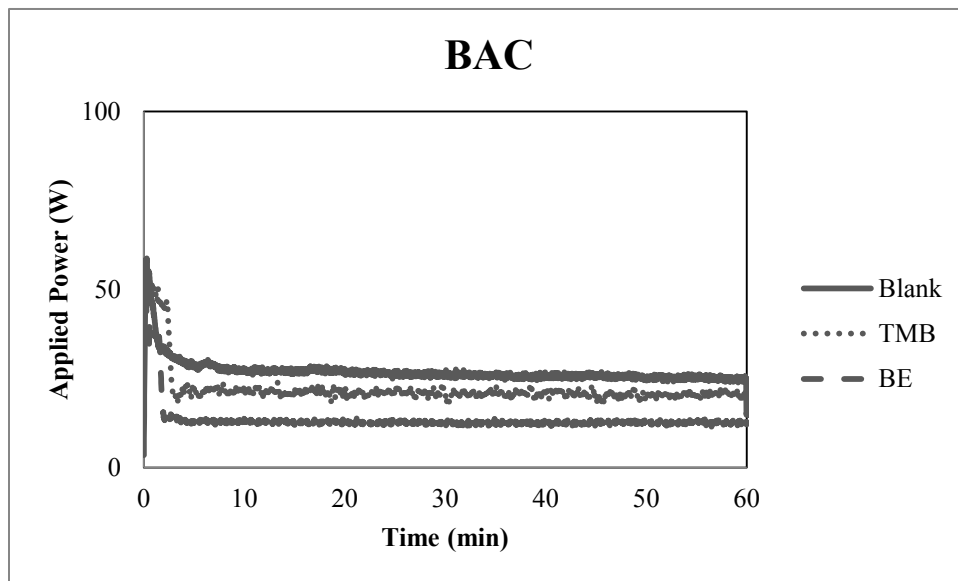**Figure B-1**: Applied power profiles during microwave regeneration of V493 samples

Figure B-2 Applied power profiles during microwave regeneration of BAC samples
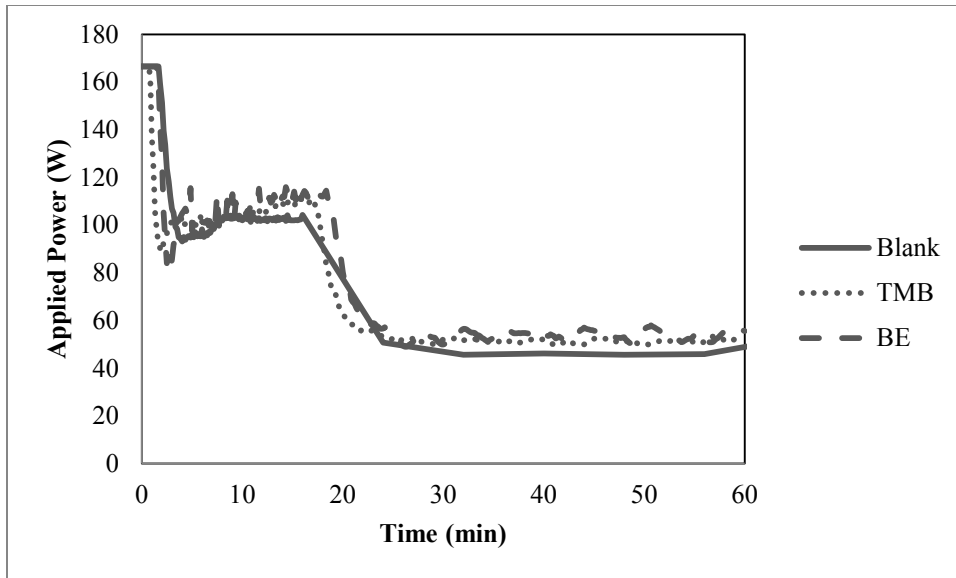
Figure B-3 Applied power profiles during conductive regeneration of V493 samples
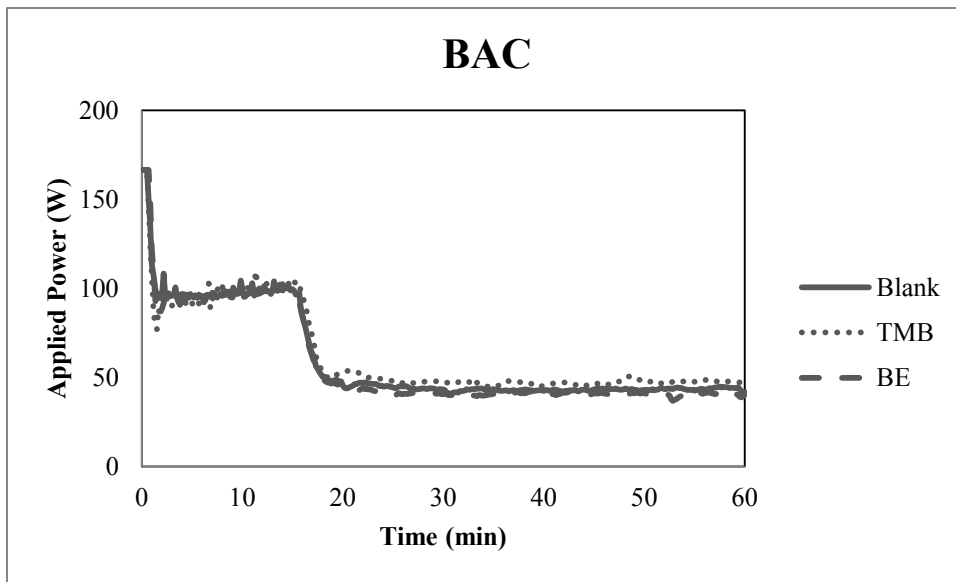

Figure B-4 Applied power profiles during conductive regeneration of BAC samples